Politecnico di Milano

SCHOOL OF INDUSTRIAL AND INFORMATION ENGINEERING

Corso di Laurea Magistrale in Ingegneria Matematica

POLITECNICO
MILANO 1863

A COUPLED SCHEME FOR THE SOLUTION OF PARABOLIC PROBLEMS ON UNBOUNDED DOMAINS

Supervisor

Prof. Luca BONAVENTURA

Co-Supervisor

Dott. Tommaso BENACCHIO

Candidate

Federico VISMARA – 913259

Academic Year 2019 – 2020

Abstract

We discuss the discretization of parabolic equations on unbounded domains by means of a spectral approach based on scaled Laguerre basis functions. Starting from the 1D advection-diffusion model problem on the positive half line, a stability analysis is first carried out: we examine several possible choices for the spatial discretization analyzing the spectrum of the corresponding matrix to determine which scheme has the best stability properties. The semi-infinite domain is then decomposed into an unbounded region, where the chosen method is employed, and a bounded one, where the problem is numerically solved using a discontinuous finite element method. A number of tests of linear and nonlinear wave propagation are carried out, showing that spurious reflections at the interface between the two subdomains are small, so that the resulting coupled approach is an efficient tool to model diffusion over arbitrarily large regions. Moreover, if a damping term is implemented in the semi-infinite part, outgoing signals are efficiently absorbed even with a small number of spectral modes, so that the proposed scheme can also be employed to efficiently implement an absorbing layer attached to the finite region of interest. The resulting setup is a computationally cheap alternative to traditional absorbing layer techniques, which usually require a large number of discretization nodes to absorb perturbations leaving the bounded domain. The thesis provides a novel extension to the parabolic case of existing stability and efficiency analyses of the same numerical setup for hyperbolic problems.

Abstract

In questa tesi si discute la discretizzazione, tramite un approccio spettrale, di equazioni differenziali a derivate parziali di tipo parabolico definite in domini illimitati. Assumendo come problema modello l'equazione di diffusione-trasporto unidimensionale su una semiretta, si conduce dapprima un'analisi di stabilità per determinare il migliore schema da adottare per la discretizzazione in spazio. In seguito, si decompone il dominio semi-infinito in una regione illimitata, dove il problema è risolto numericamente tramite il metodo precedentemente determinato, e una limitata, in cui si adotta uno schema agli elementi finiti discontinui. Si mostra che le riflessioni spurie all'interfaccia tra i due sottodomini sono trascurabili, così che lo schema accoppiato risulta essere un efficace strumento per modellare fenomeni di diffusione su domini con scale spaziali arbitrariamente grandi. Inoltre, implementando un termine di smorzamento nella sezione semi-infinita, le perturbazioni uscenti dalla regione limitata di interesse sono assorbite anche utilizzando un numero ridotto di modi spettrali; in questo modo, il modello accoppiato proposto può essere utilizzato anche per implementare in modo efficiente uno strato assorbente all'esterno del dominio in cui l'equazione viene risolta. Tale approccio risulta così essere un'efficiente alternativa agli strati assorbenti tradizionali, che spesso richiedono l'utilizzo di un gran numero di nodi e risultano pertanto essere dispendiosi dal punto di vista computazionale. Questa tesi presenta l'estensione al caso parabolico dei risultati di stabilità ed efficienza dello stesso approccio numerico, già studiati in letteratura nel caso iperbolico.

Introduction

In this thesis we analyze numerical methods for the solution of parabolic partial differential equations (PDE) in unbounded one-dimensional domains.

The correct modelling of evolution problems over arbitrarily large regions has a wide range of applications in computational physics and poses many unsolved challenges. One possible technique entails the restriction to a bounded region of interest by means of the introduction of an artificial boundary, where, in order to correctly let outgoing perturbations propagate without spurious reflections, suitable boundary conditions should be imposed that can be difficult to determine and computationally expensive. An alternative approach is represented by the so called absorbing layers, i.e. buffer regions where perturbations leaving the computational domain are damped to a prescribed external solution by an artificial reaction term. The choice of the parameters to be employed in these regions, such as grid spacing, spatial extension, and coefficients of the damping term represents the main difficulty for the numerical modelling of this kind of problems. An example of application is provided by the simulation of vertically propagating gravity waves in the Earth's atmosphere, which remains a challenge in the framework of computational space weather forecast; such a phenomenon involves a large portion of the atmosphere and may then be modeled as a wave propagation in a semi-infinite domain. Moreover, recent investigations have shown that a unified model of the upper atmosphere layers is necessary to accurately represent the processes taking place there (see e.g. [Akm11], [Rob00] and [Jac19]), so that efficient discretization schemes over arbitrarily large length scales are required.

In order to overcome the limits of currently used approaches, spectral methods based on scaled Laguerre functions were introduced in a hyperbolic

framework in [Ben10]. On the one hand, a suitable tuning of the scaling parameter allows to represent problems on arbitrarily large portions of the semi-infinite domain. On the other hand, this kind of approach may also be used to implement an absorbing layer, by attaching the semi-infinite region to a bounded one, where standard discretization schemes are employed. This coupling was applied to a spectral discretization of the shallow water equations coupled with a finite volume [BB13] and discontinuous Galerkin [BB19] discretizations on the finite domain; since a small number of spectral modes is sufficient to damp outgoing perturbations without reflections into the finite region, the proposed strategy is a computationally cheap alternative to existing absorbing layer techniques.

In this work, we extend the results of the above cited papers to the parabolic case. The discretization of differential problems involving a diffusive contribution in the form of a second-order spatial derivative is of great importance, since it allows, for example, the application of the framework proposed in [BB13], [BB19] to the discretization of the Navier-Stokes equations. More specifically:

1. We carry out a stability analysis of several possible spectral discretizations of the advection-diffusion equation on unbounded domains and we study the spectrum of the resulting system as a function of the Péclet number Pe. By doing so, we determine which methods are most appropriate to model problems in semi-infinite domains when a diffusive term is present in the equations.

2. We validate the coupling of the scheme determined in point 1 with a DG discretization on a bounded region and solve the linear advection-diffusion problem using the coupled model in order to evaluate the magnitude of the errors at the interface.

3. We implement a damping term in the semi-infinite part of the domain and we show that a small number of Laguerre modes are enough to absorb outgoing perturbations without numerical reflections spoiling the solution in the bounded domain of interest.

4. We extend the above experiments to non-linear problems.

In Chapter 1, the main results on Laguerre functions and quadrature rules on the positive half-line are reviewed. We will consider the general case of scaled basis functions, for which the scaling parameter β allows to represent arbitrarily large portions of $[0, +\infty)$ using a set number of nodes.

In Chapter 2, we derive the formulations of the model boundary value problems with parabolic terms employed as test cases for the coupled scheme, that is, the advection-diffusion equation and the Burgers' equation. We also discuss some of the features and properties of the equations to highlight their importance in numerical analysis and computational physics.

In Chapter 3 we present several alternatives based on Laguerre functions and polynomials for the discretization of the advection-diffusion equation on the positive half-line and we study their stability, so as to determine the best one to couple with the DG method in the finite region. As in [BB13] and [BB19], either modal or nodal discretizations with GLR quadrature rules, both based on scaled Laguerre functions, appear to be preferrable, since they provide the best stability properties and allow to efficiently represent functions with decay at infinity.

Chapter 4 contains the description of the coupling for a general non-linear problem with parabolic terms. We present in detail how to perform the DG discretization of the model problems in a finite region, the spectral Laguerre discretization in the unbounded part and how to couple them. In the case of the linear advection-diffusion equation, we also show that the global matrix

that represents the coupled scheme is only stable under a stability condition on the scaling parameter β. This does not represent an obstacle for the practical application of the method, since the scaling parameter can be easily adjusted so as to comply with the stability condition.

In Chapter 5 we present the results of several numerical experiments. We test the coupled scheme in the case of the homogeneous and non-homogeneous advection-diffusion equation, for which a damping term was also implemented in the semi-infinite portion of the domain; as long as the above discussed condition of β is satisfied, relative and absolute errors are comparable to those observed in [BB13] and [BB19] for the purely hyperbolic case. As a further extension of the results presented in these papers, we also considered two non-linear model problems (the Burgers' equation and a non-linear reaction equation); the errors due to the coupling are small enough to justify the accuracy of the proposed scheme for the solution of 1D problems with parabolic terms.

Finally, in Chapter 6 some conclusions are drawn and possibilities of further developments are discussed.

Contents

Chapter 1

Laguerre approximation on $[0, +\infty)$

In this chapter we present some basic notions and results on Laguerre polynomials and functions, which will be useful in the following sections. For a complete and more general analysis of orthogonal polynomials in semi-infinite domains we refer to [Ben10] and [ST06].

1.1 Zeros of orthogonal polynomials

Given the weight function $\omega \in L^1([0, +\infty)) = L^1(\mathbb{R}^+)$, we introduce the space

$$L^2_\omega(\mathbb{R}^+) = \left\{ u : [0, +\infty) \to \mathbb{R} \text{ such that } \int_0^{+\infty} |u(x)|^2 \omega(x) dx < +\infty \right\}. \tag{1.1}$$

$L^2_\omega(\mathbb{R}^+)$ is a Hilbert space with respect to the inner product

$$(u, v)_\omega = \int_0^{+\infty} u(x)v(x)\omega(x)dx. \tag{1.2}$$

Accordingly we define the norm of an element of $L^2_\omega(\mathbb{R}^+)$ as

$$\|u\|_\omega = \left(\int_0^{+\infty} |u(x)|^2 \omega(x) dx \right)^{1/2}. \tag{1.3}$$

We will also denote as $\mathbb{P}_N(\mathbb{R}^+)$ the set of all polynomials of degree at most N on $\mathbb{R}^+$ and

$$\hat{\mathbb{P}}_N = \left\{ u \text{ such that } u = ve^{-x/2}, v \in \mathbb{P}_N \right\} \tag{1.4}$$

A sequence of polynomials $\{p_n\}_{n\in\mathbb{N}}$, where $n = deg(p_n)$, is orthogonal in $L^2_\omega(\mathbb{R}^+)$ if

$$(p_n, p_m)_\omega = \int_0^{+\infty} p_n(x) p_m(x) \omega(x) dx = \|p_n\|^2_\omega \delta_{nm}. \tag{1.5}$$

The following theorem characterizes the orthogonal polynomials in terms of so-called three terms relations.

Theorem 1 *$\{p_n\}_{n\in\mathbb{N}}$ is a sequence of orthogonal polynomials in $L^2_\omega(\mathbb{R}^+)$ if and only if*

$$p_{n+1} = (a_n x - b_n) p_n - k_n p_{n-1}, \quad n \geq 0, \tag{1.6}$$

where $p_{-1} = 0$, $p_0 = 1$ and

$$a_n = \frac{c_{n+1}}{c_n}, \quad b_n = \frac{c_{n+1}}{c_n} \frac{(xp_n, p_n)_\omega}{\|p_n\|^2_\omega}, \quad k_n = \frac{c_{n+1} c_{n-1}}{c_n^2} \frac{\|p_n\|^2_\omega}{\|p_{n-1}\|^2_\omega} \tag{1.7}$$

This theorem allows us to easily compute the zeros of an orthogonal polynomial as the eigenvalues of a matrix; indeed we have the following result.

Theorem 2 *The zeros of the orthogonal polynomial p_{n+1} coincide with the eigenvalue of the tridiagonal matrix*

$$M = \begin{pmatrix} \alpha_0 & \sqrt{\beta_1} & & & \\ \sqrt{\beta_1} & \alpha_1 & \sqrt{\beta_2} & & \\ & \ddots & \ddots & \ddots & \\ & & \sqrt{\beta_{n-1}} & \alpha_{n-1} & \sqrt{\beta_n} \\ & & & \sqrt{\beta_n} & \alpha_n \end{pmatrix}$$

where

$$\alpha_j = \frac{b_j}{a_j}, \quad j \geq 0 \qquad \beta_j = \frac{k_j}{a_{j-1}a_j}, \quad j \geq 1 \tag{1.8}$$

and a_j, b_j, k_j are the coefficients of the three-terms relation defining p_{n+1}.

1.2 Laguerre polynomials

Laguerre polynomials, $\{\mathscr{L}_n\}_{n\in\mathbb{N}}$, are defined by the three-terms recurrence relation

$$(n+1)\mathscr{L}_{n+1}(x) = (2n+1-x)\mathscr{L}_n(x) - n\mathscr{L}_{n-1}(x), \tag{1.9}$$

$$\mathscr{L}_0(x) = 1, \qquad \mathscr{L}_1(x) = 1 - x.$$

Let $\omega(x) = e^{-x}$. Theorem 1 ensures that they are orthogonal with respect to the $L^2_\omega(\mathbb{R}^+)$ inner product:

$$(\mathscr{L}_n(x), \mathscr{L}_m(x))_\omega = \delta_{nm}. \tag{1.10}$$

Therefore, $\{\mathscr{L}_n\}_{n\in\mathbb{N}}$ is an orthonormal basis of $L^2_\omega(\mathbb{R}^+)$, which in turn implies that any function $u \in L^2_\omega(\mathbb{R}^+)$ can be written as

$$u(x) = \sum_{k=0}^{\infty} u_k \mathscr{L}_k(x) \qquad u_k = (u, \mathscr{L}_k)_\omega. \tag{1.11}$$

The derivative of Laguerre polynomials satisfies the relations

$$\partial_x \mathscr{L}_n(x) = -\sum_{k=0}^{n-1} \mathscr{L}_k(x), \tag{1.12}$$

$$\mathscr{L}_n(x) = \partial_x \mathscr{L}_n(x) - \partial_x \mathscr{L}_{n+1}(x), \tag{1.13}$$

$$x\partial_x \mathscr{L}_n(x) = n[\mathscr{L}_n(x) - \mathscr{L}_{n-1}(x)], \tag{1.14}$$

where $\partial_x = \dfrac{d}{dx}$.

We can now introduce two Gaussian quadrature rules for the integration over $[0, +\infty)$. We define the Gauss-Laguerre (GL) nodes $\{x_j\}_{j=0}^N$ as the zeros of $\mathscr{L}_{N+1}(x)$ and the GL weights $\{\omega_j\}_{j=0}^N$ as

$$\omega_j = \frac{x_j}{(N+1)^2[\mathscr{L}_N(x_j)]^2} \qquad 0 \le j \le N. \tag{1.15}$$

We also define the Gauss-Laguerre-Radau (GLR) nodes $\{x_j\}_{j=0}^N$ as $x_0 = 0$ and $\{x_j\}_{j=1}^N$ as the zeros of $\partial_x \mathscr{L}_{N+1}(x)$, while the GLR weights are

$$\omega_j = \frac{1}{(N+1)[\mathscr{L}_N(x_j)]^2}, \qquad 0 \le j \le N. \tag{1.16}$$

Notice that GLR nodes include the left endpoint $x = 0$ while GL nodes do not. We have the following result:

Theorem 3 *Let $\{x_j\}_{j=0}^N$ and $\{\omega_j\}_{j=0}^N$ be the GL or GLR quadrature nodes and weights. Then*

$$\int_0^{+\infty} p(x)e^{-x}dx = \sum_{j=0}^{N} p(x_j)\omega_j \qquad \forall p \in \mathbb{P}_{2N+\delta}(\mathbb{R}^+), \tag{1.17}$$

where $\delta = 1$ for GL and $\delta = 0$ for GLR quadrature.

One can show that $x_N \to +\infty$ as $N \to +\infty$.

1.3 Laguerre functions

Laguerre functions, $\{\hat{\mathscr{L}}_n\}_{n\in\mathbb{N}}$, are defined by

$$\hat{\mathscr{L}}_n(x) = e^{-x/2}\mathscr{L}_n(x) \qquad n \ge 0. \tag{1.18}$$

They satisfy the three-terms relation

$$(n+1)\hat{\mathscr{L}}_{n+1}(x) = (2n+1-x)\hat{\mathscr{L}}_n(x) - n\hat{\mathscr{L}}_{n-1}(x), \tag{1.19}$$

$$\hat{\mathscr{L}}_0(x) = e^{-x/2}, \qquad \hat{\mathscr{L}}_1(x) = (1-x)e^{-x/2} \tag{1.20}$$

and they are orthogonal in $L^2(\mathbb{R}^+)$, that is

$$\int_0^{+\infty} \hat{\mathscr{L}}_n(x)\hat{\mathscr{L}}_m(x)dx = \delta_{mn}. \tag{1.21}$$

Moreover, since

$$\partial_x \hat{\mathscr{L}}_n(x) = -\frac{1}{2}\hat{\mathscr{L}}_n(x) + e^{-x/2}\partial_x \mathscr{L}_n(x), \tag{1.22}$$

we can exploit (1.14) to obtain recurrence relations for the derivative of Laguerre functions:

$$\partial_x \hat{\mathscr{L}}_n(x) = -\sum_{k=0}^{n-1} \hat{\mathscr{L}}_k(x) - \frac{1}{2}\hat{\mathscr{L}}_n(x) \tag{1.23}$$

$$\hat{\mathscr{L}}_n(x) = \partial_x \hat{\mathscr{L}}_n(x) - \partial_x \hat{\mathscr{L}}_{n+1}(x) \tag{1.24}$$

$$x\partial_x \hat{\mathscr{L}}_n(x) = n\left[\hat{\mathscr{L}}_n(x) - \hat{\mathscr{L}}_{n-1}(x)\right] \tag{1.25}$$

We notice that, unlike Laguerre polynomials, Laguerre functions decay at infinity; precisely we have

$$|\hat{\mathscr{L}}_n(x)| \leq 1 \qquad \forall x \in \mathbb{R}^+ \tag{1.26}$$

$$\hat{\mathscr{L}}_n(x) \to 0 \qquad \text{as } x \to +\infty \tag{1.27}$$

Since $\{\hat{\mathscr{L}}_n\}_{n\in\mathbb{N}}$ is an orthonormal basis of $L^2(\mathbb{R}^+)$, we can write any $u \in L^2(\mathbb{R}^+)$ as

$$u = \sum_{k=0}^{\infty} u_k \hat{\mathscr{L}}_k, \tag{1.28}$$

where now

$$u_k = \left(u, \hat{\mathscr{L}}_k\right) = \int_0^{+\infty} u(x)\hat{\mathscr{L}}_k(x)dx. \tag{1.29}$$

Analogously to what we did with Laguerre polynomials, we can now introduce two more quadrature rules on $[0, +\infty)$: in particular we have the following result.

Theorem 4 *Let $\{x_j\}_{j=0}^N$, $\{\omega_j\}_{j=0}^N$ be the nodes and weights of Theorem 3. Set $\hat{\omega}_j = e^{x_j}\omega_j$ for all $0 \le j \le N$. Then*

$$\int_0^{+\infty} p(x)dx = \sum_{j=0}^{N} p(x_j)\hat{\omega}_j \qquad \forall p \in \hat{\mathbb{P}}_{2N+\delta}, \tag{1.30}$$

where $\delta = 1$ for GL and $\delta = 0$ for GLR quadrature.

The weights $\hat{\omega}_j$ are called modified GL and GLR quadrature weights. It can be shown that

$$\hat{\omega}_j = \frac{1}{(N+1)[\hat{\mathscr{L}}_N(x_j)]^2}, \qquad 0 \le j \le N \tag{1.31}$$

and that

$$\hat{\omega}_j \approx \frac{\sqrt{x_j}}{N+1} \tag{1.32}$$

for large N. On the other hand, the GL and GLR nodes are the same as in the polynomial case. The GL nodes can be computed as the eigenvalues of the tridiagonal matrix of Theorem 2 with

$$\alpha_j = 2j+1, \qquad 0 \le j \le N \tag{1.33}$$

$$\beta_j = j^2, \qquad 1 \le j \le N. \tag{1.34}$$

Similarly, by exploiting the relations for the derivatives of Laguerre polynomials (1.14), one can compute the zeros of $\partial_x \mathscr{L}_{N+1}$, and thus the GLR nodes.

1.4 Scaling

The possibility to introduce a scaling on Laguerre polynomials and functions allows to span arbitrarily large portions of the half line $[0, +\infty)$ with a fixed number of GL or GLR nodes. In particular, a scaling parameter β can be

introduced, which can be interpreted as the reciprocal of a typical length scale of interest L, so that

$$\beta = \frac{1}{L}. \tag{1.35}$$

We now present the main results related to the scaling referring to [GW07] and [WGW09].

Scaled Laguerre polynomials

If we choose $\omega_\beta(x) = e^{-\beta x}$ as test function, with $\beta > 0$, we obtain a new family of orthogonal polynomials: defining the n-th scaled Laguerre polynomial as

$$\mathscr{L}_n^\beta(x) = \mathscr{L}_n(\beta x) \tag{1.36}$$

we have that

$$\int_0^{+\infty} \mathscr{L}_n^\beta(x)\mathscr{L}_m^\beta(x)\omega_\beta(x)dx = \frac{1}{\beta}\delta_{nm}, \tag{1.37}$$

that is $\left\{\mathscr{L}_n^\beta\right\}_{n\in\mathbb{N}}$ is a sequence of orthogonal polynomials in $L^2_{\omega_\beta}(\mathbb{R}^+)$. Therefore we can expand any function $u \in L^2_{\omega_\beta}(\mathbb{R}^+)$ in the series of scaled Laguerre polynomials as

$$u = \sum_{k=0}^{\infty} u_k \mathscr{L}_k^\beta, \qquad u_k = \beta\left(u, \mathscr{L}_k^\beta\right)_{\omega_\beta}. \tag{1.38}$$

The three-term relation is given by

$$(n+1)\mathscr{L}_{n+1}^\beta(x) = (2n+1-\beta x)\mathscr{L}_n^\beta(x) - n\mathscr{L}_{n-1}^\beta(x), \tag{1.39}$$

$$\mathscr{L}_0^\beta(x) = 1, \qquad \mathscr{L}_1^\beta(x) = 1-\beta x, \tag{1.40}$$

and the derivatives satisfy the following properties:

$$\partial_x \mathscr{L}_n^\beta(x) = -\beta \sum_{k=0}^{n-1} \mathscr{L}_k^\beta(x) \tag{1.41}$$

$$\mathscr{L}_n^\beta(x) = \frac{1}{\beta}\left(\partial_x \mathscr{L}_n^\beta(x) - \partial_x \mathscr{L}_{n+1}^\beta(x)\right) \tag{1.42}$$

$$x\partial_x \mathscr{L}_n^\beta(x) = n\left[\mathscr{L}_n^\beta(x) - \mathscr{L}_{n-1}^\beta(x)\right] \tag{1.43}$$

We can now define the Scaled Gauss-Laguerre (SGL) nodes $\{x_j^\beta\}_{j=0}^N$ as the zeros of $\mathscr{L}_{N+1}^\beta(x)$ and the SGL weights $\{\omega_j^\beta\}_{j=0}^N$ as

$$\omega_j^\beta = \frac{x_j^\beta}{(N+1)^2[\mathscr{L}_N^\beta(x_j^\beta)]^2} \qquad 0 \le j \le N. \tag{1.44}$$

We also define the Scaled Gauss-Laguerre-Radau (SGLR) nodes $\{x_j^\beta\}_{j=0}^N$ as $x_0^\beta = 0$ and $\{x_j^\beta\}_{j=1}^N$ as the zeros of $\partial_x \mathscr{L}_{N+1}^\beta(x)$, while the GLR weights are

$$\omega_j^\beta = \frac{1}{\beta(N+1)[\mathscr{L}_N^\beta(x_j^\beta)]^2}, \qquad 0 \le j \le N. \tag{1.45}$$

The following theorem defines the SGL and SGLR quadrature rules:

Theorem 5 *Let $\{x_j^\beta\}_{j=0}^N$ and $\{\omega_j^\beta\}_{j=0}^N$ be the SGL or SGLR quadrature nodes and weights. Then*

$$\int_0^{+\infty} p(x)e^{-\beta x}dx = \sum_{j=0}^{N} p(x_j^\beta)\omega_j^\beta \qquad \forall p \in \mathbb{P}_{2N+\delta}(\mathbb{R}^+), \tag{1.46}$$

where $\delta = 1$ for GL and $\delta = 0$ for GLR quadrature.

The scaling of Laguerre polynomials modifies the distribution of the SGL and SGLR nodes with respect to the GL and GLR nodes corresponding to the same value of N. As shown in [ST06], a suitable scaling may increase the accuracy in the approximation of functions by means of Laguerre polynomials. We may also introduce the notion of scaled Laguerre functions.

Scaled Laguerre functions

We define the n-th scaled Laguerre function as

$$\hat{\mathscr{L}}_n^\beta(x) = e^{-\beta x/2}\mathscr{L}_n^\beta(x). \tag{1.47}$$

$\{\hat{\mathscr{L}}_n^\beta(x)\}_{n\in\mathbb{N}}$ is an orthogonal system in $L^2(\mathbb{R}^+)$ since

$$\int_0^{+\infty} \hat{\mathscr{L}}_n^\beta(x)\hat{\mathscr{L}}_m^\beta(x)dx = \frac{1}{\beta}\delta_{nm}, \tag{1.48}$$

therefore we can write any function $u \in L^2(\mathbb{R}^+)$ as

$$u = \sum_{k=0}^{\infty} u_k\hat{\mathscr{L}}_k^\beta(x), \qquad u_k = \beta\int_0^{+\infty} u(x)\hat{\mathscr{L}}_k^\beta(x)dx. \tag{1.49}$$

The three-term relation is

$$(n+1)\hat{\mathscr{L}}_{n+1}^\beta(x) = (2n+1-\beta x)\hat{\mathscr{L}}_n^\beta(x) - n\hat{\mathscr{L}}_{n-1}^\beta(x), \tag{1.50}$$

$$\hat{\mathscr{L}}_0^\beta(x) = e^{-\beta x/2} \qquad \hat{\mathscr{L}}_1^\beta(x) = (1-\beta x)e^{-\beta x/2} \tag{1.51}$$

while the recurrence formulas for the derivatives are

$$\partial_x\hat{\mathscr{L}}_n^\beta(x) + \frac{1}{2}\beta\hat{\mathscr{L}}_n^\beta(x) = -\beta\sum_{k=0}^{n-1}\hat{\mathscr{L}}_k^\beta(x) \tag{1.52}$$

$$\frac{1}{2}\beta\left[\hat{\mathscr{L}}_n^\beta(x) + \hat{\mathscr{L}}_{n+1}^\beta(x)\right] = \partial_x\hat{\mathscr{L}}_n^\beta(x) - \partial_x\hat{\mathscr{L}}_{n+1}^\beta(x) \tag{1.53}$$

$$x\partial_x\hat{\mathscr{L}}_n^\beta(x) = \frac{1}{2}\left[(n+1)\hat{\mathscr{L}}_{n+1}^\beta(x) - \hat{\mathscr{L}}_n^\beta(x) - n\hat{\mathscr{L}}_{n-1}^\beta(x)\right]. \tag{1.54}$$

If we define the modified weights as

$$\hat{\omega}_j^\beta = e^{\beta x_j^\beta}\omega_j^\beta, \tag{1.55}$$

we have the following theorem.

Theorem 6

$$\int_0^{+\infty} p(x)dx = \sum_{j=0}^{N} p(x_j^\beta)\hat{\omega}_j^\beta \qquad \forall p \in \hat{\mathbb{P}}_{2N+\delta} \tag{1.56}$$

where $\delta = 1$ for SGL and $\delta = 0$ for SGLR quadrature rules.

Being the zeros of $\hat{\mathscr{L}}_{N+1}^{\beta}(x)$, SGL nodes can be computed according to Theorem 2 by choosing

$$\alpha_j = \frac{2j+1}{\beta} \qquad 0 \leq j \leq N \tag{1.57}$$

$$\beta_j = \frac{j^2}{\beta^2} \tag{1.58}$$

Chapter 2

Derivation of the model problems

In this chapter we derive the expression of the model problems which will be later employed for numerical tests. We first consider the 1D advection-diffusion equation;

$$\frac{\partial q}{\partial t} - \mu \frac{\partial^2 q}{\partial z^2} + u \frac{\partial q}{\partial z} = f(z,t) \qquad z \in [0, +\infty) \quad t \in [0, T]. \tag{2.1}$$

For the sake of generality, we derive the governing equation in the general case of $\mathbb{R}^n$ and non-constant coefficients, considering also the effects of drift and reaction. We then present some results about existence, uniqueness and regularity of weak solutions of the boundary value problem associated with (2.1). The reference text is [Sal15], which discusses the problem in bounded domain; the results can be extended to the unbounded case, see for example [Pao98].

In the second part of the chapter we briefly present the homogeneous viscous Burgers' equation

$$\frac{\partial q}{\partial t} - \mu \frac{\partial^2 q}{\partial z^2} + q \frac{\partial q}{\partial z} = 0 \qquad z \in [0, +\infty) \quad t \in [0, T] \tag{2.2}$$

and its properties. In spite of the apparent similarity with (2.1), in (2.2) the advection velocity is given by the solution itself; this introduces a nonlinearity and may cause nonuniqueness of solutions. More details about existence and uniqueness can be found in [Dlo82], while [LeV92] and [LeV16] discuss the numerical approach.

2.1 Advection-diffusion equation

Equation (2.1) describes the temporal evolution of a quantity $q = q(z,t)$ which is free to diffuse in a one dimensional domain according to the coefficient μ, while being transported at velocity u. The right-hand side f is a known external source or sink acting on the system. The typical example is q being the concentration of a pollutant in a liquid with diffusivity μ and velocity u, flowing through a shallow and narrow channel; in this case f describes the quantity of pollutant which is introduced or removed from the channel at any point and time instant.

Derivation

For any point $\mathbf{x} \in \mathbb{R}^n$, if we regard the scalar quantity $q = q(\mathbf{x},t)$ as a concentration, the integral

$$\int_V q(\mathbf{x},t)d\mathbf{x} \tag{2.3}$$

is equal to the mass in the generic control volume V at time t. Mass conservation entails that the rate of growth of the mass inside any such volume is equal to the net flux into the volume plus the quantity of mass introduced from the outside. In other words,

$$\frac{d}{dt}\int_V q(\mathbf{x},t)d\mathbf{x} = -\int_{\partial V} \mathbf{j}\cdot\mathbf{n}\,d\sigma + \int_V f(\mathbf{x},t)d\mathbf{x}, \tag{2.4}$$

where ∂V denotes the boundary of V, $\mathbf{j}$ the flux through it, $\mathbf{n}$ the outward unit normal vector and $d\sigma$ the infinitesimal element of surface on ∂V. Taking the derivative inside the integral, the left-hand side becomes

$$\frac{d}{dt}\int_V q(\mathbf{x},t)d\mathbf{x} = \int_V \frac{\partial q}{\partial t}(\mathbf{x},t)d\mathbf{x}. \tag{2.5}$$

Moreover we use the divergence theorem to write

$$\int_{\partial V} \mathbf{j}\cdot\mathbf{n}\, d\sigma = \int_V \mathrm{div}\mathbf{j}\, d\mathbf{x}. \tag{2.6}$$

so that the mass conservation condition reads

$$\int_V \frac{\partial q}{\partial t}(\mathbf{x},t)d\mathbf{x} = -\int_V \mathrm{div}\mathbf{j}\, d\mathbf{x} + \int_V f(\mathbf{x},t)d\mathbf{x}. \tag{2.7}$$

Thus, assuming that both the solution and the function f are sufficiently regular, we obtain

$$\frac{\partial q}{\partial t}(\mathbf{x},t) = -\mathrm{div}\mathbf{j}(\mathbf{x},t) + f(\mathbf{x},t). \tag{2.8}$$

We are only left to define the flux $\mathbf{j}$.

The effect of transport is a translation of the quantity q without deformation, thus

$$\mathbf{j}_{adv}(\mathbf{x},t) = \mathbf{u}(\mathbf{x},t)q(\mathbf{x},t), \tag{2.9}$$

where $\mathbf{u}$ is the velocity of the flow; in the general case it is a function of both $\mathbf{x}$ and t. On the other hand, diffusion is the expansion of the pollutant from high concentration to low concentration regions; this is described by Fick's law, according to which the mass flux is proportional to the gradient of the concentration, with opposite sign. We may allow a different behaviour along each direction: defining the diffusivity μ_j as the proportionality coefficient along $\mathbf{e}_j$, this means that

$$\mathbf{j}_{diff}(\mathbf{x},t) = -\mathbf{A}(\mathbf{x},t)\nabla q(\mathbf{x},t), \tag{2.10}$$

where $\mathbf{A} \in \mathbb{R}^{n\times n}$, $a_{ij} = \mu_j \delta_{ij}$. Again, we allow the diffusivity to be a function of both time and space, so that $\mu_j = \mu_j(\mathbf{x}, t)$. Since our model takes into account both advection and diffusion, the total flux $\mathbf{j}$ will be given by a superposition of the two contributions, assumed to be independent:

$$\mathbf{j}(\mathbf{x}, t) = \mathbf{u}(\mathbf{x}, t)q(\mathbf{x}, t) - \mathbf{A}(\mathbf{x}, t)\nabla q(\mathbf{x}, t). \tag{2.11}$$

Substituting (2.11) into (2.8) and rearranging we find

$$\frac{\partial q}{\partial t} - \mathrm{div}(\mathbf{A}\nabla q + \mathbf{u}q) = f \tag{2.12}$$

To represent the most general possible situation, we add a drift contribution, $\mathbf{c} \cdot \nabla q$, and a reaction term rq, which models the decay of q. The final PDE is then

$$\frac{\partial q}{\partial t} - \mathrm{div}(\mathbf{A}\nabla q + \mathbf{u}q) + \mathbf{c} \cdot \nabla q + rq = f \qquad \mathbf{x} \in \mathbb{R}^n \quad t > 0. \tag{2.13}$$

We notice that, if $n = 1$, the coefficients are constant and $\mathbf{c} = \mathbf{0}$, $r = 0$, (2.13) reduces to (2.1).

Existence and uniqueness

We define the linear differential operator

$$\mathcal{L}q = -\mathrm{div}(\mathbf{A}\nabla q + \mathbf{u}q) + \mathbf{c} \cdot \nabla q + rq \tag{2.14}$$

and the space-time cylinder $Q_T = \Omega \times (0, T)$, where $\Omega \subset \mathbb{R}^n$ is the spatial domain of interest, and its boundary $S_T = \partial\Omega \times [0, T]$. We will also assume that

1. $\mathcal{L}$ is uniformly elliptic, i.e. $\exists\, \alpha$,M > 0 such that

$$\sum_{i,j=1}^{n} a_{ij}(\mathbf{x}, t)\xi_i\xi_j \geq \alpha|\xi|^2 \qquad |a_{ij}(\mathbf{x}, t)| \leq M, \quad \forall \xi \in \mathbb{R}^n, \text{ a.e. in } Q_T \tag{2.15}$$

2. Coefficients $\mathbf{u}$, $\mathbf{c}$ and r are bounded:

$$|u_j(\mathbf{x},t)| \le u_\infty, \quad |c_j(\mathbf{x},t)| \le c_\infty, \quad |r(\mathbf{x},t)| \le r_\infty, \qquad \text{a.e. in } Q_T \tag{2.16}$$

We will consider boundary value problems of the type

$$\begin{cases} \dfrac{\partial q}{\partial t} + \mathcal{L}q = f & \text{in } Q_T \\ q(\mathbf{x},0) = g(\mathbf{x}) & \text{in } \Omega \\ \mathcal{B}q = 0 & \text{on } S_T \end{cases} \tag{2.17}$$

where g is the initial datum and $\mathcal{B}q$ defines the boundary conditions on S_T. If Ω is unbounded, a suitable condition at infinity (typically the vanishing of the solution) is required.

Following the discussion in [Sal15], to which we refer for a complete discussion of the existence and uniqueness problem, we introduce the Hilbert triplet (V, H, V^*), where $H = L^2(\Omega)$ and $V = H_0^1(\Omega)$ (homogeneous Dirichlet boundary conditions) or $V = H^1(\Omega)$ (Neumann or Robin boundary conditions). We assume that

$$g \in H \qquad f \in L^2(0,T;V^*) \tag{2.18}$$

that is, f is an L^2 function of time such that $f(t) \in V^*$ for all $t \in (0,T)$. We look for a solution $q \in L^2(0,T;V)$ such that $\dfrac{\partial q}{\partial t} \in L^2(0,T;V^*)$. In this case, Sobolev embeddings guarantee that $q \in C([0,T];H)$.

The weak formulation of Problem (2.17) reads as follows. Given $f \in L^2(0,T;V^*)$ and $g \in H$, we look for $q \in L^2(0,T;V)$ such that $\dfrac{\partial q}{\partial t} \in L^2(0,T;V^*)$ and

$$\left\langle \frac{dq}{dt}(t), \phi \right\rangle_* + a\,(q(t),\, \phi\,;\, t) = \langle f(t),\, \phi \rangle_* \qquad \forall\, \phi \in V \tag{2.19}$$

$$q(0) = g$$

where $\langle \, . \, , . \, \rangle_*$ denotes the duality between V and V^*.

The following result holds (see [Sal15] for the proof)

Theorem 7 *Under the hypotheses* (2.15), (2.16) *and* (2.18), *problem* (2.19) *has a unique solution. Moreover*

$$\max_{t\in[0,T]} \|q(t)\|_{L^2}^2 + \alpha \int_0^T \|q(t)\|_V^2 dt \leq C \left\{ \int_0^T \|f(t)\|_*^2 dt + \|g\|_{L^2}^2 \right\} \tag{2.20}$$

$$\int_0^T \|q(t)\|_*^2 dt \leq C \left\{ \int_0^T \|f(t)\|_*^2 dt + \|g\|_{L^2}^2 \right\} \tag{2.21}$$

The inequalities provide stability estimates on the solution, whose norm is bounded, in some sense, by the norm of the data f and g.

If more regularity is attained by the coefficients, then we can gain some regularity on the solution, according to the following Theorem.

Theorem 8 *If* Ω *is a* C^2 *domain,* $\mathbf{A}$ *is symmetric and* a_{ij}, u_j, c_j, r *are smooth and independent on* t, *then the weak solution* q *belongs to* $L^2(0,T;H^2(\Omega)) \cap L^\infty(0,T;V)$ *and* $\dfrac{dq}{dt} \in L^2(0,T;H)$. *Moreover, if the coefficients are in* C^∞ *then the solution is in* $C^\infty(Q_T)$ *too.*

The case of a 1D semi-infinite domain

We apply the previous result of the particular case of interest, that is equation (2.1) complemented with a Dirichlet boundary condition at the left endpoint, a vanishing condition at infinity and an initial datum, where we take $\Omega = [0, +\infty) = \mathbb{R}^+$. The resulting strong formulation is

$$\begin{cases} \dfrac{\partial q}{\partial t} - \mu \dfrac{\partial^2 q}{\partial z^2} + u \dfrac{\partial q}{\partial z} = f(z,t) \qquad z \in [0,+\infty), \quad t \in [0,T] \\ \\ q(0,t) = q_L(t), \qquad \lim_{z\to+\infty} q(z,t) = 0 \\ \\ q(z,0) = q^0(z) \end{cases} \tag{2.22}$$

The diffusivity matrix $\mathbf{A}$ is replaced by the scalar constant μ; thus, ellipticity condition (2.15) amounts to requiring $\mu > 0$. Moreover, since the coefficients are real numbers, (2.16) is automatically satisfied; in particular the velocity u may be either positive (resp. negative), and the Dirichlet datum at the left endpoint $z = 0$ will be an inflow (resp. outflow) boundary condition.

The spatial domain is $\Omega = \mathbb{R}^+$; the Hilbert triplet will then be chosen to be

$$V = H^1(\mathbb{R}^+) \qquad H = L^2(\mathbb{R}^+) \qquad V^* = \left(H^1(\mathbb{R}^+)\right)^*. \tag{2.23}$$

The source term and initial condition are

$$f \in L^2(0,T;\left(H^1(\mathbb{R}^+)\right)^*) \qquad q^0 \in L^2(\mathbb{R}^+). \tag{2.24}$$

A straightforward consequence of the existence, uniqueness and regularity results in $\mathbb{R}^n$ is that

Corollary 8.1 *Let $\mu > 0$, $f \in L^2(0,T;(H^1(\mathbb{R}^+))^*)$ and $q^0 \in L^2(\mathbb{R}^+)$. Then problem (2.22) has a unique weak solution $q \in C^\infty(Q_T)$.*

The solution is smooth in the open half-line $(0, +\infty)$ for all $t \in [0, T]$. Regularity up to the boundary at $z = 0$ requires compatibility conditions between the initial datum q^0 and the Dirichlet value q_L; we will not go into the details.

2.2 Burgers' equation

Burgers' equation is one of the simplest examples of non-linear parabolic PDE. It appears in gas dynamics, in the theory of sound waves and traffic flow models and it is a prototype for conservation laws that can develop discontinuities in the form of shock waves.

Derivation. Conservative and advective forms

The equation was first derived by Burgers (1948) as an attempt to simplify the Navier-Stokes equation by neglecting the pressure term. The dynamics of a Newtonian incompressible fluid of kinematic viscosity ν, velocity $\mathbf{u} = \mathbf{u}(\mathbf{x}, t)$ and pressure $p = p(\mathbf{x}, t)$ with no external forces is determined by

$$\frac{\partial \mathbf{u}}{\partial t}(\mathbf{x}, t) + \mathbf{u}(\mathbf{x}, t) \cdot \nabla \mathbf{u}(\mathbf{x}, t) = -\nabla p(\mathbf{x}, t) + \nu \Delta \mathbf{u}(\mathbf{x}, t) \tag{2.25}$$

$$\nabla \cdot \mathbf{u}(\mathbf{x}, t) = 0 \tag{2.26}$$

If we drop the pressure term and we consider the one dimensional case, the first equation becomes, denoting the solution as q according to our notations,

$$\frac{\partial q}{\partial t}(z, t) + q(z, t) \frac{\partial q}{\partial z}(z, t) = \mu \frac{\partial^2 q}{\partial z^2}(z, t). \tag{2.27}$$

Notice that the equation resembles the advection-diffusion problem (2.1), but the advective velocity is now given by the solution q itself; this introduces a non-linearity and may generate shocks. (2.27) is called *viscous Burgers' equation*. It exhibits a competition between dissipation due to diffusion and steepening of the solution because of the non-linear transport. The inviscid counterpart

$$\frac{\partial q}{\partial t}(z, t) + q(z, t) \frac{\partial q}{\partial z}(z, t) = 0 \tag{2.28}$$

can be seen as the limit of (2.27) as $\mu \to 0$.

Equation (2.28) is the advective form of the inviscid Burgers' equation. We can write it as

$$\frac{\partial q}{\partial t}(z, t) + \frac{\partial}{\partial z}\left(\frac{q^2}{2}\right)(z, t) = \frac{\partial q}{\partial t}(z, t) + \frac{\partial f(q)}{\partial z}(z, t) = 0. \tag{2.29}$$

The latter expresses a conservation law, where $f(q) = q^2/2$ is the flux of q. Indeed, on each interval (a, b) it satisfies

$$\frac{d}{dt} \int_a^b q(z, t) dz = f(q(a, t)) - f(q(b, t)) \tag{2.30}$$

so that the variation of f at the endpoints equals the rate of variation of q in $[a, b]$. For this reason, (2.29) is the conservative form of the Burgers' equation; it is particularly useful for numerical integration, as we will see later.

Shock formation and vanishing viscosity approach

It is well known (see for example [Sal15]) that (2.28) exhibits a shock at time T_b when the characteristics first cross; beyond this point there is no classical solution. This happens when the solution $q(z, t)$ attains an infinite slope, so that, for $t > T_b$, it is multivalued for some z; we say that the wave breaks, and this is not admissible in many physical situations.

On the other hand, this is not the case for the viscous version (2.27). Indeed, we can see (2.28), which is a hyperbolic PDE, as the limit of (2.27), a parabolic equation, as the parameter μ tends to zero; therefore we may determine the correct physical behaviour by means of the so-called vanishing viscosity approach.

If μ is very small, the solutions of (2.27) and (2.28) look almost the same before the wave begins to break. As the slope $\dfrac{\partial q}{\partial z}$ starts to grow, though, the viscous term $\mu \dfrac{\partial^2 q}{\partial z^2}$ increases much faster and it becomes relevant. The presence of this term prevents the formation of shocks and keeps the solution smooth and single-valued for $t > T_b$. If $\mu > 0$, the discontinuity of the "inviscid" solution is replaced by a steep continuous function, whose slope gets sharper as $\mu \to 0$.

This justifies the importance of (2.27) in the framework of numerical approximation and its use as a model problem for the coupled approach.

Chapter 3

Stability analysis of spatial discretizations for the advection-diffusion equation

In this chapter we focus on the numerical solution of the advection-diffusion equation with constant coefficients on $\mathbb{R}^+ = [0, +\infty)$. The homogeneous model problem can be written either as second order partial differential equation

$$\frac{\partial q}{\partial t} - \mu \frac{\partial^2 q}{\partial z^2} + u \frac{\partial q}{\partial z} = 0 \tag{3.1}$$

or as system of first order equations

$$\begin{aligned} &\frac{\partial q}{\partial t} - \mu \frac{\partial v}{\partial z} + uv = 0 \\ &\frac{\partial q}{\partial z} - v = 0. \end{aligned} \tag{3.2}$$

We assume that solutions vanish at infinity

$$\lim_{z \to +\infty} q(z, t) = 0 \tag{3.3}$$

and that either Dirichlet boundary conditions

$$q(0,t) = q_L \tag{3.4}$$

or Neumann boundary conditions

$$\frac{\partial q}{\partial z}(0,t) = Dq_L \tag{3.5}$$

are applied at $z = 0$. Either of the two previous formulations can be employed, but we focus on (3.2) since it allows to deal with both kinds of boundary conditions in a simple way. We require that $\mu > 0$ (ellipticity condition) and $u > 0$. In this case, the Dirichlet datum at $z = 0$ corresponds to an inflow boundary condition, which guarantees well-posedness for the hyperbolic part; we will discuss the case of an outflow boundary condition, $u < 0$, in Appendix A. We analyze several possible space discretizations, in order to determine which one shows the best stability properties and can therefore be chosen to perform a coupling with a DG scheme in finite domains. We follow the procedure outlined in [BB19] for the pure advection problem: we discretize the PDE system (3.2) in space to obtain a system of ordinary differential equations of the form

$$\frac{d\mathbf{q}}{dt} = \mathbf{A}\mathbf{q} + \mathbf{g}, \tag{3.6}$$

where $\mathbf{q}$ is the unknown vector of the expansion of the solution and $\mathbf{g}$ contains the contribution of boundary conditions at $z = 0$, and we study the eigenvalue structure of the matrix $\mathbf{A}$. The corresponding discretization scheme is stable if all the eigenvalues have non-positive real part.

We analyse the following discretizations:

- *Weak form.* We multiply (3.1) or (3.2) by a test function, integrate by parts and use GLR or GL quadrature rules (as in Theorems 3 and 4) for numerical integration. We consider two different approaches:

– Modal discretization. The entries of the unknown vector $\mathbf{q}$ are the coefficients of the expansion of the solution in the Laguerre functions or polynomials orthogonal basis.

– Nodal discretization. The basis functions are Lagrange basis functions associated to the integration nodes, so that the unknown vector contains the nodal values of the approximate solution.

Furthermore, the numerical solution can be expanded in a basis of either scaled Laguerre functions or scaled Laguerre polynomials.

- *Strong form.* In this case we directly discretize the strong formulations (3.1) and (3.2) by adopting a collocation approach using GLR quadrature rules. This is the only practical choice if Dirichlet boundary conditions have to be imposed, because GLR nodes, in contrast with GL, include the left endpoint of the semi-infinite domain.

The weak forms corresponding to the formulations (3.1), (3.2) are, respectively,

$$\frac{d}{dt}\int_0^{+\infty}\varphi(z)q(z,t)\omega(z)\,dz-\mu\int_0^{+\infty}\varphi(z)\frac{\partial^2 q}{\partial z^2}(z,t)\omega(z)\,dz+ \\ +u\int_0^{+\infty}\varphi(z)\frac{\partial q}{\partial z}(z,t)\omega(z)\,dz=0 \qquad \forall\varphi \quad (3.7)$$

and

$$\frac{d}{dt}\int_0^{+\infty}\varphi(z)q(z,t)\omega(z)\,dz-\mu\int_0^{+\infty}\varphi(z)\frac{\partial v}{\partial z}(z,t)\omega(z)\,dz+ \\ +u\int_0^{+\infty}\varphi(z)v(z,t)\omega(z)\,dz=0 \qquad \forall\varphi \\ \int_0^{+\infty}\frac{\partial q}{\partial z}\varphi(z)\omega(z)\,dz-\int_0^{+\infty}v(z,t)\varphi(z)\omega(z)\,dz=0 \qquad \forall\varphi, \quad (3.8)$$

where φ denotes a test function to be chosen among a suitable test space, depending on the chosen basis, and $\omega(z)$ a non negative weight on $\mathbb{R}^+$.

3.1 Analysis of the inflow case

3.1.1 Modal discretization, Laguerre functions

We now follow the procedure outlined in [BB19] and the notation used in the same paper and in [BB13]. We focus first on the case of Neumann boundary conditions and on a discretization based on Laguerre functions, for which $\omega = 1$. For formulation (3.1), we integrate by parts and use boundary conditions to obtain

$$\frac{d}{dt}\int_0^{+\infty} \varphi(z)q(z,t)\,dz + \mu\varphi(0)Dq_L + \mu\int_0^{+\infty} \varphi'(z)\frac{\partial q}{\partial z}(z,t)\,dz + \\ + u\int_0^{+\infty} \varphi(z)\frac{\partial q}{\partial z}(z,t)\,dz = 0, \quad (3.9)$$

while for formulation (3.2), we integrate by parts only the first equation and obtain

$$\begin{aligned} &\frac{d}{dt}\int_0^{+\infty} \varphi(z)q(z,t)\,dz + \mu\varphi(0)Dq_L + \mu\int_0^{+\infty} \varphi'(z)v(z)\,dz + \\ &+u\int_0^{+\infty} \varphi(z)v(z,t)\,dz = 0 \\ &\int_0^{+\infty} \frac{\partial q}{\partial z}(z,t)\varphi(z)\,dz - \int_0^{+\infty} v(z,t)\varphi(z)\,dz = 0. \end{aligned} \quad (3.10)$$

Representing the solution as

$$q(z,t) \approx \sum_{j=0}^{M} q_j(t)\hat{\mathscr{L}}_j^{\beta}(z), \quad (3.11)$$

and taking $\varphi(z) = \hat{\mathscr{L}}_i^\beta(z)$ for $i = 0, \ldots, M$ as test functions in the previous formulae, one gets the discretization

$$\sum_{j=0}^{M} \frac{dq_j}{dt} \left(\hat{\mathscr{L}}_i^\beta, \hat{\mathscr{L}}_j^\beta \right) = -\mu \sum_{j=0}^{M} q_j(t) \left((\hat{\mathscr{L}}_i^\beta)', (\hat{\mathscr{L}}_j^\beta)' \right) - \mu \hat{\mathscr{L}}_i^\beta(0) D q_L + \\ - u \sum_{j=0}^{M} q_j(t) \left(\hat{\mathscr{L}}_i^\beta, (\hat{\mathscr{L}}_j^\beta)' \right) \tag{3.12}$$

for the formulation (3.1) and

$$\sum_{j=0}^{M} \frac{dq_j}{dt} \left(\hat{\mathscr{L}}_i^\beta, \hat{\mathscr{L}}_j^\beta \right) = -\mu \sum_{j=0}^{M} v_j(t) \left((\hat{\mathscr{L}}_i^\beta)', \hat{\mathscr{L}}_j^\beta \right) - \mu \hat{\mathscr{L}}_i^\beta(0) D q_L + \\ -u \sum_{j=0}^{M} v_j(t) \left(\hat{\mathscr{L}}_i^\beta, \hat{\mathscr{L}}_j^\beta \right) \\ \sum_{j=0}^{M} q_j(t) \left((\hat{\mathscr{L}}_j^\beta)', \hat{\mathscr{L}}_i^\beta \right) = \sum_{j=0}^{M} v_j(t) \left(\hat{\mathscr{L}}_i^\beta, \hat{\mathscr{L}}_j^\beta \right) \tag{3.13}$$

for formulation (3.2), where we have used for simplicity the notations

$$(u, v) = \int_0^{+\infty} u(z) v(z) dz.$$

and

$$(\hat{\mathscr{L}}_i^\beta)' = \frac{d}{dz} \hat{\mathscr{L}}_i^\beta \tag{3.14}$$

Exploiting now the properties

$$\left(\hat{\mathscr{L}}_i^\beta, \hat{\mathscr{L}}_j^\beta \right) = \frac{1}{\beta} \delta_{ij} \tag{3.15}$$

$$(\hat{\mathscr{L}}_i^\beta)'(z) = -\frac{\beta}{2} \hat{\mathscr{L}}_i^\beta(z) - \beta \sum_{k=0}^{i-1} \hat{\mathscr{L}}_k^\beta(z) \tag{3.16}$$

of Laguerre functions, one can notice that

$$\left((\hat{\mathscr{L}}_i^\beta)', (\hat{\mathscr{L}}_j^\beta)' \right) = -\frac{\beta}{2} \left((\hat{\mathscr{L}}_i^\beta)', \hat{\mathscr{L}}_j^\beta \right) - \beta \sum_{k=0}^{j-1} \left((\hat{\mathscr{L}}_i^\beta)', \hat{\mathscr{L}}_k^\beta \right). \tag{3.17}$$

We then recall that, as shown in [BB19], the terms $\left((\hat{\mathscr{L}}_i^\beta)', \hat{\mathscr{L}}_j^\beta\right)$ can be rewritten as

$$\begin{aligned}\left((\hat{\mathscr{L}}_i^\beta)', \hat{\mathscr{L}}_j^\beta\right) &= -\frac{\beta}{2}\left(\hat{\mathscr{L}}_i^\beta, \hat{\mathscr{L}}_j^\beta\right) - \beta\sum_{k=0}^{i-1}\left(\hat{\mathscr{L}}_k^\beta, \hat{\mathscr{L}}_j^\beta\right) \\ &= -\frac{\delta_{ij}}{2} - \sum_{k=0}^{i-1}\delta_{kj}, \end{aligned} \tag{3.18}$$

which yields $-1/2$ if $i = j$, -1 if $j < i$ and zero otherwise. Therefore, the terms $\left((\hat{\mathscr{L}}_i^\beta)', \hat{\mathscr{L}}_j^\beta\right)$ define a $(M+1)\times(M+1)$ lower triangular matrix that corresponds to the matrix denoted by $-\mathbf{L}$ in [BB19]. Therefore, denoting the entries of $\mathbf{L}$ by l_{ij}, we have that

$$l_{ij} = \begin{cases} 1/2 & i = j \\ 1 & j < i \\ 0 & j > i \end{cases} \tag{3.19}$$

and equation (3.17) yields

$$\left((\hat{\mathscr{L}}_i^\beta)', (\hat{\mathscr{L}}_j^\beta)'\right) = \frac{\beta}{2}l_{ij} + \beta\sum_{k=0}^{j-1} l_{ik} = \beta\sum_{k=0}^{j} l_{ik}\alpha_{kj},$$

where α_{kj} is equal to $1/2$ for $k = j$, 1 for $k < j$ and 0 otherwise. Therefore, the entries are those of the matrix $\mathbf{L}^T$, so that the matrix of components $\left((\hat{\mathscr{L}}_i^\beta)', (\hat{\mathscr{L}}_j^\beta)'\right)$ is indeed $\beta\mathbf{L}\mathbf{L}^T$. It follows then that, using the property $\hat{\mathscr{L}}_i^\beta(0) = 1$ and introducing the vector $\mathbf{q} = [q_0, \ldots, q_M]^T$ of the modal degrees of freedom, equation (3.12) can be rewritten in vector form as

$$\frac{d\mathbf{q}}{dt} = \mathbf{A}_{mod,Neu,Lf}\mathbf{q} + \mathbf{g}_{mod,Neu,Lf}, \tag{3.20}$$

where $\mathbf{A}_{mod,Neu,Lf} = -\mu\beta^2\mathbf{L}\mathbf{L}^T + u\beta\mathbf{L}^T$ and $\mathbf{g}_{mod,Neu,Lf} = -\mu\beta D q_L \mathbf{e}$, with $\mathbf{e} = [1, \ldots, 1]^T \in \mathbf{R}^{M+1}$. Equations (3.13) yield instead

$$\frac{d\mathbf{q}}{dt} = \mu\beta\mathbf{L}\mathbf{v} - u\mathbf{v} + \mathbf{g}$$
$$\mathbf{v} = -\beta\mathbf{L}^T\mathbf{q}, \tag{3.21}$$

from which equation (3.20) follows again.

In the case of Dirichlet boundary conditions, it is convenient to start from formulation (3.8) and integrate by parts in the second equation only, so as to obtain

$$\frac{d}{dt}\int_0^{+\infty} \varphi(z)q(z,t)\,dz - \mu\int_0^{+\infty} \varphi(z)\frac{\partial v}{\partial z}(z,t)\,dz +$$
$$+u\int_0^{+\infty} \varphi(z)v(z,t)\,dz = 0$$
$$-q_L\varphi(0) - \int_0^{+\infty} q(z)\varphi'(z)dz - \int_0^{+\infty} v(z,t)\varphi(z)dz = 0. \tag{3.22}$$

Following the previous steps, this gives

$$\sum_{j=0}^{M} \frac{dq_j}{dt}\left(\hat{\mathscr{L}}_i^\beta, \hat{\mathscr{L}}_j^\beta\right) = \mu\sum_{j=0}^{M} v_j(t)\left((\hat{\mathscr{L}}_j^\beta)', \hat{\mathscr{L}}_i^\beta\right) - u\sum_{j=0}^{M} v_j(t)\left(\hat{\mathscr{L}}_i^\beta, \hat{\mathscr{L}}_j^\beta\right)$$
$$\sum_{j=0}^{M} v_j(t)\left(\hat{\mathscr{L}}_i^\beta, \hat{\mathscr{L}}_j^\beta\right) = -q_L - \sum_{j=0}^{M} q_j(t)\left(\hat{\mathscr{L}}_j^\beta, (\hat{\mathscr{L}}_i^\beta)'\right), \tag{3.23}$$

which in vector notation yields

$$\frac{d\mathbf{q}}{dt} = -\mu\beta\mathbf{L}^T\mathbf{v} - u\mathbf{v}$$
$$\mathbf{v} = \beta\mathbf{L}\mathbf{q} + \mathbf{h}_{mod,Dir,Lf}, \tag{3.24}$$

where $\mathbf{h}_{mod,Dir,Lf} = -q_L\beta\mathbf{e}$. As a consequence, one obtains

$$\frac{d\mathbf{q}}{dt} = \mathbf{A}_{mod,Dir,Lf}\mathbf{q} + \mathbf{g}_{mod,Dir,Lf}, \tag{3.25}$$

where now $\mathbf{A}_{mod,Dir,Lf} = -\mu\beta^2\mathbf{L}^T\mathbf{L} - u\beta\mathbf{L}$ and

$$\mathbf{g}_{mod,Dir,Lf} = -\mu\beta\mathbf{L}^T\mathbf{h}_{mod,Dir,Lf} - u\mathbf{h}_{mod,Dir,Lf} = \mu\beta^2 q_L\mathbf{L}^T\mathbf{e} + uq_L\beta\mathbf{e}.$$

3.1.2 Modal discretization, Laguerre polynomials

We now examine the discretization based on Laguerre polynomials, starting from the case where a Neumann condition is imposed. In this case we employ the weight $\omega(z) = e^{-\beta z}$. For formulation (3.1), integration by parts leads to

$$\frac{d}{dt}\int_0^{+\infty} \varphi(z)q(z,t)\omega(z)\,dz + \mu\varphi(0)Dq_L + \\ + \mu\int_0^{+\infty}(\varphi'(z) - \beta\varphi(z))\frac{\partial q}{\partial z}\omega(z)\,dz + u\int_0^{+\infty}\frac{\partial q}{\partial z}\varphi(z)\omega(z)\,dz = 0, \quad (3.26)$$

while for formulation (3.2), we integrate by parts only the first equation and obtain

$$\frac{d}{dt}\int_0^{+\infty} \varphi(z)q(z,t)\omega(z)\,dz + \mu\varphi(0)Dq_L + \\ +\mu\int_0^{+\infty}(\varphi'(z) - \beta\varphi(z))v(z,t)\omega(z)\,dz + u\int_0^{+\infty} v(z,t)\varphi(z)\omega(z)\,dz = 0 \\ \int_0^{+\infty}\frac{\partial q}{\partial z}\varphi(z)\omega(z)\,dz - \int_0^{+\infty} v(z,t)\varphi(z)\omega(z)\,dz = 0. \quad (3.27)$$

where we used the fact that $\omega(0) = 1$ and $\omega' = -\beta\omega$.

We now represent the solution as

$$q(z,t) \approx \sum_{j=0}^{M} q_j(t)\mathscr{L}_j^\beta(z), \quad (3.28)$$

and take $\varphi(z) = \mathscr{L}_i^\beta(z)$ for $i = 0, \ldots, M$ as test functions. In this way we obtain

$$\sum_{j=0}^{M}\frac{dq_j}{dt}\left(\mathscr{L}_j^\beta, \mathscr{L}_i^\beta\right)_{\omega_\beta} + \mu\mathscr{L}_i^\beta(0)Dq_L + \\ + \mu\sum_{j=0}^{M} q_j\left((\mathscr{L}_j^\beta)', (\mathscr{L}_i^\beta)' - \beta\mathscr{L}_i^\beta\right)_{\omega_\beta} + u\sum_{j=0}^{M} q_j\left((\mathscr{L}_j^\beta)', \mathscr{L}_i^\beta\right)_{\omega_\beta} = 0 \quad (3.29)$$

for formulation (3.1), and

$$\sum_{j=0}^{M} \frac{dq_j}{dt} \left(\mathscr{L}_j^\beta, \mathscr{L}_i^\beta \right)_{\omega_\beta} + \mu \mathscr{L}_i^\beta(0) D q_L +$$
$$+\mu \sum_{j=0}^{M} v_j \left(\mathscr{L}_j^\beta, (\mathscr{L}_i^\beta)' - \beta \mathscr{L}_i^\beta \right)_{\omega_\beta} + u \sum_{j=0}^{M} v_j \left(\mathscr{L}_j^\beta, \mathscr{L}_i^\beta \right)_{\omega_\beta} = 0$$
$$\sum_{j=0}^{M} q_j \left((\mathscr{L}_j^\beta)', \mathscr{L}_i^\beta \right)_{\omega_\beta} - \sum_{j=0}^{M} v_j \left(\mathscr{L}_j^\beta, \mathscr{L}_i^\beta \right)_{\omega_\beta} = 0 \tag{3.30}$$

for (3.2), where we used the notation

$$(u, v)_{\omega_\beta} := \int_0^{+\infty} u(z) v(z) \omega(z)\, dz. \tag{3.31}$$

Recalling that

$$\left(\mathscr{L}_i^\beta, \mathscr{L}_j^\beta \right)_{\omega_\beta} = \frac{1}{\beta} \delta_{ij} \tag{3.32}$$

and

$$(\mathscr{L}_j^\beta)'(z) = -\beta \sum_{k=0}^{j-1} \mathscr{L}_k^\beta(z) \tag{3.33}$$

we get

$$\left((\mathscr{L}_i^\beta)', \mathscr{L}_j^\beta \right)_{\omega_\beta} = \left(-\beta \sum_{k=0}^{i-1} \mathscr{L}_k^\beta, \mathscr{L}_j^\beta \right)_{\omega_\beta} = \tag{3.34}$$
$$= -\beta \sum_{k=0}^{i-1} \left(\mathscr{L}_k^\beta, \mathscr{L}_j^\beta \right)_{\omega_\beta} = \tag{3.35}$$
$$= -\beta \sum_{k=0}^{i-1} \frac{1}{\beta} \delta_{kj} = -\sum_{k=0}^{i-1} \delta_{kj} \tag{3.36}$$

so that the entries of the matrix $\left((\mathscr{L}_i^\beta)', \mathscr{L}_j^\beta \right)_{\omega_\beta}$ are the same as the matrix $-\mathbf{L}$, where now $\mathbf{L}$ has 1 on the lower triangular portion and 0 on the main diagonal and on the upper triangular portion. Moreover, denoting by l_{ij} the

entries of $\mathbf{L}$,

$$\left((\mathscr{L}_i^\beta)', (\mathscr{L}_j^\beta)'\right)_{\omega_\beta} = -\beta \sum_{k=0}^{j-1} \left((\mathscr{L}_i^\beta)', \mathscr{L}_k^\beta\right)_{\omega_\beta} = \tag{3.37}$$

$$= \beta \sum_{k=0}^{j-1} l_{ik} = \beta \sum_{k=0}^{M} l_{ik}\alpha_{kj} \tag{3.38}$$

where α_{kj} is 1 if $k \leq j-1$, 0 otherwise; in other words, α_{kj} are the entries of $\mathbf{L}^T$, so that the entries of $\left((\mathscr{L}_i^\beta)', (\mathscr{L}_j^\beta)'\right)_{\omega_\beta}$ coincide with those of $\beta\mathbf{L}\mathbf{L}^T$. Using the fact that $\mathscr{L}_i^\beta(0) = 1$, $i = 0, \ldots, M$, equation (3.29) can be rewritten in vector form as

$$\frac{d\mathbf{q}}{dt} = \mathbf{A}_{mod,Neu,Lp}\mathbf{q} + \mathbf{g}_{mod,Neu,Lp}, \tag{3.39}$$

where

$$\mathbf{A}_{mod,Neu,Lp} = -\mu\beta^2(\mathbf{L}\mathbf{L}^T + \mathbf{L}^T) + u\beta\mathbf{L}^T \tag{3.40}$$

$$\mathbf{g}_{mod,Neu,Lp} = -\mu\beta D q_L \mathbf{e}, \tag{3.41}$$

with $\mathbf{e} = [1, \ldots, 1]^T \in \mathbf{R}^{M+1}$. Equations (3.30) yield instead

$$\begin{aligned} \frac{d\mathbf{q}}{dt} &= \mu\beta(\mathbf{L} + \mathbf{I})\mathbf{v} - u\mathbf{v} + \mathbf{g} \\ \mathbf{v} &= -\beta\mathbf{L}^T\mathbf{q}, \end{aligned} \tag{3.42}$$

from which the previous expressions follow again. Here we denoted by $\mathbf{I}$ the identity matrix.

If Dirichlet boundary conditions are imposed, we integrate by parts the second equation of (3.8), to get

$$\begin{aligned} &\frac{d}{dt}\int_0^{+\infty} \varphi(z)q(z,t)\omega(z)\,dz - \mu\int_0^{+\infty} \varphi(z)\frac{\partial v}{\partial z}(z,t)\omega(z)\,dz + \\ &+u\int_0^{+\infty} \varphi(z)v(z,t)\omega(z)\,dz = 0 \\ &\int_0^{+\infty} v\varphi(z)\omega(z)\,dz = -q_L\varphi(0) - \int_0^{+\infty} q(\varphi'(z) - \beta\varphi(z))\omega(z)\,dz \end{aligned} \tag{3.43}$$

Acting as before we obtain

$$\sum_{j=0}^{M} \frac{dq_j}{dt} \left(\mathscr{L}_i^\beta, \mathscr{L}_j^\beta \right)_{\omega_\beta} = \mu \sum_{j=0}^{M} v_j \left((\mathscr{L}_j^\beta)', \mathscr{L}_i^\beta \right)_{\omega_\beta} - u \sum_{j=0}^{M} v_j \left(\mathscr{L}_i^\beta, \mathscr{L}_j^\beta \right)_{\omega_\beta}$$

$$\sum_{j=0}^{M} v_j \left(\mathscr{L}_i^\beta, \mathscr{L}_j^\beta \right)_{\omega_\beta} = -q_L - \sum_{j=0}^{M} q_j \left(\mathscr{L}_j^\beta, (\mathscr{L}_i^\beta)' - \beta \mathscr{L}_i^\beta \right)_{\omega_\beta} \tag{3.44}$$

which gives, in vector notation,

$$\begin{aligned} \frac{d\mathbf{q}}{dt} &= (-\mu\beta \mathbf{L}^T - u\mathbf{I})\mathbf{v} \\ \mathbf{v} &= \mathbf{h}_{mod,Dir,Lp} + \beta(\mathbf{L} + \mathbf{I})\mathbf{q} \end{aligned} \tag{3.45}$$

where $\mathbf{h}_{mod,Dir,Lp} = -q_L \beta \mathbf{e}$. In the end we find

$$\frac{d\mathbf{q}}{dt} = \mathbf{A}_{mod,Dir,Lp}\mathbf{q} + \mathbf{g}_{mod,Dir,Lp} \tag{3.46}$$

where

$$\mathbf{A}_{mod,Dir,Lp} = -\mu\beta^2 \mathbf{L}^T(\mathbf{L} + \mathbf{I}) - u\beta(\mathbf{L} + \mathbf{I}) \tag{3.47}$$

$$\mathbf{g}_{mod,Dir,Lp} = -u\mathbf{h}_{mod,Dir,Lp} = uq_L\beta\mathbf{e} \tag{3.48}$$

3.1.3 Nodal discretization, Laguerre functions

We now employ a nodal discretization, where the basis functions are Lagrangian associated to the GLR or GL quadrature nodes. We start by considering the case where Laguerre functions are employed, so the weight is $\omega = 1$, and a Neumann boundary condition is imposed at the left endpoint.

Starting from (3.7), an integration by parts leads to

$$\int_0^{+\infty} \frac{\partial q}{\partial t}\varphi(z)\,dz + \mu D q_L \varphi(0) + \mu \int_0^{+\infty} \frac{\partial q}{\partial z}\varphi'(z)\,dz + u \int_0^{+\infty} \frac{\partial q}{\partial z}\varphi(z)\,dz = 0 \tag{3.49}$$

We now represent the solution as

$$q(z,t) \approx \sum_{j=0}^{M} q_j \hat{h}_j^\beta(z) \tag{3.50}$$

where

$$\hat{h}_j^\beta(z) = \frac{e^{-\beta z/2}}{e^{-\beta z_j^\beta/2}} h_j^\beta(z) \qquad j = 0, \ldots, M \tag{3.51}$$

z_j^β being the j-th GLR or GL node and $h_j^\beta(z)$ the associated Lagrangian polynomial. We then choose $\varphi = \hat{h}_i^\beta$ as test functions, with $i = 0, \ldots, M$. Plain substitution in the expression above yields

$$\sum_{j=0}^{M} \frac{dq_j}{dt} \left(\hat{h}_j^\beta, \hat{h}_i^\beta\right) + \mu D q_L \hat{h}_i^\beta(0) + \mu \sum_{j=0}^{M} q_j \left((\hat{h}_j^\beta)', (\hat{h}_i^\beta)'\right) + \\ + u \sum_{j=0}^{M} q_j \left((\hat{h}_j^\beta)', \hat{h}_i^\beta\right) = 0 \tag{3.52}$$

We now employ the GLR or GL quadrature rules.

$$\left(\hat{h}_j^\beta, \hat{h}_i^\beta\right) = \sum_{k=0}^{M} \hat{h}_j^\beta(z_k^\beta) \hat{h}_i^\beta(z_k^\beta) \hat{\omega}_k^\beta = \sum_{k=0}^{M} \delta_{jk} \delta_{ki} \hat{\omega}_k^\beta = \hat{\omega}_i^\beta \delta_{ij} \tag{3.53}$$

$$\left((\hat{h}_j^\beta)', (\hat{h}_i^\beta)'\right) = \sum_{k=0}^{M} (\hat{h}_j^\beta)'(z_k^\beta)(\hat{h}_i^\beta)'(z_k^\beta) \hat{\omega}_k^\beta = \sum_{k=0}^{M} \hat{d}_{kj}^\beta \hat{d}_{ki}^\beta \hat{\omega}_k \tag{3.54}$$

$$\left((\hat{h}_j^\beta)', \hat{h}_i^\beta\right) = \sum_{k=0}^{M} (\hat{h}_j^\beta)'(z_k^\beta) \hat{h}_i^\beta(z_k^\beta) \hat{\omega}_k^\beta = \tag{3.55}$$

$$= \sum_{k=0}^{M} \hat{d}_{kj}^\beta \delta_{ik} \hat{\omega}_k^\beta = \hat{\omega}_i^\beta \hat{d}_{ij}^\beta \tag{3.56}$$

where $\hat{\omega}_i^\beta = \omega_i^\beta e^{\beta z_i^\beta}$, being ω_i the i-the quadrature weight, and $\hat{d}_{ij}^\beta$ denotes the entries of the GLR or GL differentiation matrix $\hat{\mathbf{D}}_\beta$ associated with Laguerre functions, defined as follows:

- GL nodes

$$\hat{d}_{ij}^\beta = \begin{cases} \dfrac{\hat{\mathscr{L}}_M^\beta(z_i^\beta)}{(z_i^\beta - z_j^\beta)\hat{\mathscr{L}}_M^\beta(z_j^\beta)} & i \neq j \\ \\ -\dfrac{M+2}{2z_i^\beta} & i = j \end{cases}$$

- GLR nodes

$$\hat{d}_{ij}^{\beta} = \begin{cases} \dfrac{\hat{\mathscr{L}}_{M+1}^{\beta}(z_i^{\beta})}{(z_i^{\beta} - z_j^{\beta})\hat{\mathscr{L}}_{M+1}^{\beta}(z_j^{\beta})} & i \neq j \\ 0 & i = j \neq 0 \\ -\beta\dfrac{M+1}{2} & i = j = 0 \end{cases}$$

Defining $\hat{\mathbf{\Omega}}_\beta$ as the diagonal matrix with the quadrature weights $\hat{\omega}_i^\beta$ on the diagonal, we notice that $\left(\hat{h}_j^\beta, \hat{h}_i^\beta\right)$, $\left((\hat{h}_j^\beta)', (\hat{h}_i^\beta)'\right)$ and $\left((\hat{h}_j^\beta)', \hat{h}_i^\beta\right)$ are the entries of $\hat{\mathbf{\Omega}}_\beta$, $\hat{\mathbf{D}}_\beta^T\hat{\mathbf{\Omega}}_\beta\hat{\mathbf{D}}_\beta$ and $\hat{\mathbf{\Omega}}_\beta\hat{\mathbf{D}}_\beta$, respectively. This gives

$$\frac{d\mathbf{q}}{dt} = \mathbf{A}_{nod,Neu,Lf}\mathbf{q} + \mathbf{g}_{nod,Neu,Lf} \tag{3.57}$$

where

$$\mathbf{A}_{nod,Neu,Lf} = -\mu\hat{\mathbf{\Omega}}_\beta^{-1}\hat{\mathbf{D}}_\beta^T\hat{\mathbf{\Omega}}_\beta\hat{\mathbf{D}}_\beta - u\hat{\mathbf{D}}_\beta \tag{3.58}$$

$$\mathbf{g}_{nod,Neu,Lf} = -\mu Dq_L\hat{\mathbf{\Omega}}_\beta^{-1}\mathbf{h} \tag{3.59}$$

where $\mathbf{h} = [\hat{h}_0^\beta(0), \ldots, \hat{h}_M^\beta(0)]$. We may achieve the same result from the formulation (3.2) by integrating by parts only the first equation of (3.8), which yields (3.10). Inserting the nodal expression of the solution we get

$$\begin{aligned} &\sum_{j=0}^{M}\frac{dq_j}{dt}\left(\hat{h}_j^\beta, \hat{h}_i^\beta\right) + \mu\hat{h}_i^\beta(0)Dq_L + \mu\sum_{j=0}^{M}v_j\left(\hat{h}_j^\beta, (\hat{h}_i^\beta)'\right) + \\ &+u\sum_{j=0}^{M}v_j\left(\hat{h}_j^\beta, \hat{h}_i^\beta\right) = 0 \\ &\sum_{j=0}^{M}q_j\left((\hat{h}_j^\beta)', \hat{h}_i^\beta\right) = \sum_{j=0}^{M}v_j\left(\hat{h}_j^\beta, \hat{h}_i^\beta\right) \end{aligned} \tag{3.60}$$

which, in vector form, reads

$$\begin{aligned}\frac{d\mathbf{q}}{dt} &= (-\mu\hat{\mathbf{\Omega}}_\beta^{-1}\hat{\mathbf{D}}_\beta^T\hat{\mathbf{\Omega}}_\beta - u\mathbf{I})\mathbf{v} + \mathbf{g}_{nod,Neu,Lf} \\ \mathbf{v} &= \hat{\mathbf{D}}_\beta\mathbf{q}\end{aligned} \tag{3.61}$$

so we recover the same expressions of $\mathbf{A}_{nod,Neu,Lf}$ and $\mathbf{g}_{nod,Neu,Lf}$ already found.

If a Dirichlet condition is imposed, it is convenient to start from formulation (3.2) and integrate by parts the second equation of (3.8) only, to get (3.22). Following the same steps as before we get

$$\begin{aligned}\sum_{j=0}^{M}\frac{dq_j}{dt}\left(\hat{h}_j^\beta,\hat{h}_i^\beta\right) &= \mu\sum_{j=0}^{M}v_j\left((\hat{h}_j^\beta)',\hat{h}_i^\beta\right) - u\sum_{j=0}^{M}v_j\left(\hat{h}_j^\beta,\hat{h}_i^\beta\right) \\ \sum_{j=0}^{M}v_j\left(\hat{h}_j^\beta,\hat{h}_i^\beta\right) &= -q_L\hat{h}_i^\beta(0) - \sum_{j=0}^{M}q_j\left(\hat{h}_j^\beta,(\hat{h}_i^\beta)'\right)\end{aligned} \tag{3.62}$$

which, in vector form, reads

$$\begin{aligned}\frac{d\mathbf{q}}{dt} &= \mu\hat{\mathbf{D}}_\beta\mathbf{v} - u\mathbf{v} \\ \mathbf{v} &= -q_L\hat{\mathbf{\Omega}}_\beta^{-1}\mathbf{h} - \hat{\mathbf{\Omega}}_\beta^{-1}\hat{\mathbf{D}}_\beta^T\hat{\mathbf{\Omega}}_\beta\mathbf{q}\end{aligned} \tag{3.63}$$

In the end we obtain

$$\frac{d\mathbf{q}}{dt} = \mathbf{A}_{nod,Dir,Lf}\mathbf{q} + \mathbf{g}_{nod,Dir,Lf} \tag{3.64}$$

where

$$\mathbf{A}_{nod,Dir,Lf} = -\mu\hat{\mathbf{D}}_\beta\hat{\mathbf{\Omega}}_\beta^{-1}\hat{\mathbf{D}}_\beta^T\hat{\mathbf{\Omega}}_\beta + u\hat{\mathbf{\Omega}}_\beta^{-1}\hat{\mathbf{D}}_\beta^T\hat{\mathbf{\Omega}}_\beta \tag{3.65}$$

$$\mathbf{g}_{nod,Dir,Lf} = -q_L\mu\hat{\mathbf{D}}_\beta\hat{\mathbf{\Omega}}_\beta^{-1}\mathbf{h} + q_L u\hat{\mathbf{\Omega}}_\beta^{-1}\mathbf{h} \tag{3.66}$$

3.1.4 Nodal discretization, Laguerre polynomials

If Laguerre polynomials are employed, the weight function is now $\omega(z) = e^{-\beta z}$. Considering the case of Neumann boundary conditions first,

integration by parts of (3.7) leads now to (3.26), while for formulation (3.2) we obtain (3.27). We now represent the solution on the basis of Lagrangian functions associated to GLR and GL nodes as

$$q(z,t) \approx \sum_{j=0}^{M} q_j h_j^\beta(z) \tag{3.67}$$

and we choose $\varphi = h_i^\beta$ as test functions. We get

$$\sum_{j=0}^{M} \frac{dq_j}{dt} \left(h_j^\beta, h_i^\beta\right)_{\omega_\beta} = -\mu \sum_{j=0}^{M} q_j \left((h_j^\beta)', (h_i^\beta)' - \beta h_i^\beta\right)_{\omega_\beta} + \\ - u \sum_{j=0}^{M} q_j \left((h_j^\beta)', h_i^\beta\right)_{\omega_\beta} - \mu h_i^\beta(0) D q_L \tag{3.68}$$

for formulation (3.1) and

$$\sum_{j=0}^{M} q_j \left(h_j^\beta, h_i^\beta\right)_{\omega_\beta} = -\mu h_i^\beta(0) D q_L + \\ -\mu \sum_{j=0}^{M} v_j \left(h_j^\beta, (h_i^\beta)' - \beta h_i^\beta\right)_{\omega_\beta} - u \sum_{j=0}^{M} v_j \left(h_j^\beta, h_i^\beta\right)_{\omega_\beta} \\ \sum_{j=0}^{M} v_j \left(h_j^\beta, h_i^\beta\right) = \sum_{j=0}^{M} q_j \left((h_j^\beta)', h_i^\beta\right)_{\omega_\beta} \tag{3.69}$$

for formulation (3.2). We now use GLR and GL quadrature rules to obtain

$$\left(h_j^\beta, h_i^\beta\right)_{\omega_\beta} = \sum_{k=0}^{M} h_j^\beta(z_k^\beta) h_i^\beta(z_k^\beta) \omega_k^\beta = \sum_{k=0}^{M} \delta_{jk}\delta_{ki}\omega_k^\beta = \omega_i^\beta \delta_{ij} \tag{3.70}$$

$$\left((h_j^\beta)', (h_i^\beta)'\right)_{\omega_\beta} = \sum_{k=0}^{M} (h_j^\beta)'(z_k^\beta)(h_i^\beta)'(z_k^\beta)\omega_k^\beta = \sum_{j=0}^{M} d_{kj}^\beta d_{ki}^\beta \omega_k^\beta \tag{3.71}$$

$$\left((h_j^\beta)', h_i^\beta\right)_{\omega_\beta} = \sum_{k=0}^{M} (h_j^\beta)'(z_k^\beta) h_i^\beta(z_k^\beta)\omega_k^\beta = \\ = \sum_{k=0}^{M} d_{kj}^\beta \delta_{ik} \omega_k^\beta = \omega_i^\beta d_{ij}^\beta \tag{3.72}$$

where d_{ij}^{β} denotes the entries of the differentiation matrix $\mathbf{D}_\beta$ related to Laguerre polynomials, which are defined as:

- GL nodes

$$d_{ij}^{\beta} = \begin{cases} \dfrac{\mathscr{L}_M^{\beta}(z_i^{\beta})}{(z_i^{\beta} - z_j^{\beta})\mathscr{L}_M^{\beta}(z_j^{\beta})} & i \neq j \\ \\ \dfrac{\beta z_i^{\beta} - M - 2}{2z_i^{\beta}} & i = j \end{cases}$$

- GLR nodes

$$d_{ij}^{\beta} = \begin{cases} \dfrac{\mathscr{L}_{M+1}^{\beta}(z_i^{\beta})}{(z_i^{\beta} - z_j^{\beta})\mathscr{L}_{M+1}^{\beta}(z_j^{\beta})} & i \neq j \\ \\ \dfrac{\beta}{2} & i = j \neq 0 \\ \\ -\beta\dfrac{M}{2} & i = j = 0 \end{cases}$$

We also introduce the diagonal matrix $\mathbf{\Omega}_\beta$, with the quadrature weights ω_i^{β} on the diagonal, and we notice that $\left(h_j^{\beta}, h_i^{\beta}\right)_{\omega_\beta}$, $\left((h_j^{\beta})', (h_i^{\beta})'\right)_{\omega_\beta}$ and $\left((h_j^{\beta})', h_i^{\beta}\right)_{\omega_\beta}$ are the entries of $\mathbf{\Omega}_\beta$, $\mathbf{D}_\beta^T\mathbf{\Omega}_\beta\mathbf{D}_\beta$ and $\mathbf{\Omega}_\beta\mathbf{D}_\beta$ respectively. Thus we obtain from (3.68)

$$\frac{d\mathbf{q}}{dt} = \mathbf{A}_{nod,Neu,Lp}\mathbf{q} + \mathbf{g}_{nod,Neu,Lp} \tag{3.73}$$

where

$$\mathbf{A}_{nod,Neu,Lp} = -\mu\mathbf{\Omega}_\beta^{-1}\mathbf{D}_\beta^T\mathbf{\Omega}_\beta\mathbf{D}_\beta + \mu\beta\mathbf{D}_\beta - u\mathbf{D}_\beta \tag{3.74}$$

$$\mathbf{g}_{nod,Neu,Lp} = -Dq_L\mu\mathbf{\Omega}_\beta^{-1}\mathbf{h} \tag{3.75}$$

and $\mathbf{h} = [h_0^{\beta}(0), \ldots, h_M^{\beta}(0)]$. Analogously we can get, from (3.69),

$$\begin{aligned} \frac{d\mathbf{q}}{dt} &= -\mu\mathbf{\Omega}_\beta^{-1}(\mathbf{D}_\beta^T\mathbf{\Omega}_\beta - \beta\mathbf{\Omega}_\beta)\mathbf{v} - u\mathbf{v} + \mathbf{g}_{nod,Neu,Lp} \\ \mathbf{v} &= \mathbf{D}_\beta\mathbf{q} \end{aligned} \tag{3.76}$$

from which we recover the same expressions for $\mathbf{A}_{nod,Neu,Lp}$ and $\mathbf{g}_{nod,Neu,Lp}$.

If a Dirichlet boundary condition is imposed, we employ formulation (3.2) and we integrate by parts the second equation of (3.8) only to get (3.43). Acting as before we obtain

$$\sum_{j=0}^{M} \frac{dq_j}{dt} \left(h_i^\beta, h_j^\beta\right)_{\omega_\beta} = \mu \sum_{j=0}^{M} v_j \left((h_j^\beta)', h_i^\beta\right)_{\omega_\beta} - u \sum_{j=0}^{M} v_j \left(h_i^\beta, h_j^\beta\right)_{\omega_\beta}$$
$$\sum_{j=0}^{M} v_j \left(h_i^\beta, h_j^\beta\right)_{\omega_\beta} = -q_L h_i^\beta(0) - \sum_{j=0}^{M} q_j \left(h_j^\beta, (h_i^\beta)' - \beta h_i^\beta\right)_{\omega_\beta} \tag{3.77}$$

which gives, in vector notation,

$$\frac{d\mathbf{q}}{dt} = \mu \mathbf{D}_\beta \mathbf{v} - u\mathbf{v}$$
$$\mathbf{v} = -q_L \mathbf{\Omega}_\beta^{-1}\mathbf{h} - \mathbf{\Omega}_\beta^{-1}(\mathbf{D}_\beta^T \mathbf{\Omega}_\beta - \beta \mathbf{\Omega}_\beta)\mathbf{q} \tag{3.78}$$

In the end we obtain

$$\frac{d\mathbf{q}}{dt} = \mathbf{A}_{nod,Dir,Lp}\mathbf{q} + \mathbf{g}_{nod,Dir,Lp} \tag{3.79}$$

where

$$\mathbf{A}_{nod,Dir,Lp} = -\mu \mathbf{D}_\beta \mathbf{\Omega}_\beta^{-1} \mathbf{D}_\beta^T \mathbf{\Omega}_\beta + \mu\beta \mathbf{D}_\beta + u \mathbf{\Omega}_\beta^{-1} \mathbf{D}_\beta^T \mathbf{\Omega}_\beta - u\beta \mathbf{I} \tag{3.80}$$

$$\mathbf{g}_{nod,Dir,Lp} = -q_L \mu \mathbf{D}_\beta \mathbf{\Omega}_\beta^{-1} \mathbf{h} + q_L u \mathbf{\Omega}_\beta^{-1} \mathbf{h} \tag{3.81}$$

3.1.5 Strong form discretization, Laguerre functions

Let us now discretize (3.1) in strong form, by inserting the expansion of the solution on the basis of Lagrangian functions and evaluating it at the GLR interpolation nodes, which are the only practical alternative in this case, since they include the point $z = 0$. We start from the case of a Dirichlet boundary condition imposed at the left endpoint. This implies

$$q(0,t) = \sum_{j=0}^{M} q_j \hat{h}_j^\beta(0) = \sum_{j=0}^{M} q_j \delta_{j0} = q_0 = q_L, \tag{3.82}$$

so that the solution can be represented as

$$q(z,t) \approx \sum_{j=0}^{M} q_j(t)\hat{h}_j^{\beta}(z) \tag{3.83}$$

We then insert the expansion of the solution into (3.1) and evaluate it at z_i, $i = 1, \ldots, M$, to get

$$\sum_{j=0}^{M} \frac{dq_j}{dt}\hat{h}_j^{\beta}(z_i) - \mu \sum_{j=0}^{M} q_j(\hat{h}_j^{\beta})''(z_i) + u \sum_{j=0}^{M} q_j(\hat{h}_j^{\beta})'(z_i) = 0 \tag{3.84}$$

Since the basis is Lagrangian, we have $\hat{h}_j^{\beta}(z_i) = \delta_{ij}$:

$$\frac{dq_i}{dt} = \mu q_L(\hat{h}_0^{\beta})''(z_i) + \mu \sum_{j=1}^{M}(\hat{h}_j^{\beta})''(z_i)q_j - uq_L(\hat{h}_0^{\beta})'(z_i) - u\sum_{j=1}^{M}(\hat{h}_j^{\beta})'(z_i)q_j \tag{3.85}$$

which in vector form is

$$\frac{d\mathbf{q}}{dt} = \mathbf{A}_{coll,Dir,Lf}\mathbf{q} + \mathbf{g}_{coll,Dir,Lf} \tag{3.86}$$

where

$$\mathbf{A}_{coll,Dir,Lf} = \mu(\hat{\mathbf{D}}_{\beta}^2)_M - u(\hat{\mathbf{D}}_{\beta})_M \tag{3.87}$$

$$\mathbf{g}_{coll,Dir,Lf} = \mu q_L \tilde{\mathbf{g}}_{\mathbf{1}} - uq_L\tilde{\mathbf{g}}_{\mathbf{2}} \tag{3.88}$$

being $\tilde{\mathbf{g}}_{\mathbf{1}} = [(\hat{h}_0^{\beta})''(z_1), \ldots, (\hat{h}_0^{\beta})''(z_M)]$, $\tilde{\mathbf{g}}_{\mathbf{2}} = [(\hat{h}_0^{\beta})'(z_1), \ldots, (\hat{h}_0^{\beta})'(z_M)]$ and $(\hat{\mathbf{D}}_{\beta})_M$ is obtained from the differentiation matrix $\hat{\mathbf{D}}_{\beta}$ by removing the first row and the first column.

If a Neumann condition is imposed at $z = 0$ it is convenient to start from formulation (3.2). In this case the boundary condition implies

$$\frac{\partial q}{\partial z}(0,t) = v(0,t) = \sum_{j=0}^{M} v_j\hat{h}_j^{\beta}(0) = \sum_{j=0}^{M} v_j\delta_{j0} = v_0 = Dq_L \tag{3.89}$$

The second equation gives

$$\sum_{j=0}^{M} q_j (\hat{h}_j^\beta)'(z_i^\beta) - \sum_{j=0}^{M} v_j \hat{h}_j^\beta(z_i^\beta) = 0 \tag{3.90}$$

$$\sum_{j=0}^{M} q_j \hat{d}_{ij}^\beta - \sum_{j=0}^{M} v_j \delta_{ij} = 0 \tag{3.91}$$

$$v_i = \sum_{j=0}^{M} \hat{d}_{ij}^\beta q_j \qquad i = 1, \ldots, M \tag{3.92}$$

so that

$$\mathbf{v} = (\hat{\mathbf{D}}_\beta)_0 \mathbf{q} + D q_L \mathbf{e_1} \tag{3.93}$$

where $(\hat{\mathbf{D}}_\beta)_0$ is the matrix obtained from $\hat{\mathbf{D}}_\beta$ by replacing the first row with zeros, and $\mathbf{e_1} = [1, 0, \ldots, 0]^T$. The first equation gives

$$\sum_{j=0}^{M} \frac{dq_j}{dt} \hat{h}_j^\beta(z_i^\beta) - \mu \sum_{j=0}^{M} v_j (\hat{h}_j^\beta)'(z_i^\beta) + u \sum_{j=0}^{M} v_j \hat{h}_j^\beta(z_i^\beta) = 0 \tag{3.94}$$

which, in vector form, reads

$$\frac{d\mathbf{q}}{dt} = \mu \hat{\mathbf{D}}_\beta \mathbf{v} - u\mathbf{v} \tag{3.95}$$

In the end we obtain

$$\frac{d\mathbf{q}}{dt} = \mathbf{A}_{coll,Neu,Lf}\mathbf{q} + \mathbf{g}_{coll,Neu,Lf} \tag{3.96}$$

where

$$\mathbf{A}_{coll,Neu,Lf} = \mu \hat{\mathbf{D}}_\beta (\hat{\mathbf{D}}_\beta)_0 - u(\hat{\mathbf{D}}_\beta)_0 \tag{3.97}$$

$$\mathbf{g}_{coll,Neu,Lf} = \mu D q_L \hat{\mathbf{D}}_\beta \mathbf{e_1} - u D q_L \mathbf{e_1} = \mu D q_L \tilde{\mathbf{g_2}} - u D q_L \mathbf{e_1} \tag{3.98}$$

3.1.6 Strong form discretization, Laguerre polynomials

We repeat the same steps as above, replacing the Lagrangian basis functions related to Laguerre functions, $\hat{h}_i^\beta$, with the ones based of Laguerre polyno-

mials, h_i^β. Hence, the differentiation matrix $\hat{\mathbf{D}}_\beta$ will be replaced by $\mathbf{D}_\beta$. We find, if a Dirichlet boundary condition is imposed,

$$\frac{d\mathbf{q}}{dt} = \mathbf{A}_{coll,Dir,Lp}\mathbf{q} + \mathbf{g}_{coll,Dir,Lp} \tag{3.99}$$

where

$$\mathbf{A}_{coll,Dir,Lf} = \mu(\hat{\mathbf{D}}_\beta^2)_M - u(\hat{\mathbf{D}}_\beta)_M \tag{3.100}$$

$$\mathbf{g}_{coll,Dir,Lf} = \mu q_L \tilde{\mathbf{g}}_\mathbf{1} - u q_L \tilde{\mathbf{g}}_\mathbf{2} \tag{3.101}$$

being $\tilde{\mathbf{g}}_\mathbf{1} = [(h_0^\beta)''(z_1), \ldots, (h_0^\beta)''(z_M)]$, $\tilde{\mathbf{g}}_\mathbf{2} = [(h_0^\beta)'(z_1), \ldots, (h_0^\beta)'(z_M)]$ and $(\mathbf{D}_\beta)_M$ is obtained from the differentiation matrix $\mathbf{D}_\beta$ by removing the first row and the first column.

In the case of a Neumann boundary condition we find

$$\frac{d\mathbf{q}}{dt} = \mathbf{A}_{coll,Neu,Lp}\mathbf{q} + \mathbf{g}_{coll,Neu,Lp} \tag{3.102}$$

where

$$\mathbf{A}_{coll,Neu,Lp} = \mu\mathbf{D}_\beta(\mathbf{D}_\beta)_0 - u(\mathbf{D}_\beta)_0 \tag{3.103}$$

$$\mathbf{g}_{coll,Neu,Lp} = \mu D q_L \mathbf{D}_\beta \mathbf{e}_\mathbf{1} - u D q_L \mathbf{e}_\mathbf{1} = \mu D q_L \tilde{\mathbf{g}}_\mathbf{2} - u D q_L \mathbf{e}_\mathbf{1} \tag{3.104}$$

3.2 Analysis of the results

The following table shows the expressions for matrix $\mathbf{A}$ in the different schemes, for both Dirichlet and Neumann boundary conditions at the left endpoint of the semi-infinite domain.

Coll, LF, Dir	$\mu(\hat{\mathbf{D}}_\beta^2)_M - u(\hat{\mathbf{D}}_\beta)_M$
Coll, LF, Neu	$\mu\hat{\mathbf{D}}_\beta(\hat{\mathbf{D}}_\beta)_0 - u(\hat{\mathbf{D}}_\beta)_0$
Coll, LP, Dir	$\mu(\mathbf{D}_\beta^2)_M - u(\mathbf{D}_\beta)_M$
Coll, LP, Neu	$\mu\mathbf{D}_\beta(\mathbf{D}_\beta)_0 - u(\mathbf{D}_\beta)_0$
Nod, LF, Dir	$-\mu\hat{\mathbf{D}}_\beta\hat{\mathbf{\Omega}}_\beta^{-1}\hat{\mathbf{D}}_\beta^T\hat{\mathbf{\Omega}}_\beta + u\hat{\mathbf{\Omega}}_\beta^{-1}\hat{\mathbf{D}}_\beta^T\hat{\mathbf{\Omega}}_\beta$
Nod, LF, Neu	$-\mu\hat{\mathbf{\Omega}}_\beta^{-1}\hat{\mathbf{D}}_\beta^T\hat{\mathbf{\Omega}}_\beta\hat{\mathbf{D}}_\beta - u\hat{\mathbf{D}}_\beta$
Nod, LP, Dir	$-\mu\mathbf{D}_\beta\mathbf{\Omega}_\beta^{-1}\mathbf{D}_\beta^T\mathbf{\Omega}_\beta + \mu\beta\mathbf{D}_\beta + u\mathbf{\Omega}_\beta^{-1}\mathbf{D}_\beta^T\mathbf{\Omega}_\beta - u\beta\mathbf{I}$
Nod, LP, Neu	$-\mu\mathbf{\Omega}_\beta^{-1}\mathbf{D}_\beta^T\mathbf{\Omega}_\beta\mathbf{D}_\beta + \mu\beta\mathbf{D}_\beta - u\mathbf{D}_\beta$
Mod, LF, Dir	$-\mu\beta^2\mathbf{L}^T\mathbf{L} - u\beta\mathbf{L}$
Mod, LF, Neu	$-\mu\beta^2\mathbf{L}\mathbf{L}^T + u\beta\mathbf{L}^T$
Mod, LP, Dir	$-\mu\beta^2\mathbf{L}^T(\mathbf{L}+\mathbf{I}) - u\beta(\mathbf{L}+\mathbf{I})$
Mod, LP, Neu	$-\mu\beta^2(\mathbf{L}+\mathbf{I})\mathbf{L}^T + u\beta\mathbf{L}^T$

Table 3.1: Matrix $\mathbf{A}$. 'Coll': collocation, 'Nod': nodal, 'Mod': modal, 'Dir': Dirichlet b.c., 'Neu': Neumann b.c., 'LF': Laguerre Functions, 'LP': Laguerre Polynomials.

The matrix $\mathbf{L}$ is defined as

- LF

$$l_{ij} = \begin{cases} 1/2 & i = j \\ 1 & i > j \\ 0 & i < j \end{cases}$$

- LP

$$l_{ij} = \begin{cases} 1 & i > j \\ 0 & i \leq j \end{cases}$$

In the following tables, we collect the results of the stability analysis carried out computing numerically the eigenvalues of the different matrices $\mathbf{A}$ defined in Table 3.1. As customary for the advection-diffusion problem, the stability property can be a function of the Péclet number, which is usually defined as $Pe = uL/\mu$, where L is a reference length scale. Since the proposed discretization employs the scaling parameter β, which has been assumed in (1.35) to be defined as $\beta = 1/L$, we will also use here the definition $Pe_\beta = u/\mu\beta$. Notice that Pe is determined by the physics of the problem, while Pe_β depends on the chosen discretization because of the presence of β; we present the stability results using both definitions. We start from Pe_β; we fix $M = 50$, $\beta = \mu = 1$ and we let Pe_β vary, determining u as $Pe_\beta\mu\beta$. The ranges of Pe_β for which each discretization is stable are shown in Table 3.2.

			LF	
			Neu	Dir
Strong			$\forall Pe_\beta$	$\forall Pe_\beta$
Weak	Nodal	GLR	$Pe_\beta \leq 1.7$	$\forall Pe_\beta$
		GL	$Pe_\beta \leq 0.5$	$\forall Pe_\beta$
	Modal		$Pe_\beta \leq 1.7$	$\forall Pe_\beta$

			LP	
			Neu	Dir
Strong			$Pe_\beta \geq 0.4$	$Pe_\beta \geq 0.33$
Weak	Nodal	GLR	$0.35 \leq Pe_\beta \leq 62$	$Pe_\beta \geq 0.35$
		GL	$0.5 \leq Pe_\beta \leq 4.1$	$Pe_\beta \geq 0.12$
	Modal		$0.35 \leq Pe_\beta \leq 62$	$Pe_\beta \geq 0.35$

Table 3.2: Stability of $\mathbf{A}$ as a function of $Pe_\beta = u/\mu\beta$: condition under which the largest real part of the eigenvalues is non-positive. $M = 50$, $\beta = \mu = 1$. 'Neu': Neumann b.c., 'Dir': Dirichlet b.c., 'LF': Laguerre Functions, 'LP': Laguerre Polynomials.

As an example, Figure 3.1 shows the maximum real part of the eigenvalues of $\mathbf{A}$ in four of the above mentioned cases. As we can see, if a Dirichlet condition is imposed, the choice of Laguerre functions is unconditionally stable for all discretizations; on the other hand, Laguerre polynomials are not stable for the discretization of the purely diffusive problem, nonetheless

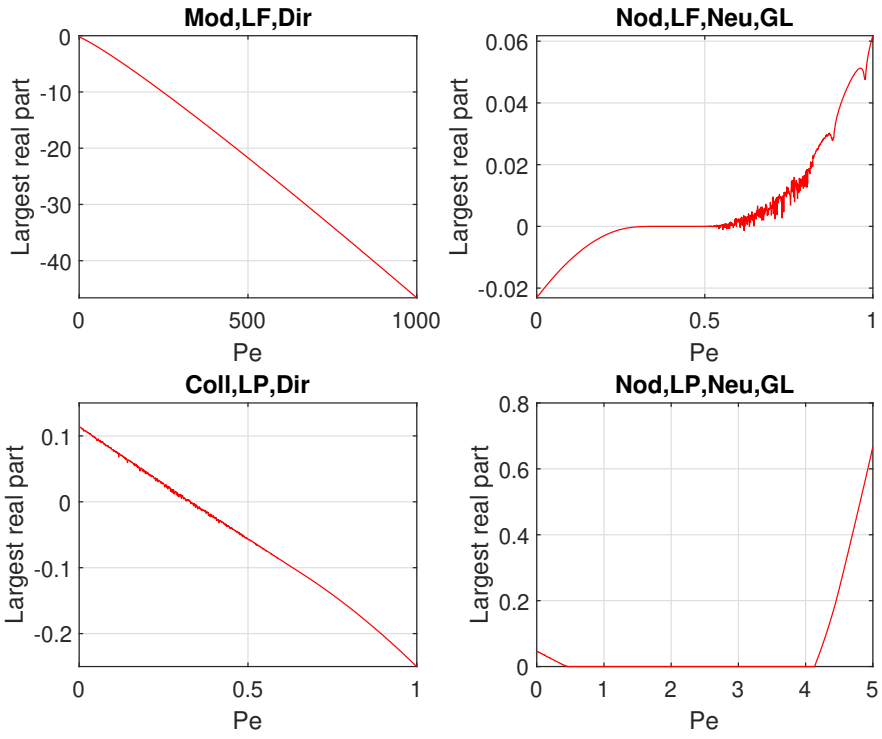

Figure 3.1: Maximum real part of the eigenvalues of $\mathbf{A}$ as a function of Pe_β. $M = 50$, $mu = \beta = 1$, $u = Pe_\beta \mu \beta$.

they achieve stability above a small value of Pe_β. If the problem is subject to a Neumann condition, the schemes are found to be unstable for large values of the Péclet number, except for the collocation method. In this case, Laguerre polynomials yield wider stability ranges if compared to the ones achieved by the Laguerre functions. For the same reason we can argue that GLR nodes are proved to be a better choice than GL.

If instead we consider the more standard definition of the Péclet number, namely $Pe = uL/\mu$, we look for the values of the scaling parameter β which make each discretization stable for a fixed value of Pe. This approach is complementary to the one adopted previously, where we fixed the value of β and let Pe_β, defined in terms of β, vary. With this new definition, Pe is only determined by the physical parameters of the problem, and letting β vary corresponds to choosing the spatial resolution. The first step is to rewrite the matrices of Tables 3.1 and in terms of Pe; for simplicity we choose the length scale $L = 1$, to obtain the results in Table 3.2. Next, we set $\mu = 1$ and we analyze the stability of $\mathbf{A}$ for a fixed value of Pe; the corresponding ranges for β are shown in Table 3.4 for both scaled Laguerre functions and polynomials. The results correspond to those relative to Pe_β.

Coll, LF, Dir	$\mu\left[(\hat{\mathbf{D}}_\beta^2)_M - Pe(\hat{\mathbf{D}}_\beta)_M\right]$
Coll, LF, Neu	$\mu\left[\hat{\mathbf{D}}_\beta(\hat{\mathbf{D}}_\beta)_0 - Pe(\hat{\mathbf{D}}_\beta)_0\right]$
Coll, LP, Dir	$\mu\left[(\mathbf{D}_\beta^2)_M - Pe(\mathbf{D}_\beta)_M\right]$
Coll, LP, Neu	$\mu\left[\mathbf{D}_\beta(\mathbf{D}_\beta)_0 - Pe(\mathbf{D}_\beta)_0\right]$
Nod, LF, Dir	$\mu\left[-\hat{\mathbf{D}}_\beta\hat{\mathbf{\Omega}}_\beta^{-1}\hat{\mathbf{D}}_\beta^T\hat{\mathbf{\Omega}}_\beta + Pe\hat{\mathbf{\Omega}}_\beta^{-1}\hat{\mathbf{D}}_\beta^T\hat{\mathbf{\Omega}}_\beta\right]$
Nod, LF, Neu	$\mu\left[-\hat{\mathbf{\Omega}}_\beta^{-1}\hat{\mathbf{D}}_\beta^T\hat{\mathbf{\Omega}}_\beta\hat{\mathbf{D}}_\beta - Pe\hat{\mathbf{D}}_\beta\right]$
Nod, LP, Dir	$\mu\left[-\mathbf{D}_\beta\mathbf{\Omega}_\beta^{-1}\mathbf{D}_\beta^T\mathbf{\Omega}_\beta + \beta\mathbf{D}_\beta + Pe\mathbf{\Omega}_\beta^{-1}\mathbf{D}_\beta^T\mathbf{\Omega}_\beta - Pe\beta\mathbf{I}\right]$
Nod, LP, Neu	$\mu\left[-\mathbf{\Omega}_\beta^{-1}\mathbf{D}_\beta^T\mathbf{\Omega}_\beta\mathbf{D}_\beta + \beta\mathbf{D}_\beta - Pe\mathbf{D}_\beta\right]$
Mod, LF, Dir	$\mu\left[-\beta^2\mathbf{L}^T\mathbf{L} - Pe\beta\mathbf{L}\right]$
Mod, LF, Neu	$\mu\left[-\beta^2\mathbf{L}\mathbf{L}^T + Pe\beta\mathbf{L}^T\right]$
Mod, LP, Dir	$\mu\left[-\beta^2\mathbf{L}^T(\mathbf{L}+\mathbf{I}) - Pe\beta(\mathbf{L}+\mathbf{I})\right]$
Mod, LP, Neu	$\mu\left[-\beta^2(\mathbf{L}+\mathbf{I})\mathbf{L}^T + Pe\beta\mathbf{L}^T\right]$

Table 3.3: Matrix **A**. 'Coll': collocation, 'Nod': nodal, 'Mod': modal, 'Dir': Inflow Dirichlet b.c., 'Neu': Neumann b.c., 'LF': Laguerre Functions, 'LP': Laguerre Polynomials.

			LF	
			Neu	Dir
Strong			$\forall\beta$	$\forall\beta$
Weak	Nodal	GLR	$\beta \geq 0.58Pe$	$\forall\beta$
		GL	$\beta \geq 2Pe$	$\forall\beta$
	Modal		$\beta \geq 0.58Pe$	$\forall\beta$

			LP	
			Neu	Dir
Strong			$\beta \leq 2.6Pe$	$\beta \leq 3Pe$
Weak	Nodal	GLR	$0.017Pe \leq \beta \leq 2.83Pe$	$\beta \leq 3Pe$
		GL	$0.25Pe \leq \beta \leq 2Pe$	$\beta \leq 8.5Pe$
	Modal		$0.017Pe \leq \beta \leq 2.83Pe$	$\beta \leq 3Pe$

Table 3.4: Stability of $\mathbf{A}$ as a function of β: condition under which the largest real part of the eigenvalues is non-positive. $M = 50$, $\mu = 1$. 'Neu': Neumann b.c., 'Dir': Dirichlet b.c., 'LF': Laguerre Functions, 'LP': Laguerre Polynomials.

As we saw in Section 1, the GLR and GL nodes $\{x_i\}_{i=0}^N$ are such that $x_N \to +\infty$ as $N \to +\infty$, so that also $\mathscr{L}_N(x_N) \to +\infty$. At the same time, the associated quadrature weights decay exponentially for large x_j. This implies that any numerical quadrature involving Laguerre polynomials is usually ill-conditioned. Moreover, the fact that the expansion polynomials of a function $u \in L^2_\omega(\mathbb{R}^+)$ are unbounded as $x \to +\infty$ while the weight function

$\omega = e^{-\beta x}$ decays exponentially causes the approximation by means of Laguerre polynomials to be less and less accurate as x grows. For these reasons we consider the approaches based on Laguerre functions to be preferable. Based on the results of the analysis, in the following we will consider a modal discretization in weak form based on scaled Laguerre functions.

These conclusions extend the results provided in [BB19], where the pure advection problem is discussed; in particular, as expected, the results coincide in the limit $Pe_\beta \to +\infty$, or, equivalently, $Pe \to +\infty$. To the best of the author's knowledge, this is the first stability analysis of this kind for advection-diffusion equations.

Chapter 4

Coupled scheme for general non-linear model problems

In this chapter we show how to solve the model problems of Chapter 2 by means of a coupled approach. For the sake of generality, we will take into account both the hyperbolic and the parabolic terms by considering the problem

$$\frac{\partial q}{\partial t} + \frac{\partial f(q)}{\partial z} = \frac{\partial}{\partial z}\left(\mu(z,t)\frac{\partial q}{\partial z}\right) + s(q,z,t) \qquad z \in (0,+\infty), \quad t > 0, \quad (4.1)$$

from which we recover the advection-diffusion equation and the Burgers' equation by choosing μ constant and $f(q) = uq$ and $f(q) = \frac{q^2}{2}$, respectively. We require that the diffusion μ is sufficiently regular and there are two positive constants μ_0 and μ_1 such that

$$0 < \mu_0 \leq \mu(z,t) \leq \mu_1 \qquad \forall z \in (0,+\infty), \quad \forall t > 0. \quad (4.2)$$

The function $s(q,z,t)$ corresponds to a reaction contribution and it may also contain a source term. We impose a Dirichlet condition

$$q(0,t) = a(t) \qquad t > 0 \quad (4.3)$$

at the left endpoint, and we require that the solution q vanishes at infinity. We also assign the initial datum

$$q(z,0) = q^0(z) \qquad z \in [0, +\infty). \tag{4.4}$$

Since we already discussed the linear problem in the previous chapter, we now take into account the case where f and s are, possibly, non-linear functions of the solution q.

As a first step, the semi-infinite domain is subdivided into a bounded region $[0, L]$, where the equation is discretized with a standard DG method on a Legendre polynomial basis, and an unbounded region $[L, +\infty)$, where the equation is discretized, according to the results of Chapter 3, on the basis of scaled Laguerre functions. In particular, following the notation of [BB19], we introduce a computational mesh $\{K_m\}_{m=1}^N$ of size Δz_m on $[0, L]$, where $K_m = [z_{m-1/2}, z_{m+\frac{1}{2}}]$, so that $[0, L] = \cup_{m=1}^N K_m$. We denote by z_m the midpoint of the generic element K_m. With this definition, $0 = z_{1/2}$ and $L = z_{N+1/2}$. We choose as basis functions

$$\phi_l^m(z) = \sqrt{2l+1} L_l \left(2 \frac{z - z_m}{\Delta z_m} \right), \qquad l = 0, \dots, p \quad m = 1, \dots, N, \tag{4.5}$$

where L_l is the Legendre polynomial of degree l, defined on the reference interval $[-1, 1]$. The solution q will be approximated by

$$q_h(z,t) = \sum_{j=0}^{p} \alpha_m^j(t) \phi_j^m(z), \qquad z \in K_m, \quad m = 1, \dots, N \tag{4.6}$$

On the other hand, concerning the semi-infinite part $K_{N+1} = [L, +\infty)$, we choose to expand the solution on the basis of Laguerre functions, where a suitable translation is performed on the independent variable z:

$$q_M(z,t) = \sum_{j=0}^{M} q_j(t) \hat{\mathscr{L}}_j^{\beta}(z - L), \qquad z \in [L, +\infty). \tag{4.7}$$

In this way, we may regard the resulting coupled scheme as a global modal approach, where the chosen basis is given by Legendre polynomials in the sub-intervals K_m for $m = 1, \dots, N$ and by scaled Laguerre functions in the rightmost interval K_{N+1}, which spans the whole region $[L, +\infty)$. We arrange the unknown coefficients in the vectors

$$\mathbf{q}_{DG}(t) = (\alpha_1^0(t), \dots, \alpha_1^p(t), \dots, \alpha_N^0(t), \dots, \alpha_N^p(t))^T \in \mathbb{R}^{N(p+1)}, \tag{4.8}$$

and

$$\mathbf{q}_{mod}(t) = (q_0(t), \dots, q_M(t)) \in \mathbb{R}^{M+1}, \tag{4.9}$$

so that the global vector of degrees of freedom is

$$\mathbf{q}(t) = (\mathbf{q}_{DG}(t), \mathbf{q}_{mod}(t))^T \in \mathbb{R}^{N(p+1)+M+1}. \tag{4.10}$$

The coupling requires a correct implementation of fluxes at the interface, located at $z = L$. In the following sections, we describe this coupling procedure in detail. We refer to [Riv08] for a complete discussion of the DG discretization of the diffusive term, while our references for the analysis of the hyperbolic part will be [CL89] and [BB19].

A note about the coupling technique The coupling may be implemented in two different ways. As a first approach, one may see the point $z = L$ as an interface between two separate schemes, i.e. the right endpoint of a DG discretization on $[0, L]$ and the left endpoint of a Laguerre discretization on $[L, +\infty)$; in this case, the coupling merely consists in setting $q_M(L^+, t)$ and $q_h(L^-, t)$ as right and left boundary conditions for the two problems, respectively. An alternative perspective would consider $z = L$ as an internal interface of a global DG scheme. In this case we no longer distinguish between the two discretizations, but we interpret the coupled model as

a full DG scheme where a different basis is chosen in the semi-infinite interval K_{N+1}: accordingly, the penalization of jumps of the numerical solution at $z = L$ would be implemented as for $z_{m+1/2}$ with $m = 1, \dots, N-1$. We will take into account both techniques in the following sections. Even if they both entail the coupling between a DG and a Laguerre discretization, we will refer at them for clarity as "coupled DG-Laguerre scheme" and "fully DG scheme", respectively.

4.1 Coupled DG-Laguerre scheme

4.1.1 DG discretization on the finite domain

We start from the Discontinuous Galerkin discretization of (4.1) in the bounded region $[0, L]$. For any non-negative integer p, we denote by $\mathbb{P}_p(K_m)$, the set of all polynomials of degree p on K_m, so that the discontinuous finite element space is

$$V_h^p = \{v \in L^2([0, L]) : v|_{K_m} \in \mathbb{P}_p(K_m) \quad m = 1, \dots, N\}. \tag{4.11}$$

Then we define the jump and average of $v \in V_h^p$ at the endpoints of K_m as

$$[[v(z_{m+\frac{1}{2}})]] = v(z^-_{m+\frac{1}{2}}) - v(z^+_{m+\frac{1}{2}}), \qquad m = 1, \dots, N-1 \tag{4.12}$$

$$\{v(z_{m+\frac{1}{2}})\} = \frac{1}{2}(v(z^-_{m+\frac{1}{2}}) + v(z^+_{m+\frac{1}{2}})), \qquad m = 1, \dots, N-1. \tag{4.13}$$

We extend these definitions at the endpoints of the domain $[0, L]$ as

$$[[v(0)]] = -v(0^+), \quad \{v(0)\} = v(0^+), \quad [[v(L)]] = v(L^-), \quad \{v(L)\} = v(L^-). \tag{4.14}$$

We also recall that, thanks to the orthogonality properties of Legendre polynomials, the basis functions ϕ_l^m satisfy

$$\int_{z_{m-1/2}}^{z_{m+\frac{1}{2}}} \phi_p^m(z)\phi_q^m(z)dz = \Delta z_m \delta_{pq}. \tag{4.15}$$

We can now multiply (4.1) by a test function $v \in V_h^p$ and integrate by parts on each interval K_m (for notational simplicity we omit the dependences on time):

$$\begin{aligned}
&\int_{K_m} \frac{\partial q}{\partial t} v dz + f(q(z_{m+\frac{1}{2}}))v(z^-_{m+\frac{1}{2}}) - f(q(z_{m-1/2}))v(z^+_{m-1/2}) + \\
&- \int_{K_m} f(q)v' dz = \mu(z_{m+\frac{1}{2}})\frac{\partial q}{\partial z}(z_{m+\frac{1}{2}})v(z^-_{m+\frac{1}{2}}) + \\
&- \mu(z_{m-1/2})\frac{\partial q}{\partial z}(z_{m-1/2})v(z^+_{m-1/2}) - \int_{K_m} \mu \frac{\partial q}{\partial z} v' dz + \int_{K_m} svdz \qquad \forall v \in V_h^p
\end{aligned} \tag{4.16}$$

By adding all N equations above and applying the definitions of jump and average we obtain

$$\begin{aligned}
&\sum_{m=1}^{N} \int_{K_m} \frac{\partial q}{\partial t} v dz + \sum_{m=0}^{N} f(q(z_{m+\frac{1}{2}})) \left[\left[v(z_{m+\frac{1}{2}})\right]\right] - \sum_{m=1}^{N} \int_{K_m} f(q)v' dz = \\
&- \sum_{m=1}^{N} \int_{K_m} \mu \frac{\partial q}{\partial z} v' dz + \sum_{m=0}^{N} \left[\left[\mu(z_{m+\frac{1}{2}})\frac{\partial q}{\partial z}(z_{m+\frac{1}{2}})v(z_{m+\frac{1}{2}})\right]\right] + \\
&+ \sum_{m=1}^{N} \int_{K_m} svdz \quad \forall v \in V_h^p
\end{aligned}$$

If $1 \leq m \leq N-1$, i.e. at interior interfaces, the following relation holds true ([ABCM02],[Qua17]):

$$\begin{aligned}
&\left[\left[\mu(z_{m+\frac{1}{2}})\frac{\partial q}{\partial z}(z_{m+\frac{1}{2}})v(z_{m+\frac{1}{2}})\right]\right] = \\
&= \left\{\mu(z_{m+\frac{1}{2}})\frac{\partial q}{\partial z}(z_{m+\frac{1}{2}})\right\}\left[\left[v(z_{m+\frac{1}{2}})\right]\right] + \\
&+ \left\{v(z_{m+\frac{1}{2}})\right\}\left[\left[\mu(z_{m+\frac{1}{2}})\frac{\partial q}{\partial z}(z_{m+\frac{1}{2}})\right]\right].
\end{aligned} \tag{4.17}$$

Notice that, since we are considering a DG discretization on the domain $[0, L]$ alone, we do not consider the node $z = L$ as an interior interface, so we will not penalize the jumps of the solution there; this will no longer be the case

for the fully DG approach, as we will se in the next section. Theorem 8 and regularity of μ entail

$$\left[\left[\mu(z_{m+\frac{1}{2}})\frac{\partial q}{\partial z}(z_{m+\frac{1}{2}})\right]\right] = 0 \quad \left[\left[q(z_{m+\frac{1}{2}})\right]\right] = 0, \qquad m = 1, \dots, N-1 \tag{4.18}$$

thus

$$\begin{aligned}
&\sum_{m=1}^{N}\int_{K_m}\frac{\partial q}{\partial t}v dz + \sum_{m=1}^{N-1} f(q(z_{m+\frac{1}{2}}))\left[\left[v(z_{m+\frac{1}{2}})\right]\right] - \sum_{m=1}^{N}\int_{K_m} f(q)v' dz = \\
&= -\sum_{m=1}^{N}\int_{K_m}\mu\frac{\partial q}{\partial z}v' dz + \sum_{m=0}^{N}\left\{\mu(z_{m+\frac{1}{2}})\frac{\partial q}{\partial z}(z_{m+\frac{1}{2}})\right\}\left[\left[v(z_{m+\frac{1}{2}})\right]\right] + \\
&- \varepsilon\sum_{m=0}^{N}\left\{\mu(z_{m+\frac{1}{2}})v'(z_{m+\frac{1}{2}})\right\}\left[\left[q(z_{m+\frac{1}{2}})\right]\right] + \sum_{m=1}^{N}\int_{K_m} svdz + \\
&- \varepsilon\mu(0)v'(0)q(0) + \varepsilon\mu(L)v'(L)q(L) + f(q(0))v(0) - f(q(L))v(L) \qquad \forall v
\end{aligned}$$

Even if, in principle, ε may be any natural number, since the term it multiplies is always zero if q is the exact solution of (4.1), we only consider the cases $\varepsilon \in \{-1, 0, 1\}$, which correspond to the SIPG method (*Symmetric Interior Penalty Galerkin*) [Whe78][Arn82], NIPG method (*Non-symmetric Interior Penalty Galerkin*) [RWG99] and IIPG method (*Incomplete Interior Penalty Galerkin*) [DSW04].

The values of $q(0)$ and $q(L)$, involved in the discretization of the diffusion term, are provided by the Dirichlet condition (4.3) and by the spectral Laguerre discretization in the semi-infinite part K_{N+1}, respectively; in particular we have

$$q(0) = a(t) \tag{4.19}$$

$$q(L) = \sum_{j=0}^{M} q_j(t)\hat{\mathscr{L}}_j^{\beta}(0) = \sum_{j=0}^{M} q_j(t). \tag{4.20}$$

We now want to substitute the solution q with its approximation $q_h \in V_h^p$; in this case, the values of $f(q_h(z_{m+\frac{1}{2}}))$ and $f(q_h(L))$, coming from the discre-

tization of the hyperbolic contribution, are not defined, since q_h exhibits a jump at the interfaces $z_{m+\frac{1}{2}}$. To solve this issue we have to introduce a suitable numerical flux. In particular, we will employ the Rusanov flux, which, in our specific case, implies

$$f(q_h(z_{m+\frac{1}{2}},t)) = \frac{1}{2}\left[f(q_h(z^+_{m+\frac{1}{2}},t)) + f(q_h(z^-_{m+\frac{1}{2}},t))\right] + \\ - \frac{\Lambda_{m+1/2}(t)}{2}\left[q_h(z^+_{m+\frac{1}{2}},t) - q_h(z^-_{m+\frac{1}{2}},t)\right], \quad (4.21)$$

where

$$\Lambda_{m+1/2}(t) = \max\left(\left|\frac{df}{dq}(q_h(z^+_{m+\frac{1}{2}},t))\right|, \left|\frac{df}{dq}(q_h(z^+_{m+\frac{1}{2}},t))\right|\right). \quad (4.22)$$

At the interface $z = L = z_{N+1/2}$, this condition reads

$$f(q_h(L,t)) = \frac{1}{2}\left[f(q_M(L^+,t)) + f(q_h(L^-,t))\right] + \\ - \frac{\Lambda_{m+1/2}(t)}{2}\left[q_M(L^+,t) - q_h(L^-,t)\right], \quad (4.23)$$

so that another exchange of information between the two discretizations is performed. We may now define the bilinear form $a_\varepsilon : V_h^p \times V_h^p \times [0,+\infty) \to \mathbb{R}$ as

$$\begin{aligned} a_\varepsilon(w,v,t) = &\sum_{m=1}^{N}\int_{K_m}\mu\frac{\partial w}{\partial z}v'dz + \\ &- \sum_{m=0}^{N}\left\{\mu(z_{m+\frac{1}{2}},t)\frac{\partial w}{\partial z}(z_{m+\frac{1}{2}})\right\}\left[\left[v(z_{m+\frac{1}{2}})\right]\right] + \\ &+ \varepsilon\sum_{m=0}^{N}\left\{\mu(z_{m+\frac{1}{2}},t)v'(z_{m+\frac{1}{2}})\right\}\left[\left[w(z_{m+\frac{1}{2}})\right]\right] + \\ &+ \sum_{m=0}^{N}\frac{\sigma}{\Delta z_m}\left[\left[w(z_{m+\frac{1}{2}})\right]\right]\left[\left[v(z_{m+\frac{1}{2}})\right]\right], \end{aligned} \quad (4.24)$$

and $b : V_h^p \times V_h^p \to \mathbb{R}$ as

$$b(w,v) = \sum_{m=1}^{N-1} f(w(z_{m+\frac{1}{2}})) \left[\left[v(z_{m+\frac{1}{2}})\right]\right] + \\ - \sum_{m=1}^{N} \int_{K_m} f(w)v'dz - \sum_{m=1}^{N} \int_{K_m} s(w)vdz. \tag{4.25}$$

a_ε and b correspond to the discretizations of the diffusion and transport terms, respectively. We remark that, due to non-linearity of f and s, b will be in general a non-linear function of w and v. We also introduce
$g : V_h^p \times V_h^p \to \mathbb{R}$, $h : V_h^p \times V_h^p \to \mathbb{R}$ as

$$g(w,v,t) = \varepsilon\mu(L,t)v'(L)w(L) + \frac{\sigma}{\Delta z_N} v(L)w(L) \tag{4.26}$$

$$h(w,v) = -f(w(L))v(L) \tag{4.27}$$

and the linear operator $L : V_h^p \times [0,+\infty) \to \mathbb{R}$

$$L(v,t) = -\varepsilon\mu(0,t)v'(0)a(t) + \frac{\sigma}{\Delta z_1} v(0)a(t) + f(a(t))v(0). \tag{4.28}$$

In the definitions of a_ε, g and L we added the terms with σ to penalize jumps at the interfaces in the numerical solution. This does not spoil the consistency of the method, since the jumps of the exact solution are zero inside the domain, but it improves its stability properties; indeed, while the NIPG method is stable for any $\sigma > 0$, SIPG and IIPG require a sufficiently large σ in order to reach stability. The bilinear form g encodes the coupling of the discretizations of the diffusion term between the two domains, while h contains the exchange of information concerning the non-linear advection part. The linear operator L is related to the Dirichlet condition at the left endpoint $z = 0$. Again, because of the presence of f, h will be non-linear in its first argument.

The weak formulation reads then as follows: for all $t > 0$ we want to find $q_h(t) \in V_h^p$ such that

$$\int_0^L \frac{\partial q_h}{\partial t} v dz + a_\varepsilon(q_h, v, t) + b(q_h, v) = L(v, t) + g(q_h, v, t) + h(q_h, v) \quad \forall v \in V_h^p. \tag{4.29}$$

Next we choose q_h as in (4.6), we insert this expansion in (4.29) and test it against $v = \phi_i^l$, $l = 1, \ldots, N$, $i = 0, \ldots, p$. The approximation q_h is completely determined when the coefficients α_m^j are known for all $m = 1, \ldots, N$ and $j = 0, \ldots, p$. Therefore, (4.29) reads now

$$\begin{aligned} &\forall t > 0, \text{ find } \alpha_m^j(t), \quad m = 1, \ldots, N, \quad j = 0, \ldots, p \quad \text{ such that} \\ &\sum_{j=0}^{p} \frac{d\alpha_m^j(t)}{dt} \int_0^L \phi_j^m(z)\phi_i^l(z)dz + \sum_{j=0}^{p} \alpha_m^j(t) a_\varepsilon(\phi_j^m(z), \phi_i^l(z), t) + \\ &+ b\left(\sum_{j=0}^{p} \alpha_m^j(t)\phi_j^m(z), \phi_i^l(z)\right) = L(\phi_i^l(z), t) + g(q_h, \phi_i^l(z), t) + \\ &+ h\left(q_h, \phi_i^l(z)\right) \\ &\forall l = 1, \ldots, N, \quad i = 0, \ldots, p. \end{aligned} \tag{4.30}$$

Because of the local support of the basis functions, we have

$$\int_0^L \phi_j^m(z)\phi_i^l(z)dz = \Delta z_m \delta_{ji}\delta_{ml}, \tag{4.31}$$

thus, assuming a uniform grid, $\Delta z_m = \Delta z \quad \forall m$,

$$\begin{aligned} \frac{d\alpha_l^i(t)}{dt} = &- \frac{1}{\Delta z} \sum_{j=0}^{p} a_\varepsilon(\phi_j^m(z), \phi_i^l(z), t)\alpha_m^j(t) + \\ &- \frac{1}{\Delta z} b\left(\sum_{j=0}^{p} \alpha_m^j(t)\phi_j^m(z), \phi_i^l(z)\right) + \frac{1}{\Delta z} L(\phi_i^l(z), t) + \\ &+ \frac{1}{\Delta z} g(q_h, \phi_i^l(z), t) + \frac{1}{\Delta z} h\left(q_h, \phi_i^l(z)\right). \end{aligned} \tag{4.32}$$

We now want to rewrite this problem in vector form. We introduce the

$N(p+1) \times N(p+1)$ square matrix $\mathbf{A}_{DG}(t)$, whose entries are

$$a_{l(i+1),m(j+1)}(t) = -\frac{1}{\Delta z} a_\varepsilon(\phi_j^m(z), \phi_i^l(z), t), \quad l, m = 1, \ldots, N \quad i, j = 0, \ldots, p, \tag{4.33}$$

and the vector $\mathbf{b}_{DG}(\mathbf{q}_{DG}(t)) \in \mathbb{R}^{N(p+1)}$ as

$$b_{l(i+1)}(\mathbf{q}_{DG}(t)) = -\frac{1}{\Delta z} b\left(\sum_{j=0}^{p} \alpha_m^j(t)\phi_j^m(z), \phi_i^l(z)\right), \tag{4.34}$$

which is the discrete counterpart of the non-linear hyperbolic part of the model problem. The integral in the definition of a_ε will be computed using a suitable quadrature rule.

We define $\mathbf{g}_{DG}(t) \in \mathbb{R}^{N(p+1)}$ as

$$(g_{DG})_{l(i+1)}(t) = \frac{1}{\Delta z}\left(-\varepsilon\mu(0,t)(\phi_i^l)'(0)a(t) + \frac{\sigma}{\Delta z}\phi_i^l(0)a(t) + \phi_i^l(0)f(a(t))\right), \tag{4.35}$$

which encodes the contribution of the linear operator (4.28) due to the Dirichlet condition at the left endpoint. Because of the local support of the basis functions, only the first $p+1$ entries of $\mathbf{g}_{DG}$, corresponding to the leftmost sub-interval K_1, will be non-zero. By substituting the expression for $q_h(L)$ in the definition of g, we find

$$\frac{1}{\Delta z} g(q_h, \phi_i^l) = \frac{1}{\Delta z}\left(\varepsilon\mu(L,t)(\phi_i^l)'(L)\sum_{j=0}^{M} q_j + \frac{\sigma}{\Delta z}\phi_i^l(L)\sum_{j=0}^{M} q_j\right). \tag{4.36}$$

We then define the coupling matrix $\mathbf{A}_{DG,mod}(t) \in \mathbb{R}^{N(p+1)\times(M+1)}$. Because of the local support of the basis functions ϕ_i^l we have

$$(a_{DG,mod})_{l(i+1),j} = \begin{cases} 0 & l \leq N-1 \\ \\ \dfrac{1}{\Delta z}\left(\varepsilon\mu(L,t)(\phi_i^l)'(L) + \dfrac{\sigma}{\Delta z}\phi_i^l(L)\right) & l = N, \quad i = 0, \ldots, p \end{cases}$$

We notice that the only non-zero entries appear in the bottom $p+1$ rows. We can now write

$$g(q_h, \phi_i^l, t) = \sum_{j=1}^{M+1} (a_{DG,mod})_{l(i+1),j}(t)(q_{mod})_j. \tag{4.37}$$

Finally, substituting the expression for $f(q_h(L))$ in the definition of h according to the Rusanov flux we have

$$\begin{aligned}\frac{1}{\Delta z}h(q_h, \phi_i^l) = -\frac{1}{\Delta z}(\frac{1}{2}\left[f(q_M(L^+, t)) + f(q_h(L^-, t))\right] + \\ - \frac{\Lambda_{m+1/2}(t)}{2}\left[q_M(L^+, t) - q_h(L^-, t)\right])\phi_i^l(L) = (h_{DG})_{l,i+1}(\mathbf{q}(t)).\end{aligned} \tag{4.38}$$

Because of the exchange of information, the vector $\mathbf{h}_{DG} \in \mathbb{R}^{N(p+1)}$ depends on the unknown coefficients of both the bounded and unbounded subdomains. The resulting formulation is then

$$\begin{aligned}\frac{d\mathbf{q}_{DG}(t)}{dt} = \mathbf{A}_{DG}(t)\mathbf{q}_{DG}(t) + \mathbf{A}_{DG,mod}(t)\mathbf{q}_{mod}(t) + \\ + \mathbf{b}_{DG}(\mathbf{q}_{DG}(t)) + \mathbf{g}_{DG}(t) + \mathbf{h}_{DG}(\mathbf{q}(t)).\end{aligned} \tag{4.39}$$

As we can see, the equation for $\mathbf{q}_{DG}$ contains a dependence on the unknown coefficients q_j of the Laguerre expansion in K_{N+1}. This coupling consists of a linear part, through the matrix $\mathbf{A}_{DG,mod}$ related to the (linear) diffusion term, and a non-linear one, with the vector $\mathbf{h}_{DG}$ containing the flux exchange at the interface for the hyperbolic part. We remark that, due to the dependence of the diffusion μ on time, both matrices $\mathbf{A}_{DG}$ and $\mathbf{A}_{DG,mod}$ are, in general, functions of t.

4.1.2 Spectral discretization on the semi-infinite domain

We now describe how to discretize (4.1) in the semi-infinite part of the domain. We multiply it by a test function v and we integrate by parts on the

whole semi-infinite sub-interval $K_{N+1} = [L, +\infty)$, applying the asymptotic condition at infinity.

$$\int_L^{+\infty} \frac{\partial q}{\partial t} v dz - f(q(L,t))v(L) - \int_L^{+\infty} f(q)\frac{\partial v}{\partial z} dz = \tag{4.40}$$
$$= -\int_L^{+\infty} \mu \frac{\partial q}{\partial z}\frac{\partial v}{\partial z} dz + \mu(L,t)\frac{\partial q}{\partial z}(L,t)v(L) + \int_L^{+\infty} s(q)v dz.$$

The value of $\dfrac{\partial q}{\partial z}(L,t)$ is provided by the expansion of the solution in the bounded region $[0, L]$ as

$$\frac{\partial q}{\partial z}(L^-,t) = \sum_{j=0}^{p} \alpha_N^j(t)(\phi_j^N)'(L) \tag{4.41}$$

If we now replace q with its expansion q_M as in (4.7), we have to define the value of $f(q_M(L,t))$, appearing in the second summand. Again, we apply the Rusanov flux to get

$$f(q_M(L,t)) = \frac{1}{2}\left[f(q_M(L^+,t)) + f(q_h(L^-,t))\right] + \\ - \frac{\Lambda_{m+1/2}(t)}{2}\left[q_M(L^+,t) - q_h(L^-,t)\right], \tag{4.42}$$

where

$$q_M(L^+,t) = \sum_{j=0}^{M} q_j(t)\hat{\mathscr{L}}_j^{\beta}(0) = \sum_{j=0}^{M} q_j(t) \tag{4.43}$$

and

$$q_h(L^-,t) = \sum_{j=0}^{p} \alpha_N^j(t)\phi_i^N(L^-). \tag{4.44}$$

Moreover, by choosing $v = \hat{\mathscr{L}}_i^{\beta}(z-L)$ in (4.40) (we will omit the dependence on the independent variable in the following), with $i = 0, \ldots, M$, the Galerkin formulation (4.40) reads as follows: for any $t > 0$, find $q_i(t)$,

$i = 0, \dots, M$, such that

$$\sum_{j=0}^{M} \frac{dq_j(t)}{dt} \left(\hat{\mathscr{L}}_j^\beta, \hat{\mathscr{L}}_i^\beta \right) - f(q_M(L,t)) \hat{\mathscr{L}}_i^\beta(0) + \tag{4.45}$$
$$- \left(f\left(\sum_{j=0}^{M} q_j(t) \hat{\mathscr{L}}_j^\beta \right), (\hat{\mathscr{L}}_i^\beta)' \right) =$$
$$= - \sum_{j=0}^{M} q_j(t) \left(\mu(\hat{\mathscr{L}}_j^\beta)', (\hat{\mathscr{L}}_i^\beta)' \right) +$$
$$+ \left(s\left(\sum_{j=0}^{M} q_j(t) \hat{\mathscr{L}}_j^\beta \right), \hat{\mathscr{L}}_i^\beta \right) + \mu(L,t) \sum_{j=0}^{p} \alpha_N^j(t) (\phi_j^N)'(L) \hat{\mathscr{L}}_i^\beta(0),$$

where we used the shorthand notation $(.\,,.)$ to denote the integral of the product on $[L, +\infty)$. Problem (4.45) can now be written in vector form: arranging the unknown $q_j(t)$ in a vector $\mathbf{q}_{mod}(t)$ we find

$$\frac{d\mathbf{q}_{mod}(t)}{dt} = \mathbf{A}_{mod}(t)\mathbf{q}_{mod}(t) + \mathbf{A}_{mod,DG}(t)\mathbf{q}_{DG}(t) + \mathbf{b}_{mod}\left(\mathbf{q}_{mod}(t)\right) + \mathbf{h}_{mod}(\mathbf{q}(t)), \tag{4.46}$$

where

$$(a_{mod})_{ij} = -\beta \left(\mu(\hat{\mathscr{L}}_j^\beta)', (\hat{\mathscr{L}}_i^\beta)' \right), \tag{4.47}$$
$$(b_{mod})_i(\mathbf{q}_{mod}(t)) = \beta \left(f\left(\sum_{j=0}^{M} q_j(t) \hat{\mathscr{L}}_j^\beta \right), (\hat{\mathscr{L}}_i^\beta)' \right) +$$
$$+ \beta \left(s\left(\sum_{j=0}^{M} q_j(t) \hat{\mathscr{L}}_j^\beta \right), \hat{\mathscr{L}}_i^\beta \right),$$
$$(h_{mod})_i(\mathbf{q}(t)) = \beta f(q_M(L,t))[1, \dots, 1]^T,$$

while the entries of the coupling matrix $\mathbf{A}_{mod,DG} \in \mathbb{R}^{(M+1)\times N(p+1)}$ are

$$(a_{mod,DG})_{i,j(k+1)} = \begin{cases} 0 & j \leq N-1 \\ -\mu(L,t)\beta(\phi_k^N)'(L) & j = N, \quad k = 0, \dots, p \end{cases}.$$

The entries of $\mathbf{A}_{mod}$ are computed by means of GLR quadrature rules. Analogously to the previous section, the vector $\mathbf{b}_{mod}$ comes from the discretization

of the non-linear advective part of the equation, while $\mathbf{h}_{mod}$ couples the finite and semi-infinite parts through the Rusanov flux at the interface. Moreover, the coupling matrix $\mathbf{A}_{mod,DG}$ allows the exchange of information at the interface due to the integration by part of the linear diffusive term; its entries are mostly zero, except for the rightmost $p+1$ columns, since only the last sub-interval K_M of the bounded region is involved. We remark again the dependence on time of both matrices in (4.46).

4.2 Fully DG scheme

In this section we examine a different approach to the coupling, namely a full DG scheme on the whole half-line, where we consider the point $z = L$ as an internal interface. The finite element space is here defined as

$$V_h^p = \{v \in L^2([0,+\infty)) : v|_{K_m} \in \mathbb{P}_p(K_m) \quad m = 1,\dots,N\} \tag{4.48}$$

and (4.18) hold true for $m = N$ as well. Therefore, we multiply (4.1) by a test function in V_h^p and we integrate by parts on each interval K_m with $m = 1,\dots,N+1$. We then add the resulting $N+1$ equations and use (4.18) to obtain

$$\begin{aligned}
&\sum_{m=1}^{N+1}\int_{K_m}\frac{\partial q}{\partial t}v\,dz + \sum_{m=1}^{N} f(q(z_{m+\frac{1}{2}}))\left[\left[v(z_{m+\frac{1}{2}})\right]\right] - \sum_{m=1}^{N+1}\int_{K_m} f(q)v'dz = \\
&= -\sum_{m=1}^{N+1}\int_{K_m}\mu\frac{\partial q}{\partial z}v'dz + \sum_{m=0}^{N}\left\{\mu(z_{m+\frac{1}{2}})\frac{\partial q}{\partial z}(z_{m+\frac{1}{2}})\right\}\left[\left[v(z_{m+\frac{1}{2}})\right]\right] + \\
&- \varepsilon\sum_{m=0}^{N}\left\{\mu(z_{m+\frac{1}{2}})v'(z_{m+\frac{1}{2}})\right\}\left[\left[q(z_{m+\frac{1}{2}})\right]\right] + \sum_{m=1}^{N+1}\int_{K_m} svdz + \\
&- \varepsilon\mu(0)v'(0)q(0) + f(q(0))v(0) \qquad \forall v \in V_h^p.
\end{aligned}$$

We may now define the bilinear form $a_\varepsilon : V_h^p \times V_h^p \times [0, +\infty) \to \mathbb{R}$ as

$$\begin{aligned} a_\varepsilon(w, v, t) = &\sum_{m=1}^{N+1} \int_{K_m} \mu \frac{\partial w}{\partial z} v' dz + \\ &- \sum_{m=0}^{N} \left\{ \mu(z_{m+\frac{1}{2}}, t) \frac{\partial w}{\partial z}(z_{m+\frac{1}{2}}) \right\} \left[\left[v(z_{m+\frac{1}{2}}) \right] \right] + \\ &+ \varepsilon \sum_{m=0}^{N} \left\{ \mu(z_{m+\frac{1}{2}}, t) v'(z_{m+\frac{1}{2}}) \right\} \left[\left[w(z_{m+\frac{1}{2}}) \right] \right] + \\ &+ \sum_{m=0}^{N} \frac{\sigma}{\Delta z_m} \left[\left[w(z_{m+\frac{1}{2}}) \right] \right] \left[\left[v(z_{m+\frac{1}{2}}) \right] \right], \end{aligned} \tag{4.49}$$

and $b : V_h^p \times V_h^p \to \mathbb{R}$ as

$$\begin{aligned} b(w, v) = &\sum_{m=1}^{N} f(w(z_{m+\frac{1}{2}})) \left[\left[v(z_{m+\frac{1}{2}}) \right] \right] + \\ &- \sum_{m=1}^{N+1} \int_{K_m} f(w) v' dz - \sum_{m=1}^{N+1} \int_{K_m} s(w) v dz. \end{aligned} \tag{4.50}$$

Notice the difference with (4.24) and (4.25): here, the point $L = z_{N+1/2}$ is also included in the sums, since it is considered as an internal interface of a full DG scheme. We also introduce $h : V_h^p \times V_h^p \to \mathbb{R}$ as

$$h(w, v) = -f(w(L))v(L) \tag{4.51}$$

and the linear operator $L : V_h^p \times [0, +\infty) \to \mathbb{R}$

$$L(v, t) = -\varepsilon \mu(0, t) v'(0) a(t) + \frac{\sigma}{\Delta z_1} v(0) a(t) + f(a(t)) v(0). \tag{4.52}$$

The weak formulation reads then as follows: for all $t > 0$ we want to find $q_h(t) \in V_h^p$ such that

$$\int_0^{+\infty} \frac{\partial q_h}{\partial t} v dz + a_\varepsilon(q_h, v, t) + b(q_h, v) = L(v, t) + h(q_h, v) \quad \forall v \in V_h^p. \tag{4.53}$$

Next we choose q_h as in (4.6) or (4.7), we insert this expansion in (4.53) and test it against $v = \phi_i^l$, for $l = 1, \ldots, N$, $i = 0, \ldots, p$ and $v = \hat{\mathscr{L}}_j^\beta(z - L)$,

for $j = 0, \ldots, M$, respectively. Considering the bounded region $[0, L]$, we use the expansion (4.6) and the test functions $v = \phi_i^l$; therefore, (4.53) reads

$$\begin{aligned} &\forall t > 0, \text{ find } \alpha_m^j(t), \quad m = 1, \ldots, N, \quad j = 0, \ldots, p \quad \text{such that} \\ &\sum_{j=0}^{p} \frac{d\alpha_m^j(t)}{dt} \int_0^{+\infty} \phi_j^m(z)\phi_i^l(z)dz + \sum_{j=0}^{p} \alpha_m^j(t) a_\varepsilon(\phi_j^m(z), \phi_i^l(z), t) + \\ &+b\left(\sum_{j=0}^{p} \alpha_m^j(t)\phi_j^m(z), \phi_i^l(z)\right) = L(\phi_i^l(z), t) + h\left(q_h, \phi_i^l(z)\right) \\ &\forall l = 1, \ldots, N, \quad i = 0, \ldots, p. \end{aligned} \tag{4.54}$$

Because of the local support of the basis functions, we have

$$\int_0^{+\infty} \phi_j^m(z)\phi_i^l(z)dz = \Delta z_m \delta_{ji}\delta_{ml}, \tag{4.55}$$

thus, assuming a uniform grid, $\Delta z_m = \Delta z \quad \forall m$,

$$\begin{aligned} \frac{d\alpha_l^i(t)}{dt} = &- \frac{1}{\Delta z} \sum_{j=0}^{p} a_\varepsilon(\phi_j^m(z), \phi_i^l(z), t)\alpha_m^j(t) + \\ &- \frac{1}{\Delta z} b\left(\sum_{j=0}^{p} \alpha_m^j(t)\phi_j^m(z), \phi_i^l(z)\right) + \frac{1}{\Delta z} L(\phi_i^l(z), t) + \\ &+ \frac{1}{\Delta z} h\left(q_h, \phi_i^l(z)\right). \end{aligned} \tag{4.56}$$

On the other hand, in the sub-interval $[L, +\infty)$ we use scaled Laguerre basis functions. Thus, by choosing $v = \hat{\mathscr{L}}_i^\beta(z - L)$ in (4.53) (we will omit the dependence on the independent variable in the following), with $i = 0, \ldots, M$, the weak formulation reads as follows: for any $t > 0$, find $q_i(t)$,
$i = 0, \ldots, M$, such that

$$\begin{aligned} &\sum_{j=0}^{M} \frac{dq_j(t)}{dt} \left(\hat{\mathscr{L}}_j^\beta, \hat{\mathscr{L}}_i^\beta\right) + \sum_{j=0}^{M} q_j(t) a_\varepsilon(\hat{\mathscr{L}}_j^\beta, \hat{\mathscr{L}}_i^\beta) + \\ &+b\left(\sum_{j=0}^{M} q_j(t)\hat{\mathscr{L}}_j^\beta, \hat{\mathscr{L}}_i^\beta\right) = h(q_h, \hat{\mathscr{L}}_i^\beta), \end{aligned} \tag{4.57}$$

where, thanks to the orthogonality properties of scaled Laguerre functions,

$$\left(\hat{\mathscr{L}}_j^\beta, \hat{\mathscr{L}}_i^\beta\right) = \frac{1}{\beta}\delta_{ij}, \tag{4.58}$$

so that

$$\begin{aligned}\frac{dq_i(t)}{dt} =& -\beta \sum_{j=0}^{M} q_j(t) a_\varepsilon(\hat{\mathscr{L}}_j^\beta, \hat{\mathscr{L}}_i^\beta) + \\ & -\beta b\left(\sum_{j=0}^{M} q_j(t)\hat{\mathscr{L}}_j^\beta, \hat{\mathscr{L}}_i^\beta\right) + \beta h(q_h, \hat{\mathscr{L}}_i^\beta).\end{aligned} \tag{4.59}$$

As for the hyperbolic part, we define $f(q_h(L,t))$ in terms of the Rusanov flux (4.21); we now focus on the penalization of jumps at the interface $z = z_{N+1/2} = L$. At this point, the contribution to the bilinear form a_ε is given by

$$-\left\{\mu(L)\frac{\partial q}{\partial z}(L)\right\}[[v(L)]] + \varepsilon\left\{\mu(L)v'(L)\right\}[[q(L)]] + \frac{\sigma}{\Delta z}[[q(L)]][[v(L)]]. \tag{4.60}$$

Expanding the definitions of averages and jumps and assuming that μ is continuous across the interface we find

$$\begin{aligned}&-\frac{\mu(L)}{2}\left(\frac{\partial q}{\partial z}(L^+) + \frac{\partial q}{\partial z}(L^-)\right)(v(L^-) - v(L^+)) + \\ &+\mu(L)\varepsilon\frac{v'(L^+) + v'(L^-)}{2}(q(L^-) - q(L^+)) + \\ &+\frac{\sigma}{\Delta z}(q(L^-) - q(L^+))(v(L^-) - v(L^+)).\end{aligned} \tag{4.61}$$

If we insert the expansion of the solution and we choose

$$v(L^-) = \phi_i^N(L) \qquad v(L^+) = \hat{\mathscr{L}}_i^\beta(0) = 1 \tag{4.62}$$

$$v'(L^-) = (\phi_i^N(L))' \qquad v'(L^+) = (\hat{\mathscr{L}}_i^\beta)'(0) \tag{4.63}$$

we can identify the matrices $\mathbf{A}'_{DG} \in \mathbb{R}^{(p+1)\times(p+1)}$ and $\mathbf{A}'_{mod} \in \mathbb{R}^{(M+1)\times(M+1)}$,

defined as

$$(a'_{DG})_{i+1,j+1} = \frac{1}{\Delta z}\Big(\frac{\mu}{2}(\phi_j^N)'(L)\phi_i^N(L) - \frac{\mu\varepsilon}{2}(\phi_i^N)'(L)\phi_j^N(L) + \\ - \frac{\sigma}{\Delta z}\phi_i^N(L)\phi_j^N(L)\Big) \tag{4.64}$$

$$(a'_{mod})_{i+1,j+1} = \beta\left(-\frac{\mu}{2}(\hat{\mathscr{L}}_j^\beta)'(0) + \frac{\mu\varepsilon}{2}(\hat{\mathscr{L}}_i^\beta)'(0) - \frac{\sigma}{\Delta z}\right) \tag{4.65}$$

and the two coupling matrices $\mathbf{A}_{DG,mod} \in \mathbb{R}^{N(p+1)\times(M+1)}$ and $\mathbf{A}_{mod,DG} \in \mathbb{R}^{(M+1)\times N(p+1)}$. Their entries $(a_{DG,mod})_{l(i+1),j+1}$ and $(a_{mod,DG})_{i+1,j(k+1)}$ are given by

$$\begin{cases} 0 & l \leq N-1 \\ \\ \dfrac{1}{\Delta z}\left(\dfrac{\mu}{2}\phi_i^N(L)(\hat{\mathscr{L}}_j^\beta)'(0) + \dfrac{\mu\varepsilon}{2}(\phi_i^N)'(L) + \dfrac{\sigma}{\Delta z}\phi_i^N(L)\right) & l = N, \end{cases} \tag{4.66}$$

and

$$\begin{cases} 0 & j \leq N-1 \\ \\ \beta\left(-\dfrac{\mu}{2}(\phi_j^N)'(L) - \dfrac{\mu\varepsilon}{2}\phi_j^N(L)(\hat{\mathscr{L}}_i^\beta)'(0) + \dfrac{\sigma}{\Delta z}\phi_j^N(L)\right) & j = N, \end{cases} \tag{4.67}$$

respectively. We notice that the coupling matrices for this fully DG approach contain parameters related both to the DG scheme, i.e. ε and σ, and to the Laguerre discretization, i.e. β; this was not the case in the coupling matrices of Section 4.1. We can further simplify their expressions by recalling that

$$(\hat{\mathscr{L}}_i^\beta)'(0) = -\beta\sum_{k=0}^{i-1}\hat{\mathscr{L}}_k^\beta(0) - \frac{\beta}{2}\hat{\mathscr{L}}_i^\beta(0) = -\beta\left(i+\frac{1}{2}\right) \tag{4.68}$$

We also introduce the $N(p+1)\times N(p+1)$ square matrix $\mathbf{A}_{DG}(t)$, whose

entries are

$$a_{l(i+1),m(j+1)}(t) = \begin{cases} -\dfrac{1}{\Delta z} a_\varepsilon(\phi_j^m(z), \phi_i^l(z), t) & l, m = 1, \dots, N-1, \\ \\ (a'_{DG})_{i+1,j+1} & l = m = N \end{cases} \tag{4.69}$$

and the vector $\mathbf{b}_{DG}(\mathbf{q}_{DG}(t)) \in \mathbb{R}^{N(p+1)}$ as

$$b_{l(i+1)}(\mathbf{q}_{DG}(t)) = -\frac{1}{\Delta z} b\left(\sum_{j=0}^{p} \alpha_m^j(t)\phi_j^m(z), \phi_i^l(z)\right), \tag{4.70}$$

which is the discrete counterpart of the non-linear hyperbolic part of the model problem. The integral in the definition of a_ε will be computed using a suitable quadrature rule.

We define $\mathbf{g}_{DG}(t) \in \mathbb{R}^{N(p+1)}$ as

$$(g_{DG})_{l(i+1)}(t) = \frac{1}{\Delta z}\left(-\varepsilon\mu(0,t)(\phi_i^l)'(0)a(t) + \frac{\sigma}{\Delta z}\phi_i^l(0)a(t) + \phi_i^l(0)f(a(t))\right), \tag{4.71}$$

which encodes the contribution of the linear operator (4.52) due to the Dirichlet condition at the left endpoint. Finally, substituting the expression for $f(q_h(L))$ in the definition of h according to the Rusanov flux we have

$$\begin{aligned} \frac{1}{\Delta z} h(q_h, \phi_i^l) = -\frac{1}{\Delta z}(&\frac{1}{2}\left[f(q_h(L^+,t)) + f(q_h(L^-,t))\right] + \\ &- \frac{\Lambda_{m+1/2}(t)}{2}\left[q_h(L^+,t) - q_h(L^-,t)\right])\phi_i^l(L) = (h_{DG})_{l,i+1}(\mathbf{q}(t)). \end{aligned} \tag{4.72}$$

Because of the exchange of information, the vector $\mathbf{h}_{DG} \in \mathbb{R}^{N(p+1)}$ depends on the unknown coefficients of both the bounded and unbounded subdomains. The resulting formulation for this part of the domain is then

$$\begin{aligned} \frac{d\mathbf{q}_{DG}(t)}{dt} = \mathbf{A}_{DG}(t)\mathbf{q}_{DG}(t) + \mathbf{A}_{DG,mod}(t)\mathbf{q}_{mod}(t) + \\ + \mathbf{b}_{DG}(\mathbf{q}_{DG}(t)) + \mathbf{g}_{DG}(t) + \mathbf{h}_{DG}(\mathbf{q}(t)). \end{aligned} \tag{4.73}$$

Concerning the infinite sub-interval K_{N+1}, we define

$$(a_{mod})_{ij} = -\beta\left(\mu(\hat{\mathscr{L}}_j^\beta)', (\hat{\mathscr{L}}_i^\beta)'\right) + (a'_{mod})_{ij}, \tag{4.74}$$

$$(b_{mod})_i(\mathbf{q}_{mod}(t)) = -\beta b\left(\sum_{j=0}^{M} q_j(t)\hat{\mathscr{L}}_j^\beta(z), \hat{\mathscr{L}}_i^\beta(z)\right),$$

$$(h_{mod})_i(\mathbf{q}(t)) = \beta f(q_h(L,t))[1,\ldots,1]^T,$$

where again $f(q_h(L,t))$ is written in terms of the Rusanov flux, so that

$$\frac{d\mathbf{q}_{mod}(t)}{dt} = \mathbf{A}_{mod}(t)\mathbf{q}_{mod}(t) + \mathbf{A}_{mod,DG}(t)\mathbf{q}_{DG}(t) + \\ + \mathbf{b}_{mod}\left(\mathbf{q}_{mod}(t)\right) + \mathbf{h}_{mod}(\mathbf{q}(t)). \tag{4.75}$$

4.3 Coupling of the two discretizations and time integration

We now collect the results of the previous sections in a unified discretization scheme on the whole domain $[0, +\infty)$. Regardless of the approach employed for the coupling, we may define the global unknown vector as

$$\mathbf{q}(t) = (\mathbf{q}_{DG}(t), \mathbf{q}_{mod}(t))^T \in \mathbb{R}^{N(p+1)+M+1}, \tag{4.76}$$

the global vectors

$$\mathbf{b}(\mathbf{q}(t)) = (\mathbf{b}_{DG}(\mathbf{q}_{DG}(t)), \mathbf{b}_{mod}(\mathbf{q}_{mod}(t)))^T \in \mathbb{R}^{N(p+1)+M+1}, \tag{4.77}$$

$$\mathbf{h}(\mathbf{q}) = (\mathbf{h}_{DG}(\mathbf{q}), \mathbf{h}_{mod}(\mathbf{q}))^T \in \mathbb{R}^{N(p+1)+M+1}, \tag{4.78}$$

and

$$\mathbf{g}(t) = (\mathbf{g}_{DG}(t), 0, \ldots, 0)^T \in \mathbb{R}^{N(p+1)+M+1}. \tag{4.79}$$

The global matrix is

$$\mathbf{A}(t) = \begin{pmatrix} \mathbf{A}_{DG}(t) & \mathbf{A}_{DG,mod}(t) \\ \mathbf{A}_{mod,DG}(t) & \mathbf{A}_{mod}(t) \end{pmatrix} \in \mathbb{R}^{(N(p+1)+M+1)\times(N(p+1)+M+1)} \tag{4.80}$$

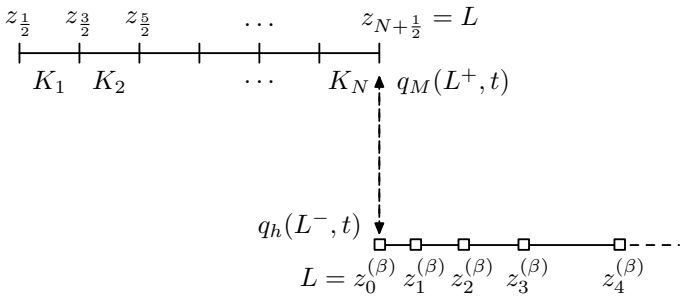

Figure 4.1: Scheme of the coupling between a DG and a Laguerre discretization for the solution of parabolic problems. Squares: Laguerre modes in the unbounded domain. Arrows: flux exchange at the interface.

so that the coupled semi-discrete formulation reads

$$\frac{d\mathbf{q}(t)}{dt} = \mathbf{A}(t)\mathbf{q}(t) + \mathbf{b}(\mathbf{q}(t)) + \mathbf{h}(\mathbf{q}(t)) + \mathbf{g}(t). \tag{4.81}$$

The matrix $\mathbf{A}$ is the discrete counterpart of the diffusion term; the vector $\mathbf{b}$ corresponds to the discretization of the non-linear advective part and the source-reaction term; the vector $\mathbf{h}$ contains the flux exchange at the interface $z = L$ by means of the application of the Rusanov flux to the flux function f; finally, the vector $\mathbf{g}$ encodes the Dirichlet condition at the left endpoint $q(0) = a(t)$. The scheme with the corresponding notations is shown in Figure 4.1. We remark that, because of the vectors $\mathbf{b}$ and $\mathbf{h}$, problem (4.81) is non-linear. However, if the functions f and s in (4.1) are linear, then $\mathbf{b}(\mathbf{q}(t))$ and $\mathbf{h}(\mathbf{q}(t))$ can be written as the product between a matrix and the unknown vector $\mathbf{q}(t)$. In this case, (4.81) is a linear system of equations; moreover, if μ is constant, then $\mathbf{A}$ does not depend on t and we recover the results of Chapter 3.

We now want to discretize Problem (4.81) in time. To this end we subdivide the time interval of interest $[0, T]$ as $0 = t^0 < t^1 < \cdots < t^n = T$, where we assume for simplicity $t^{i+1} - t^i = \Delta t$ for all $i = 0, \ldots, n-1$. We also define

$\mathbf{q}^i := \mathbf{q}(t^i)$. We now need an approximation of the initial datum $q^0(z)$. With the usual notation, we write $\mathbf{q}^0_{DG} := \mathbf{q}_{DG}(0)$. Using (4.6) we can compute the entries of the initial vector as

$$\alpha^i_m(0) = \frac{1}{\Delta z}\int_{K_m} q^0(z)\phi^m_i(z)dz, \qquad m = 1,\dots,N, \quad i = 0,\dots,p, \tag{4.82}$$

and

$$\mathbf{q}^0_{DG} = (\alpha^0_1(0),\dots,\alpha^p_1(0),\dots,\alpha^0_N(0),\dots,\alpha^p_N(0))^T. \tag{4.83}$$

In a similar fashion, using (4.7) we have

$$q_k(0) = \beta\int_L^{+\infty} q^0(z)\hat{\mathscr{L}}^\beta_k(z-L)dz, \quad k = 0,\dots,M. \tag{4.84}$$

and

$$\mathbf{q}^0_{mod} = [q_0(0),\dots,q_M(0)]^T. \tag{4.85}$$

According to the definition of $\mathbf{q}$, the initial vector will be given by

$$\mathbf{q}^0 = (\mathbf{q}^0_{DG}, \mathbf{q}^0_{mod})^T, \tag{4.86}$$

where $\mathbf{q}^0_{DG}$ and $\mathbf{q}^0_{mod}$ are defined by (4.83) and (4.85) respectively. The integrals appearing in (4.82) and (4.84) will be computed by means of appropriate quadrature rules, e.g. Gauss-Legendre and Gauss-Laguerre-Radau respectively.

To account for the most general possible case, we write (4.81) as

$$\frac{d\mathbf{q}(t)}{dt} = \mathbf{f}(t,\mathbf{q}(t)). \tag{4.87}$$

This problem can now be solved in time by using the θ-method, which amounts to setting

$$\frac{\mathbf{q}^{i+1}-\mathbf{q}^i}{\Delta t} = \theta(\mathbf{f}(t^{i+1},\mathbf{q}^{i+1})) + (1-\theta)(\mathbf{f}(t^i,\mathbf{q}^i)) \qquad i = 0,\dots,n-1, \tag{4.88}$$

where $\theta \in [0,1]$. Forward Euler (FE), backward Euler (BE) and Crank-Nicolson (CN) methods are special cases corresponding to $\theta = 0$, $\theta = 1$

and $\theta = 1/2$ respectively. All θ-methods are first-order accurate, except for CN which is second-order. Moreover all the θ-methods for $\frac{1}{2} \leq \theta \leq 1$ are unconditionally stable (see for example [QSS07]).

If $\theta > 0$ the method is implicit, meaning that, in the general non-linear case, we have to solve a non-linear system of equations at each time step. Instead, we may also discretize the problem by employing the Runge-Kutta method defined as

$$\mathbf{q}^{n+1} = \mathbf{q}^n + \frac{\Delta t}{6}(\mathbf{K}_1 + \mathbf{K}_2 + 4\mathbf{K}_3) \tag{4.89}$$

$$\mathbf{K}_1 = \mathbf{f}(t^n, \mathbf{q}^n); \tag{4.90}$$

$$\mathbf{K}_2 = \mathbf{f}(t^n + \Delta t, \mathbf{q}^n + \Delta t \mathbf{K}_1); \tag{4.91}$$

$$\mathbf{K}_3 = \mathbf{f}\left(t^n + \frac{\Delta t}{2}, \mathbf{q}^n + \frac{\Delta t}{4}(\mathbf{K}_1 + \mathbf{K}_2)\right). \tag{4.92}$$

This scheme provides third-order convergence, but it requires a small time step being an explicit method.

4.4 Stability of the global matrix

We consider the global semi-discrete formulation (4.81) and we study the spectral stability of the matrix $\mathbf{A}$ as a function of the Péclet number Pe. In particular, we fix $L = 1\ m$, $\beta = 1$ and we set $p = 3$, $p = 2$ or $p = 1$. As in Chapter 3, we require that the maximum real part of its eigenvalues is non-positive; it turns out that this only happens if the number of intervals in the bounded region $[0, L]$ is large enough, or, equivalently, if the spacing Δz is sufficiently small.

Coupled DG-Laguerre scheme

The parameter for the DG discretization are $\epsilon = -1$ and $\sigma = 200$. As for u and μ, we examine two different cases: in each of them we choose one parameter equal to 1 and we set the second according to the value of Pe. The critical values Δz_{cr} for different values of M are shown in Tables 4.1 and 4.2; the coupling matrix is stable if $\Delta z < \Delta z_{cr}$, unstable otherwise.

Pe		0.001	10	100	500	1000
$M = 180$	$p = 3$	1/2	1/2	1/2	1/25	1/57
$M = 180$	$p = 2$	1/2	1/2	1/3	1/53	1/122
$M = 180$	$p = 1$	1/2	1/2	1/8	1/176	1/422
$M = 90$	$p = 3$	1/2	1/2	1/4	1/29	1/61
$M = 90$	$p = 2$	1/2	1/2	1/7	1/61	1/131
$M = 90$	$p = 1$	1/2	1/2	1/21	1/211	1/461
$M = 50$	$p = 3$	1/2	1/2	1/5	1/31	1/63
$M = 50$	$p = 2$	1/2	1/2	1/10	1/65	1/135
$M = 50$	$p = 1$	1/2	1/2	1/31	1/228	1/480
$M = 20$	$p = 3$	1/2	1/2	1/6	1/32	1/65
$M = 20$	$p = 2$	1/2	1/2	1/12	1/68	1/138
$M = 20$	$p = 1$	1/2	1/2	1/41	1/242	1/494

Table 4.1: Critical value of the finite domain grid spacing Δz for the stability of $\mathbf{A}$. $\mu = 1$, $u = Pe\mu$.

As we can see, if the Péclet number is small enough, approximately less than 100, the whole spectrum of $\mathbf{A}$ has negative real part regardless of the spacing Δz: 2 sub-elements in the unit interval are enough to make the scheme stable. On the other hand, high values of Pe require a fine grid in

Pe		0.001	10	100	500	1000
$M = 180$	$p = 3$	1/2	1/2	1/2	1/24	1/54
$M = 180$	$p = 2$	1/2	1/2	1/2	1/49	1/114
$M = 180$	$p = 1$	1/2	1/2	1/4	1/175	1/418
$M = 90$	$p = 3$	1/2	1/2	1/2	1/27	1/58
$M = 90$	$p = 2$	1/2	1/2	1/6	1/57	1/123
$M = 90$	$p = 1$	1/2	1/2	1/21	1/209	1/457
$M = 50$	$p = 3$	1/2	1/2	1/4	1/29	1/60
$M = 50$	$p = 2$	1/2	1/2	1/9	1/61	1/127
$M = 50$	$p = 1$	1/2	1/2	1/31	1/226	1/476
$M = 20$	$p = 3$	1/2	1/2	1/6	1/30	1/61
$M = 20$	$p = 2$	1/2	1/2	1/12	1/64	1/130
$M = 20$	$p = 1$	1/2	1/2	1/41	1/240	1/490

Table 4.2: Critical value of the finite domain grid spacing Δz for the stability of $\mathbf{A}$. $u = 1$, $\mu = u/Pe$.

$[0, L]$ to prevent spurious growth caused by eigenvalues with positive real part; the minimum number of sub-intervals N increases quite rapidly with Pe and also depends on the polynomial degree p. In particular, high-degree polynomials allow us to use larger sub-intervals without losing stability.

Fully DG scheme

We now examine the stability of the global matrix if a fully DG approach is used for the coupling. Results for different values of ε are shown in Tables 4.3 and 4.4 for $\sigma = 200$ and $\sigma = 20$, respectively.

		$Pe = 100$		$Pe = 500$		$Pe = 1000$	
M	p	$\varepsilon = -1$	$\varepsilon = 1$	$\varepsilon = -1$	$\varepsilon = 1$	$\varepsilon = -1$	$\varepsilon = 1$
180	3	1/2	1/2	1/4	1/3	1/9	1/9
180	2	1/2	1/2	1/8	1/7	1/20	1/20
180	1	1/2	1/2	1/9	1/9	1/20	1/20
90	3	1/2	1/2	1/5	1/5	1/13	1/13
90	2	1/2	1/2	1/9	1/9	1/21	1/21
90	1	1/2	1/2	1/10	1/10	1/21	1/21
50	3	1/2	1/2	1/6	1/6	1/10	1/10
50	2	1/2	1/2	1/10	1/10	1/22	1/22
50	1	1/2	1/2	1/10	1/10	1/21	1/21
20	3	1/2	1/2	1/5	1/5	1/8	1/8
20	2	1/2	1/2	1/10	1/10	1/22	1/22
20	1	1/2	1/2	1/10	1/10	1/21	1/21

Table 4.3: Critical value of the finite domain grid spacing Δz for the stability of $\mathbf{A}$ in the fully DG scheme. $\mu = 1$, $u = Pe\mu$, $\sigma = 200$.

The value of Δz shows no particular dependence on ε, while a higher penalization on jumps, corresponding to high values of σ, allows to take larger sub-intervals without losing stability. Unlike the previous approach, a reduction of M does not lead to a decrease of the critical Δz values; indeed, once the polynomial degree p is fixed, the critical value of the spacing appears to

		$Pe = 100$		$Pe = 500$		$Pe = 1000$	
M	p	$\varepsilon = -1$	$\varepsilon = 1$	$\varepsilon = -1$	$\varepsilon = 1$	$\varepsilon = -1$	$\varepsilon = 1$
180	3	1/6	1/2	1/21	1/12	1/40	1/37
180	2	1/7	1/2	1/35	1/33	1/73	1/73
180	1	1/6	1/2	1/30	1/31	1/61	1/62
90	3	1/5	1/2	1/20	1/19	1/34	1/30
90	2	1/7	1/5	1/37	1/37	1/75	1/77
90	1	1/5	1/2	1/30	1/31	1/61	1/62
50	3	1/4	1/3	1/18	1/16	1/30	1/26
50	2	1/7	1/6	1/37	1/38	1/75	1/79
50	1	1/5	1/3	1/30	1/31	1/61	1/62
20	3	1/5	1/4	1/15	1/13	1/27	1/24
20	2	1/8	1/8	1/38	1/40	1/76	1/80
20	1	1/7	1/7	1/30	1/31	1/61	1/62

Table 4.4: Critical value of the finite domain grid spacing Δz for the stability of $\mathbf{A}$ in the fully DG scheme. $\mu = 1$, $u = Pe\mu$, $\sigma = 20$.

be independent from M. As in the first coupling technique, higher values of the Péclet number require a finer grid to achieve stability.

As a consequence of this analysis, we will always make sure to choose N large enough in the following tests, especially in advection-dominated regimes.

Chapter 5

Numerical results

This chapter presents the results of several numerical experiments testing the accuracy of the schemes described in the previous chapters.

In Section 5.1 we take the advection-diffusion equation as a model problem and we consider a stand-alone modal approach on the basis of scaled Laguerre functions, checking that the rates of convergence in time and space are in accordance with theoretical results.

In Section 5.2 we consider the coupled scheme and we test it on the linear advection-diffusion equation, both homogeneous and non-homogeneous, on the Burgers' equation and on a non-linear reaction equation. We compare the results with a stand-alone DG discretization on a larger domain. By varying the number of sub-intervals in the bounded region, and the number of Laguerre nodes accordingly, we show that relative errors are small enough to prove the accuracy of the coupling.

Finally, in Section 5.3 we implement an absorbing layer in the semi-infinite part. Again, we examine the linear case, by considering outgoing perturbations both in the forms of single Gaussian profiles and wave trains, and the non-linear Burgers' equation, and we show that signals are damped with

negligible reflections at the interface.

5.1 Stand-alone Laguerre discretization

First, we evaluate the accuracy of the spectral discretization of the advection-diffusion equation with constant coefficients in the half-line to justify its coupling with a DG discretization on a bounded domain. In particular, our model problem will be

$$\frac{\partial q}{\partial t} - \mu \frac{\partial^2 q}{\partial z^2} + u \frac{\partial q}{\partial z} = f(z,t) \qquad z \in [0, +\infty), \quad t > 0 \tag{5.1}$$

We assume that the solution vanishes at infinity:

$$\lim_{z \to +\infty} q(z,t) = 0. \tag{5.2}$$

Denoting by q_h and q the numerical and exact solution and exploiting the GLR quadrature rules with nodes $\{z_j^\beta\}_{j=0}^M$ and weights $\{\hat{\omega}_j^\beta\}_{j=0}^M$, we define the absolute errors as

$$\mathcal{E}_{L^2} = \sqrt{\sum_{j=0}^{M} \left(q_h(z_j^\beta) - q(z_j^\beta) \right)^2 \hat{\omega}_j^\beta} \tag{5.3}$$

$$\mathcal{E}_{H^1} = \sqrt{\mathcal{E}_{L^2}^2 + \sum_{j=0}^{M} \left(q_h'(z_j^\beta) - q'(z_j^\beta) \right)^2 \hat{\omega}_j^\beta} \tag{5.4}$$

$$\mathcal{E}_{L^1} = \sum_{j=0}^{M} |q_h(z_j^\beta) - q(z_j^\beta)| \hat{\omega}_j^\beta \tag{5.5}$$

$$\mathcal{E}_{L^\infty} = \max_{j=0,\ldots,M} |q_h(z_j^\beta) - q(z_j^\beta)| \tag{5.6}$$

We also want to determine the rate of time convergence of the method. Assuming that the error behaves like $\mathcal{E}(\Delta t) = K \Delta t^r$, where K is a constant independent on Δt, we have

$$\mathcal{E}(\Delta t) = K \Delta t^r, \qquad \mathcal{E}\left(\frac{\Delta t}{2}\right) = K \left(\frac{\Delta t}{2}\right)^r, \tag{5.7}$$

so that, dividing the two relations and solving for r,

$$r = \log_2 \frac{\mathcal{E}(\Delta t)}{\mathcal{E}(\Delta t/2)}. \tag{5.8}$$

We consider as exact solution, as in [Ben10],

$$q(z,t) = ze^{-z}\sin^2(z-t). \tag{5.9}$$

Since the spectral discretization on the half line will be coupled to the DG scheme on the bounded region by means of a flux condition at the interface, we impose a Neumann datum at $z = 0$, so that the matrix of the linear system will be the one denoted by Mod,LF,Neu in Table 3.1. We recall that, unlike the case of Dirichlet boundary conditions, this matrix is only stable if β is above a certain threshold depending on the Péclet number Pe, as shown in Table 3.4; since the values of Pe is set by the problem itself, we will choose the scaling parameter β to satisfy this bound and avoid numerical instabilities.

The first test concerns stability issues related to the Péclet number. The initial datum is

$$q_0(z) = q(z,0) = ze^{-z}\sin^2(z). \tag{5.10}$$

The number of Laguerre modes is $M = 50$ as in the analysis of spectral stability carried out in Chapter 3. We run the simulation until $T = 10\ s$ with $n = 200$ time intervals.

Table 5.1 shows the relative L^∞ errors for different choices of β, and the corresponding value of Pe_β. As expected, errors blow up if β is not large enough, or, equivalently, if Pe_β is not kept under control. Therefore, the value of the scaling parameter β can be set so as to and prevent instabilities. This is another relevant benefit provided by the scaling, which not only allows for the representation of arbitrarily large domains with a fixed number of spectral modes, but is also crucial to achieve stability.

μ	u	β	Pe_β	$\mathcal{E}_{L^\infty}$
1	100	1	100	2.4280e+15
1	100	15	6.67	1.1326e+09
1	100	20	5	2.4370e-02
0.01	1	1	100	9.8163e+10
0.01	1	10	10	2.6189e-03
1	1	0.01	100	4.2769e+04
1	1	0.1	10	1.4016e+00
1	1	1	1	2.9775e-04

Table 5.1: Absolute L^∞ errors as functions of β. Stand-alone Laguerre discretization of the advection-diffusion equation. $M = 50$, $\theta = 1/2$, $T = 10\,s$, $n = 200$.

We now analyze spatial error convergence; therefore, we fix a small time step, $n = 2000$ (so that $\Delta t = 0.005\,s$), and we compute the absolute L^2, H^1, L^1 and L^∞ errors with respect to the exact solution as we let M vary. We set $\mu = 4\,m^2/s$, $u = 8\,m/2$ and $\beta = 1$ so that $Pe_\beta = 2$. For each case, we also compute the Courant number, defined as $C = u\Delta t/\delta$, where δ is the distance between the first and the second GLR nodes. Results are reported in Figure 5.1 and Tables 5.2 and 5.3 for $\theta = 1/2$ and $\theta = 1$ respectively. As expected, the errors decay exponentially for small values of M (straight lines in the semi-logarithmic plots); when M is sufficiently large, the temporal error dominates and a constant level is attained.

As for time convergence, we fix a large number of modes, $M = 160$ and we reduce the time step Δt; the other parameters are kept as before. Tables 5.4 and 5.5 and the logarithmic plot in Figure 5.2 show that the expected rates of convergence are achieved by the implemented method. Note the different

values on the y axes for $\theta = 1/2$ and $\theta = 1$ in Figures 5.1 and 5.2.

M	C	$\mathcal{E}_{L^2}$	$\mathcal{E}_{H^1}$	$\mathcal{E}_{L^1}$	$\mathcal{E}_{L^\infty}$
10	0.1196	0.1911	0.4213	0.7315	0.1167
20	0.2287	0.0352	0.0957	0.1419	0.0160
40	0.4469	8.8581e-04	0.0281	0.0065	3.2054e-04
80	0.8830	3.2096e-06	0.0111	2.5095e-05	1.0008e-06
160	1.7544	3.1239e-06	0.0041	2.3237e-05	8.0047e-07

Table 5.2: Absolute L^2, H^1, L^1 and L^∞ errors and Courant number for space convergence, Laguerre stand-alone discretization of the advection-diffusion equation, $\theta = 1/2$, $\Delta t = 0.005\,s$, $\mu = 4\,m^2/s$, $u = 8\,m/s$, $\beta = 1$.

M	C	$\mathcal{E}_{L^2}$	$\mathcal{E}_{H^1}$	$\mathcal{E}_{L^1}$	$\mathcal{E}_{L^\infty}$
10	0.1196	0.1910	0.4215	0.7263	0.1164
20	0.2287	0.0352	0.0955	0.1437	0.0159
40	0.4469	0.0034	0.0283	0.0300	7.1656e-04
80	0.8830	0.0032	0.0115	0.0277	6.1982e-04
160	1.7544	0.0032	0.0052	0.0277	6.2404e-04

Table 5.3: Absolute L^2, H^1, L^1 and L^∞ errors and Courant number for space convergence, Laguerre stand-alone discretization of the advection-diffusion equation, $\theta = 1$, $\Delta t = 0.005\,s$, $\mu = 4\,m^2/s$, $u = 8\,m/s$, $\beta = 1$.

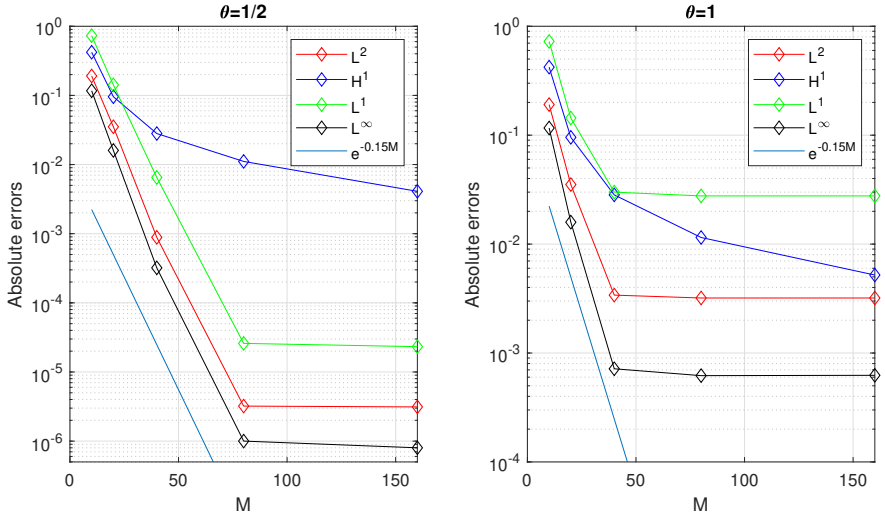

Figure 5.1: Absolute errors for space convergence, Laguerre stand-alone discretization of the advection-diffusion equation. Absolute L^2, H^1, L^1 and L^∞ errors. $n = 2000$, $T = 10\,s$, $\Delta t = 0.005\,s$.

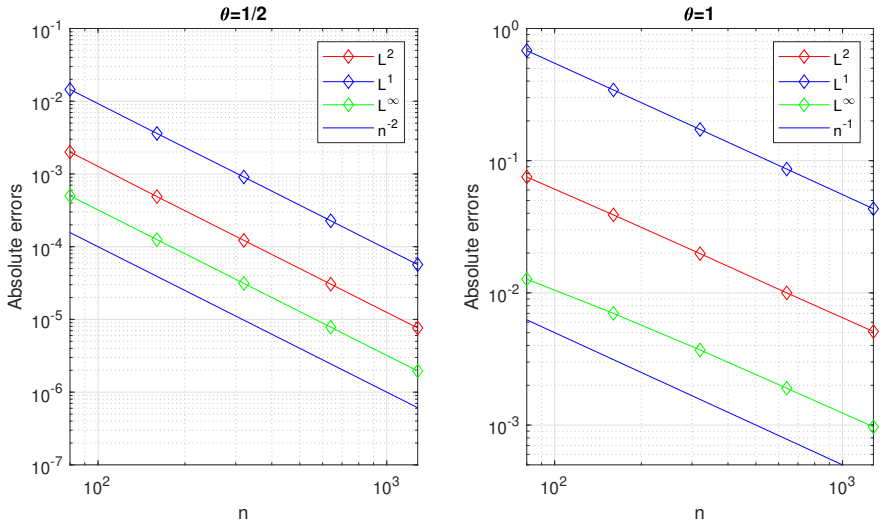

Figure 5.2: Absolute errors for time convergence, Laguerre stand-alone discretization of the advection-diffusion equations. Absolute L^2, L^1 and L^∞ errors. $M = 160$, $T = 10\,s$.

Δt	$\mathcal{E}_{L^2}$	r_{L^2}	$\mathcal{E}_{L^1}$	r_{L^1}	$\mathcal{E}_{L^\infty}$	r_{L^∞}
0.125	0.0020	-	0.0145	-	5.0090e-04	-
0.0625	4.8797e-04	1.9988	0.0036	1.9977	1.2511e-04	2.0013
0.0313	1.2202e-04	1.9997	9.0753e-04	1.9992	3.1271e-05	2.0003
0.0156	3.0506e-05	1.9999	2.2692e-04	1.9998	7.8172e-06	2.0001
0.0078	7.6267e-06	2.0000	5.6731e-05	1.9999	1.9543e-06	2.0000

Table 5.4: Absolute L^2, L^1 and L^∞ errors and rates for time convergence, Laguerre stand-alone discretization of the advection-diffusion equation, $\theta = 1/2$, $M = 160$, $T = 10\,s$.

Δt	$\mathcal{E}_{L^2}$	r_{L^2}	$\mathcal{E}_{L^1}$	r_{L^1}	$\mathcal{E}_{L^\infty}$	r_{L^∞}
0.125	0.0753	-	0.6813	-	0.0127	-
0.0625	0.0389	0.9545	0.3428	0.9908	0.0070	0.8535
0.0313	0.0198	0.9697	0.1722	0.9930	0.0037	0.9182
0.0156	0.0100	0.9818	0.0864	0.9956	0.0019	0.9568
0.0078	0.0051	0.9899	0.0433	0.9978	9.6961e-04	0.9778

Table 5.5: Absolute L^2, L^1 and L^∞ errors and rates for time convergence, Laguerre stand-alone discretization of the advection-diffusion equation, $\theta = 1$, $M = 160$, $T = 10\,s$.

5.2 Validation of the coupling method

We now consider the coupled scheme (4.81) and we compute the errors on the finite region $[0, L]$ using a suitable Gaussian quadrature rule on the subintervals K_m, whose width is Δz for all $m = 1, \ldots, M$. In particular, we introduce the discrete norms

$$\|u_h\|_{L^2} = \sqrt{\sum_{m=1}^{N} \frac{\Delta z}{2} \sum_{k=1}^{ng} \left[u_h \left(\frac{\Delta z}{2} x_k + z_m \right) \right]^2 w_k} \tag{5.11}$$

$$\|u_h\|_{L^1} = \sum_{m=1}^{N} \frac{\Delta z}{2} \sum_{k=1}^{ng} \left| u_h \left(\frac{\Delta z}{2} x_k + z_m \right) \right| w_k \tag{5.12}$$

$$\|u_h\|_{L^\infty} = \max_{m=1,\ldots,N} \max_{k=1,\ldots,ng} \left| u_h \left(\frac{\Delta z}{2} x_k + z_m \right) \right|, \tag{5.13}$$

where $\{x_k\}_{k=1}^{ng}$ and $\{w_k\}_{k=1}^{ng}$ are the Gaussian nodes and weights on the reference interval $[-1, 1]$; the absolute errors with respect to the exact solution for the analysis of the non-homogeneous problem are defined as

$$\mathcal{E}_{L^2} = \|q_h - q\|_{L^2} \tag{5.14}$$

$$\mathcal{E}_{L^1} = \|q_h - q\|_{L^1} \tag{5.15}$$

$$\mathcal{E}_{L^\infty} = \|q_h - q\|_{L^\infty}, \tag{5.16}$$

where q_h and q are the numerical and the exact solution, respectively. In the homogeneous case we will be interested in relative errors with respect to a full DG discretization. Denoting by q_{DG} the reference solution, we define

$$\mathcal{E}^{rel}_{L^2} = \frac{\|q_h - q_{DG}\|_{L^2}}{\|q_{DG}\|_{L^2}} \tag{5.17}$$

$$\mathcal{E}^{rel}_{L^1} = \frac{\|q_h - q_{DG}\|_{L^1}}{\|q_{DG}\|_{L^1}} \tag{5.18}$$

$$\mathcal{E}^{rel}_{L^\infty} = \frac{\|q_h - q_{DG}\|_{L^\infty}}{\|q_{DG}\|_{L^\infty}}. \tag{5.19}$$

All the following tests will employ a SIPG scheme, corresponding to $\epsilon = -1$. This discretization is stable as long as the penalization parameter σ is large

enough ([Riv08],[Whe78]). We found that setting $\sigma = 200$ allows to achieve stability in all the experiments; therefore, we will consider $\sigma = 200$ unless otherwise specified.

5.2.1 Advection-diffusion equation

Test 1. Non-homogeneous problem

We first examine the non-homogeneous case, that is, equation (5.1) with $f \neq 0$. The exact solution is given by $q(z,t) = ze^{-z}\sin^2(z-t)$. We evolve the coupled scheme until the final time $T = 10\,s$ and find good agreement with the exact solution (Figure 5.3).

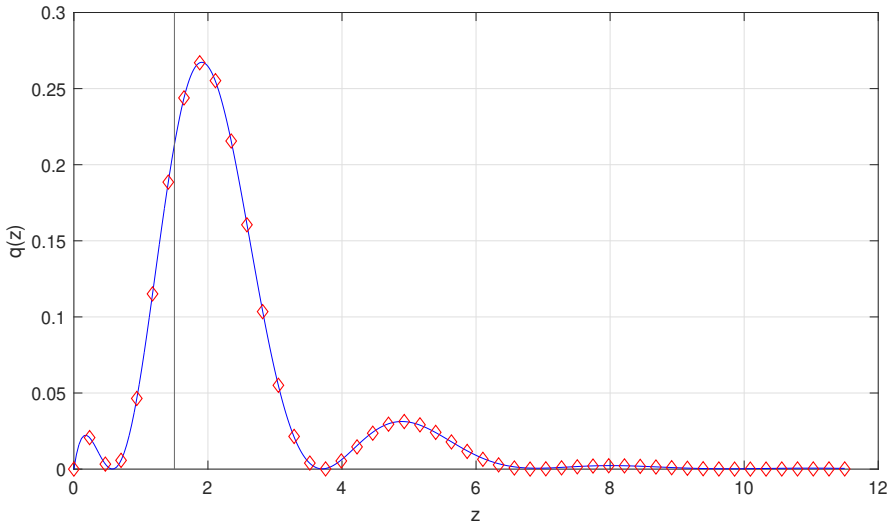

Figure 5.3: Coupled model, Test 1, solution at the final time $T = 10\,s$. Exact solution: $q(z,t) = ze^{-z}\sin^2(z-t)$. $N = 20$, $L = 1.5\,m$, $p = 2$, $M = 30$, $\varepsilon = -1$, $\sigma = 100$, $\beta = 1$, $\mu = 10\,m^2/s$, $u = 2\,m/s$, $n = 50$, $\theta = 1/2$. Blue solid line: solution computed by the coupled scheme. Red diamonds: exact solution.

First we carry out some experiments to evaluate the rate of convergence in time and space of the DG discretization in the finite domain. We fix a fine spacing in the finite domain and a large number of spectral modes in the semi-infinite domain, namely $N = 100$ and $M = 180$ and we run the code until the final time of $T = 10\,s$. The interface is placed at $L = 2\,m$, so that $\Delta z = 0.02\,m$, and piecewise quadratic basis functions ($p = 2$) are used in $[0, L]$; we choose $\mu = 1\,m^2/s$, $u = 1\,m/s$, $\beta = 1$, while the parameters for the DG scheme are $\varepsilon = -1$ and $\sigma = 200$. We compute the L^2 norm of the error, $\mathcal{E}_2$, with respect to the exact solution. The results as a function of the time step n for the cases $\theta = 1/2$ and $\theta = 1$ are reported in Tables 5.6 and 5.7, while the logarithmic plots are shown in Figures 5.4 and 5.5 respectively; results corresponding to the fully DG method are shown in tables 5.8 and 5.9.

n	10	20	40	80	160
Δt	1	0.5	0.25	0.125	0.0625
$\mathcal{E}_{L^2}$	0.0340	0.0071	0.0017	4.3383e-04	1.1424e-04
r	-	2.2481	2.0493	1.9934	1.9250

Table 5.6: L^2 errors and rate of time convergence, coupled model, Test 1, $\theta = 1/2$, $N = 100$, $M = 180$, $\Delta z = 0.02\,m$.

n	10	20	40	80	160
Δt	1	0.5	0.25	0.125	0.0625
$\mathcal{E}_{L^2}$	0.0531	0.0301	0.0162	0.0084	0.0043
r	-	0.8194	0.8943	0.9449	0.9731

Table 5.7: L^2 errors and rate of time convergence, coupled model, Test 1, $\theta = 1$, $N = 100$, $M = 180$, $\Delta z = 0.02\,m$.

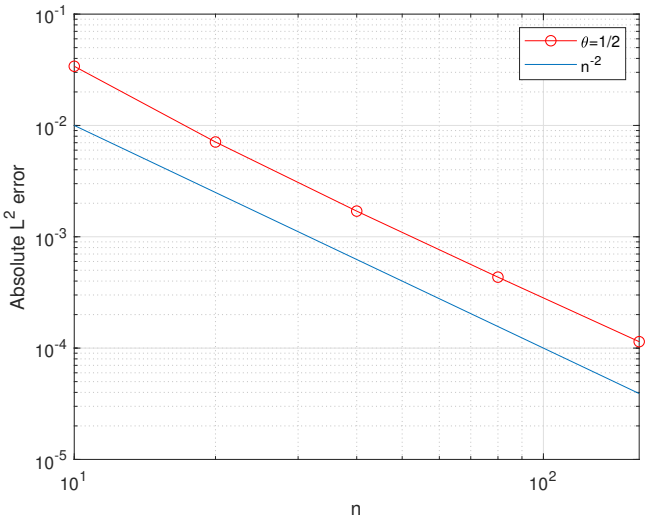

Figure 5.4: Absolute L^2 errors for time convergence, coupled model, Test 1. $\theta = 1/2$, $N = 100$, $M = 180$, $\Delta z = 0.01\,m$.

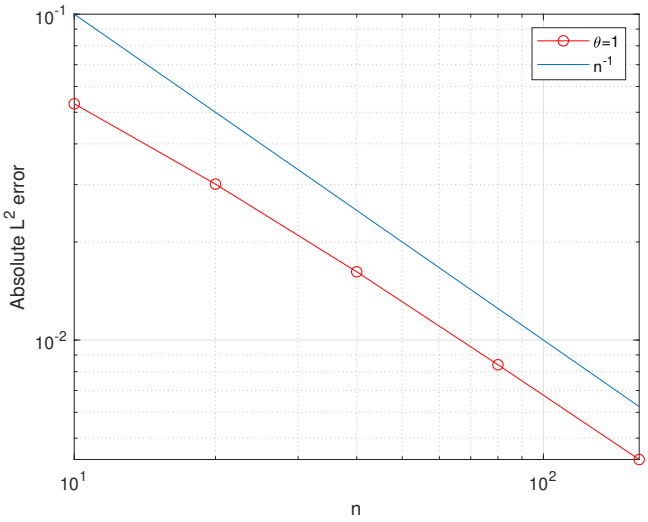

Figure 5.5: Absolute L^2 errors for time convergence, coupled model, Test 1. $\theta = 1$, $N = 100$, $M = 180$, $\Delta z = 0.01\,m$.

n	10	20	40	80	160
Δt	1	0.5	0.25	0.125	0.0625
$\mathcal{E}_{L^2}$	0.0340	0.0071	0.0017	4.2601e-04	1.0623e-04
r	-	2.2493	2.0543	2.0133	2.0036

Table 5.8: L^2 errors and rate of time convergence, fully DG model, Test 1, $\theta = 1/2$, $N = 100$, $M = 180$, $\Delta z = 0.02\,m$.

n	10	20	40	80	160
Δt	1	0.5	0.25	0.125	0.0625
$\mathcal{E}_{L^2}$	0.0531	0.0301	0.0162	0.0084	0.0043
r	-	0.8192	0.8939	0.9441	0.9715

Table 5.9: L^2 errors and rate of time convergence, coupled model, Test 1, $\theta = 1$, $N = 100$, $M = 180$, $\Delta z = 0.02\,m$.

As expected, we have linear convergence for $\theta = 1$ and quadratic for $\theta = 1/2$ for both techniques.

Next we test the space convergence by fixing a small time step, $n = 1000$, corresponding to $\Delta t = 0.01\,s$, and letting N vary; we also modify the value of β in such a way that the distance between the first and the second spectral modes is approximately equal to the spacing $\Delta z = L/N$. We choose $\theta = 1/2$ and we distinguish the cases where piecewise quadratic, $p = 2$ and piecewise linear, $p = 1$, basis functions are employed. The results for the coupled approach are shown in Table 5.10 and Figure 5.6, while the errors related to the fully DG scheme are in Table 5.11. We note that the latter are smaller than the former once all the parameters are fixed. In both cases the L^2 error stabilizes for large values of N because the time error dominates; this may be improved by choosing time integration methods of higher orders. For the first

			$p=2$		$p=1$	
N	Δz	β	$\mathcal{E}_{L^2}$	C	$\mathcal{E}_{L^2}$	C
10	0.2	0.1	1.05e-03	0.1	1.10e-02	0.05
20	0.1	0.2	2.63e-04	0.2	4.04e-03	0.1
40	0.05	0.4	6.72e-05	0.4	1.67e-03	0.2
80	0.025	0.8	1.84e-05	0.8	7.55e-04	0.4
160	1.25e-02	1.6	6.36e-06	1.6	3.58e-04	0.8
320	6.25e-03	3.2	3.54e-06	3.2	1.74e-04	1.6
640	3.12e-03	6.4	2.91e-06	6.4	8.52e-05	3.2
1280	1.56e-03	12.8	2.77e-06	12.8	4.20e-05	6.4
2560	7.81e-04	25.6	2.73e-06	25.6	2.06e-05	12.8

Table 5.10: Absolute L^2 errors for space convergence, coupled model, Test 1, $\theta = 1/2$, $\Delta t = 0.01\,s$, $M = 180$.

steps of refinement, the error reduction is quadratic for $p = 2$ and linear for $p = 1$. We remark that the Courant number is now defined as $C = up\Delta t/\Delta z$ to account for the polynomial degree employed in the DG discretization.

Now we examine the accuracy of the coupling as a function of the Péclet number, Pe. In this case we compute the relative L^1, L^2 and L^∞ errors with respect to the numerical solution achieved by a full DG discretization on $[0, 5L]$. We recall that, in order to ensure stability, the number of intervals in $[0, L]$ has to be chosen large enough. Therefore, we set $L = 2\,m$, $p = 2$, $\beta = 1$, $\mu = 1\,m^2/s$, $u = 2Pe\mu$ and a final time $T = 10\,s$ with $n = 200$ time steps, while $N > N_{cr}$, where N_{cr} is the minimum number of sub-intervals required in the bounded region to make the global scheme stable (see Tables 4.1 and 4.2). The characteristic length scale in the definition of Pe has been set to $1/2$ according to (1.35). The number of Laguerre modes M is such

			$p=2$		$p=1$	
N	Δz	β	$\mathcal{E}_{L^2}$	C	$\mathcal{E}_{L^2}$	C
10	0.2	0.1	1.72e-04	0.1	0.0039	0.05
20	0.1	0.2	2.11e-05	0.2	0.0010	0.1
40	0.05	0.4	3.55e-06	0.4	2.54e-04	0.2
80	0.025	0.8	2.71e-06	0.8	6.33e-05	0.4
160	1.25e-02	1.6	2.71e-06	1.6	1.57e-05	0.8
320	6.25e-03	3.2	2.72e-06	3.2	4.44e-06	1.6
640	3.12e-03	6.4	2.72e-06	6.4	2.74e-06	3.2
1280	1.56e-03	12.8	2.72e-06	12.8	2.69e-06	6.4
2560	7.81e-04	25.6	2.72e-06	25.6	2.70e-06	12.8

Table 5.11: Absolute L^2 errors for space convergence, fully DG scheme, Test 1, $\theta = 1/2$, $\Delta t = 0.01\,s$, $M = 180$.

that the distance between the first and the second node in the semi-infinite domain is approximately the same as the spacing Δz. Relative errors are shown in Tables 5.12 and 5.13 for the coupled scheme and the fully DG scheme, respectively. The second case provides smaller errors, and it has the further advantage that N_{cr} is small for high values of Pe, so that it is not necessary to increase N and M as diffusion dominates; these remarks show that the fully DG approach exhibits better features in terms of efficiency and stability.

Finally we fix the number of sub-intervals in the DG domain, $N = 100$ and we reduce the number of modes M. We choose $\mu = 1\,m^2/s$, $u = 1\,m/s$, $p = 2$, $\theta = 1/2$, $n = 2000$ (corresponding to $\Delta t = 0.005\,s$) and β according to the spacing Δz, while the other parameters are kept as before. The relative errors are shown in Tables 5.14 and 5.15; as long as M is small we have an

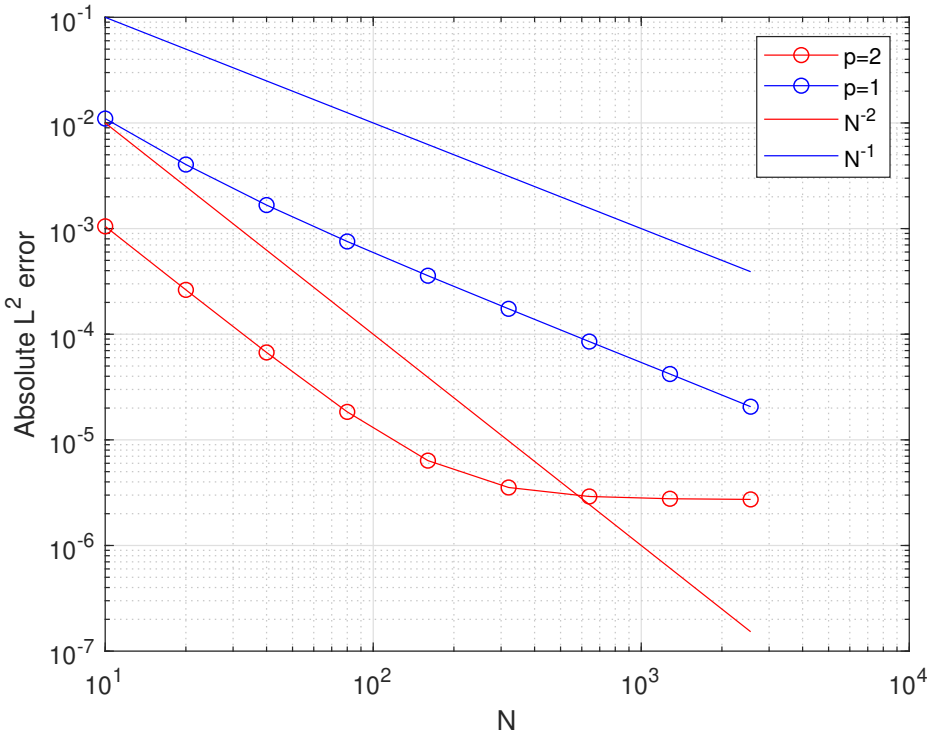

Figure 5.6: Coupled model, Test 1. L^2 error as a function of N for quadratic (red dots) and linear (blue dots) polynomials. $\theta = 1/2$, $\Delta t = 0.01\,s$, $M = 180$.

exponential reduction, while, starting from $M \approx 20$, increasing the number of modes has no effects on the errors. This happens, again, because of the time discretization employed, which limits the accuracy of the scheme. We also notice that the relative errors are low, at most around a few percent, even if a small number of modes is employed in the semi-infinite domain. Again, if the coupling is performed using a global DG approach, relative errors appear to be much lower.

Pe	0.001	10	100	500	1000
N_{cr}	2	2	8	106	244
N	100	100	100	120	250
M	180	180	180	220	350
$\mathcal{E}_2^{rel}$	6.7058e-05	2.2816e-06	6.8365e-08	1.6824e-07	2.3390e-08
$\mathcal{E}_1^{rel}$	7.6783e-05	1.0206e-06	1.0736e-08	1.9466e-08	1.8109e-09
$\mathcal{E}_\infty^{rel}$	6.9416e-05	7.3078e-06	4.8501e-07	1.7828e-06	3.6115e-07

Table 5.12: Coupled model, Test 1. L^2, L^1 and L^∞ relative errors as functions of Pe. $\Delta z = 0.01\,m$, $\Delta t = 0.05\,s$.

Pe	0.001	10	100	500	1000
N_{cr}	2	2	2	8	20
N	100	100	100	100	100
M	180	180	180	180	180
$\mathcal{E}_2^{rel}$	9.5798e-09	1.5563e-08	5.5664e-09	7.1439e-08	2.5828e-07
$\mathcal{E}_1^{rel}$	6.8142e-09	7.1110e-09	6.6474e-10	1.0369e-08	5.9035e-08
$\mathcal{E}_\infty^{rel}$	7.1773e-08	4.6508e-08	5.5162e-08	6.5700e-07	1.9148e-06

Table 5.13: Fully DG scheme, Test 1. L^2, L^1 and L^∞ relative errors as functions of Pe. $\Delta z = 0.01\,m$, $\Delta t = 0.05\,s$.

M	5	10	20	40	80
β	30	16	8	4	2
$\mathcal{E}_2^{rel}$	0.0539	0.0023	5.0184-05	5.0182e-05	5.0182e-05
$\mathcal{E}_1^{rel}$	0.0543	0.0024	5.2144e-05	5.2141e-05	5.2141e-05
$\mathcal{E}_\infty^{rel}$	0.0792	0.0032	6.3515e-05	6.3513e-05	6.3513e-05

Table 5.14: Coupled model, Test 1. L^2, L^1 and L^∞ relative errors as functions of M. $\Delta t = 0.005\,s$, $\Delta z = 0.02\ m$, $C = 0.25$.

M	5	10	20	40	80
β	30	16	8	4	2
$\mathcal{E}_2^{rel}$	0.0539	0.0024	1.8085-08	4.8592e-08	4.8592e-08
$\mathcal{E}_1^{rel}$	0.0543	0.0025	1.6993e-08	4.1506e-08	4.1505e-08
$\mathcal{E}_\infty^{rel}$	0.0792	0.0032	2.9806e-08	9.6897e-08	9.6799e-08

Table 5.15: Fully DG scheme, Test 1. L^2, L^1 and L^∞ relative errors as functions of M. $\Delta t = 0.005\,s$, $\Delta z = 0.02\ m$, $C = 0.25$.

Test 2. Homogeneous problem

We now examine the homogeneous case, that is equation (5.1) with $f = 0$, and we consider as initial datum a Gaussian profile of unitary amplitude

$$q^0(z) = \exp\left[-\left(\frac{z - z_q}{\sigma_q}\right)^2\right]. \tag{5.20}$$

The interface is located at $L = 10\,m$ and the initial hump is placed inside the bounded interval $[0, L]$ by choosing $z_q = 8\,m$ and $z_q = 5\,m$. The velocity is $u = 1\,m/s$ and the final time is $T = 4\,s$, so that the peak of the Gaussian crosses the interface in the first case but not in the second. We set $\Delta t = 0.02\,s$, $M = 10$ or $M = 40$ modes in the semi-infinite region, $N = 500$ sub-intervals for the DG scheme, so that $\Delta z = 0.02\,m$, and we compute the relative L^2, L^1 and L^∞ errors with respect to a full DG discretization on $[0, 50]$. Figure 5.7 depicts the process for $z_q = 8\,m$, $\sigma_q = 1\,m$: the initial hump expands and its amplitude decreases because of diffusion. As we can see from Tables 5.16 and 5.17, 10 modes for Laguerre discretization are enough to keep the errors in the bounded domain below a few percent. With $M = 40$ all the relative errors drastically reduce to the order of magnitude of 10^{-7}. As in the previous tests, the full DG coupling approach yields better relative errors, specially for $M = 40$, as seen in Tables 5.18 and 5.19.

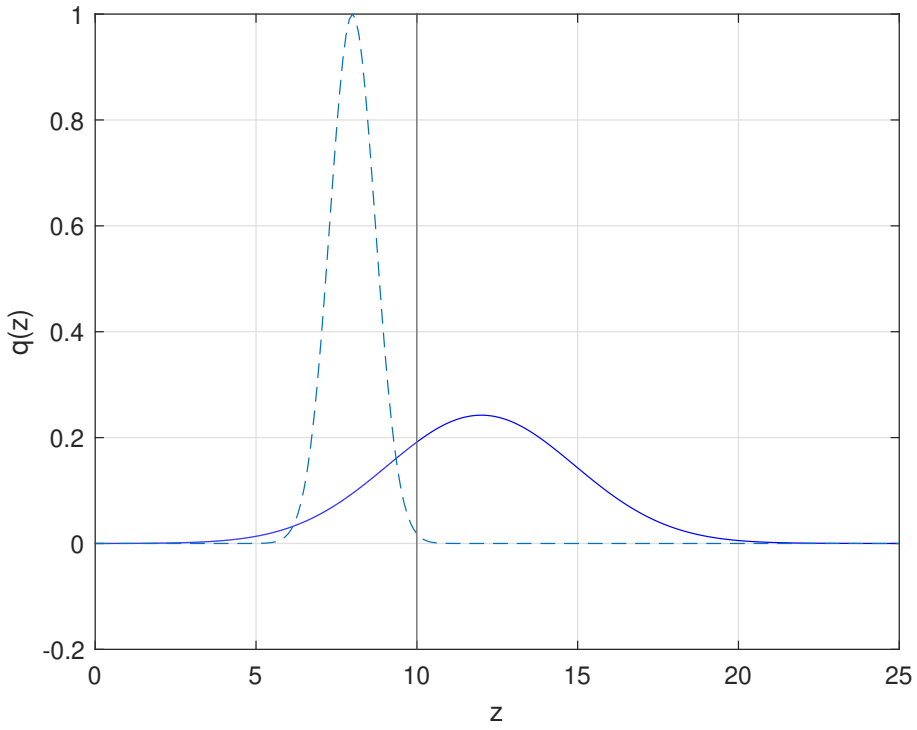

Figure 5.7: Coupled model, Test 2. Dashed line: initial datum. Solid line: DG-Laguerre solution at $T = 4$. $z_q = 8\,m$, $\sigma_q = 1\,m$, $M = 40$, $\beta = 4$, $\Delta z = 0.02\,m$, $\Delta t = 0.02\,s$, $\mu = 1\,m^2/s$, $u = 1\,m/s$.

z_q	σ_q	$\mathcal{E}_2^{rel}$	$\mathcal{E}_1^{rel}$	$\mathcal{E}_\infty^{rel}$
8	1	0.0190	0.0112	0.0380
	2	0.0198	0.0113	0.0410
	0.5	0.0187	0.0111	0.0371
5	1	0.0014	5.8133e-04	0.0049
	2	0.0020	8.7381e-04	0.0073
	0.5	0.0012	5.1314e-04	0.0044

Table 5.16: Coupled model, Test 2, L^2, L^1 and L^∞ relative errors. $M = 10$, $\beta = 16$, $\Delta z = 0.02\ m$, $\Delta t = 0.02\ s$, $C = 1$.

z_q	σ_q	$\mathcal{E}_2^{rel}$	$\mathcal{E}_1^{rel}$	$\mathcal{E}_\infty^{rel}$
8	1	4.9880e-07	4.5332e-07	4.6756e-07
	2	5.2517e-07	4.9364e-07	4.7604e-07
	0.5	3.1715e-07	6.5379e-07	2.7090e-07
5	1	4.3415e-07	1.2434e-06	2.1077e-07
	2	3.5954e-07	1.0264e-06	1.7643e-07
	0.5	4.5910e-07	1.3151e-06	2.2267e-07

Table 5.17: Coupled model, Test 2, L^2, L^1 and L^∞ relative errors. $M = 40$, $\beta = 4$, $\Delta z = 0.02\ m$, $\Delta t = 0.02\ s$, $C = 1$.

z_q	σ_q	$\mathcal{E}_2^{rel}$	$\mathcal{E}_1^{rel}$	$\mathcal{E}_\infty^{rel}$
8	1	0.0190	0.0111	0.0379
	2	0.0197	0.0113	0.0410
	0.5	0.0187	0.0111	0.0370
5	1	0.0014	5.7830e-04	0.0049
	2	0.0020	8.7031e-04	0.0072
	0.5	0.0012	5.1025e-04	0.0044

Table 5.18: Coupled model, Test 2, L^2, L^1 and L^∞ relative errors. $M = 10$, $\beta = 16$, $\Delta z = 0.02\ m$, $\Delta t = 0.02\ s$, $C = 1$.

z_q	σ_q	$\mathcal{E}_2^{rel}$	$\mathcal{E}_1^{rel}$	$\mathcal{E}_\infty^{rel}$
8	1	4.6269e-09	2.3089e-09	5.7648e-08
	2	3.7002e-09	2.8320e-09	5.6288e-09
	0.5	2.4680e-09	1.9425e-09	2.8789e-09
5	1	9.2343e-10	3.9790e-10	3.1233e-09
	2	8.7252e-10	3.7657e-10	3.6162e-09
	0.5	9.4017e-10	4.0560e-10	3.1924e-09

Table 5.19: Fully DG scheme, Test 2, L^2, L^1 and L^∞ relative errors. $M = 40$, $\beta = 4$, $\Delta z = 0.02\ m$, $\Delta t = 0.02\ s$, $C = 1$.

5.2.2 Burgers' equation

Next, we examine the case of the viscous Burgers' equation, which is (4.1) with $f(q) = q^2/2$ and $s(q) = 0$. The initial datum is the Gaussian profile $q_0(z) = \exp(-(z-3)^2)$. As time t evolves, the profile moves rightward increasing its steepness according to the value of the viscosity μ; in order to avoid the formation of shocks we choose $\mu = 0.05\, m^2/s$. Since the closed form of the solution is not available, we compute the errors with respect to a stand-alone DG discretization on a larger domain with the same spacing Δz.

We place the interface between the coupled schemes at $L = 3\ m$ and we run the simulation until $T = 1\ s$. Because of the explicit time integration, a small time step is required to achieve stability, so we choose $\Delta t = 10^{-6}\ s$ and $N = 30$, with $\epsilon = -1$ and $\sigma = 200$ in (4.24) and (4.28). Regarding the modal discretization on the semi-infinite domain, we choose $M = 60$ modes. The plot of the numerical solution corresponding to these parameters is shown in Figure 5.8. We recall that, because of the non-linearity of the problem, a third-order Runge-Kutta scheme has been employed for time discretization. Tables 5.20 and 5.21 report the relative L^2, L^1 and L^∞ errors in the bounded sub-domain $[0, L]$ for $N = 15$ and $N = 30$, respectively; they are obtained by varying the number of modes in the semi-infinite domain, and, accordingly, the scaling parameter β so that the distance between the first two nodes is approximately equal to the grid spacing in $[0, L]$, and keeping all the other parameters unchanged. The corresponding results for the fully DG approach are shown in Tables 5.22 and 5.23. We notice that small values of M are enough to keep the coupling error around a few percent.

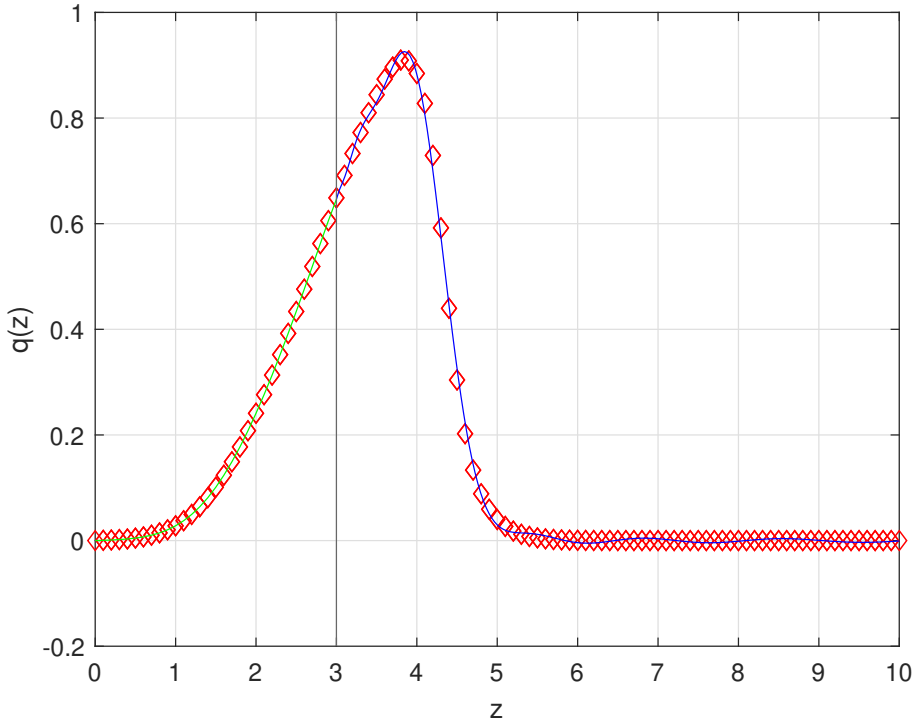

Figure 5.8: Coupled scheme for viscous Burgers' equation with Gaussian initial datum $q_0(z) = \exp(-(z-3)^2)$. Solution at $T = 1\,s$ with $N = 30$, $M = 60$, $\Delta t = 10^{-6}\,s$. Green line: Coupled DG. Blue line: Coupled Laguerre. Red diamonds: Stand-alone DG.

M	10	20	40	80
β	1.6	0.85	0.45	0.23
$\mathcal{E}_2^{rel}$	0.0121	0.0089	0.0036	0.0021
$\mathcal{E}_1^{rel}$	0.0059	0.0044	0.0018	0.0011
$\mathcal{E}_\infty^{rel}$	0.0201	0.0147	0.0059	0.0035

Table 5.20: Relative L^2, L^1 and L^∞ errors in the bounded region for the coupled Burgers' equation, $T = 1\,s$, $\Delta t = 10^{-6}\,s$, $N = 15$.

M	10	30	60	100
β	3.6	1.2	0.6	0.36
$\mathcal{E}_2^{rel}$	0.0036	0.0030	0.0028	0.0027
$\mathcal{E}_1^{rel}$	0.0010	8.3909e-04	7.7184e-04	7.4412e-04
$\mathcal{E}_\infty^{rel}$	0.0085	0.0071	0.0066	0.0063

Table 5.21: Relative L^2, L^1 and L^∞ errors in the bounded region for the coupled Burgers' equation, $T = 1\,s$, $\Delta t = 10^{-6}\,s$, $N = 30$.

M	10	20	40	80
β	1.6	0.85	0.45	0.23
$\mathcal{E}_2^{rel}$	0.0012	0.0012	0.0013	0.0013
$\mathcal{E}_1^{rel}$	3.9101e-04	4.0620e-04	4.3301e-04	4.3976e-04
$\mathcal{E}_\infty^{rel}$	0.0043	0.0044	0.0047	0.0047

Table 5.22: Relative L^2, L^1 and L^∞ errors in the bounded region for the coupled Burgers' equation, fully DG scheme, $T = 1\,s$, $\Delta t = 10^{-5}\,s$, $N = 15$.

M	10	30	60	100
β	3.6	1.2	0.6	0.36
$\mathcal{E}_2^{rel}$	4.0343e-04	5.3347e-04	5.8155e-04	6.0289e-04
$\mathcal{E}_1^{rel}$	9.3222e-05	1.2266e-04	1.3305e-04	1.3762e-04
$\mathcal{E}_\infty^{rel}$	0.0021	0.0028	0.0030	0.0032

Table 5.23: Relative L^2, L^1 and L^∞ errors in the bounded region for the coupled Burgers' equation, fully DG scheme, $T = 1\,s$, $\Delta t = 10^{-5}\,s$, $N = 30$.

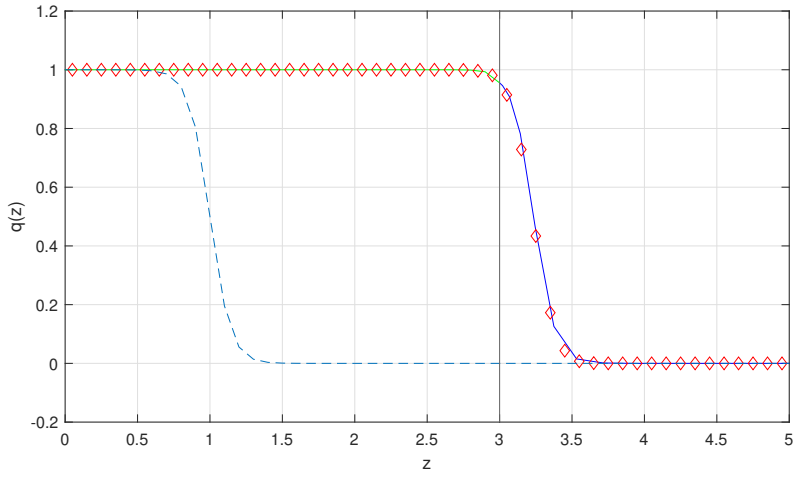

Figure 5.9: Coupled scheme for non linear diffusion-reaction equation. Solution at $T = 3\,s$. $p = 1$, $L = 3\,m$, $N = 30$, $M = 180$, $\beta = 1$, $\Delta t = 10^{-5}\,s$. Dashed line: Initial datum. Green line: Coupled DG. Blue line: Coupled Laguerre. Red diamonds: Full DG.

5.2.3 Reaction-diffusion equation

Finally, we consider a non-linear reaction contribution by setting $s(q) = \gamma q^2(1-q)$ in (4.1). We choose as initial datum

$$q_0(z) = \frac{1}{1 + \exp(\lambda(z-1))} \tag{5.21}$$

with $\lambda = \frac{1}{2}\sqrt{\frac{2\gamma}{\mu}}$, $\mu = \frac{1}{\gamma} = 0.05\,m^2/s$. We run the simulation until $T = 3\ s$, when the bump has crossed the interface, with $\Delta t = 10^{-5}\ s$; we place the interface, placed as before at $L = 3\ m$, and we choose $N = 30$ to ensure the stability of the explicit time integration scheme. The plot of the numerical solution provided by the coupled model with $M = 180$ and $\beta = 1$ is shown in Figure 5.9, in comparison with the one obtained by a stand-alone DG discretization on $[0, 10]$ with the same spacing Δz.

The results of the analysis of the relative errors for different choices of

the parameters are reported in Tables 5.24 and 5.25. Once again, a small number of modes is sufficient to keep under control the errors in the bounded region, proving the efficiency of the coupling.

M	10	20	40	80
β	1.6	0.85	0.45	0.23
$\mathcal{E}_2^{rel}$	0.0065	1.8365e-04	2.0168e-04	2.0930e-04
$\mathcal{E}_1^{rel}$	0.0020	6.2614e-05	7.0923e-05	7.4531e-05
$\mathcal{E}_\infty^{rel}$	0.0230	6.6436e-04	7.4003e-04	7.7181e-04

Table 5.24: Relative L^2, L^1 and L^∞ errors in the bounded region for the coupled diffusion-reaction equation, $T = 3\,s$, $\Delta t = 10^{-5}\,s$, $N = 15$.

M	10	30	60	100
β	3.6	1.2	0.6	0.36
$\mathcal{E}_2^{rel}$	1.0905e-04	1.8365e-04	2.0168e-04	2.0930e-04
$\mathcal{E}_1^{rel}$	3.7923e-05	6.2614e-05	7.0923e-05	7.4531e-05
$\mathcal{E}_\infty^{rel}$	3.9756e-04	6.6436e-04	7.4003e-04	7.7181e-04

Table 5.25: Relative L^2, L^1 and L^∞ errors in the bounded region for the coupled diffusion-reaction equation, $T = 3\,s$, $\Delta t = 10^{-5}\,s$, $N = 30$.

5.3 Absorbing layer

We now want to assess the possibility to employ the semi-infinite part of the computational domain as an absorbing layer to damp perturbations leaving the finite region. This can be done by implementing a reaction coefficient $\gamma \neq 0$ in $[L, +\infty)$. As in [Ben10] and [BB19], we choose a sigmoid of the form

$$\gamma(z) = \frac{\Delta\gamma}{1 + \exp\left(\dfrac{\alpha L_0 - z + L}{\sigma_D}\right)}, \tag{5.22}$$

where $\Delta\gamma$ is the sigmoid amplitude, $\alpha \in [0, 1]$ the position of the sigmoid inside the absorbing layer, L_0 the spatial extension of the semi-infinite region, i.e. the distance between the first and the last GLR nodes, and σ_D determines the sigmoid steepness.

We will first examine the case of a single Gaussian perturbation leaving the bounded region; in this case we expect spurious reflections at the interface to be minimal, and absolute L^2, L^1 and L^∞ errors with respect to the zero solution will then be computed in the finite region $[0, L]$. In a second test, we will consider a wavelike Dirichlet boundary condition at the left endpoint, so that a wave-train will cross the finite portion of the domain before being damped, and we will compute the relative errors in the bounded part of the domain with respect to a reference standalone DG discretization on the interval $[0, 2L]$. Finally, we will also test the efficiency of the absorbing layer on a non-linear problem, namely the Burgers' equation.

5.3.1 Gaussian perturbation

We place the interface at $L = 1000\ m$ and we consider an initial datum as (5.20), with $\mu_q = 750\ m$ and $\sigma_q = 50\ m$. We set $u = 1\, m/s$ and $\mu = 1\, m^2/s$,

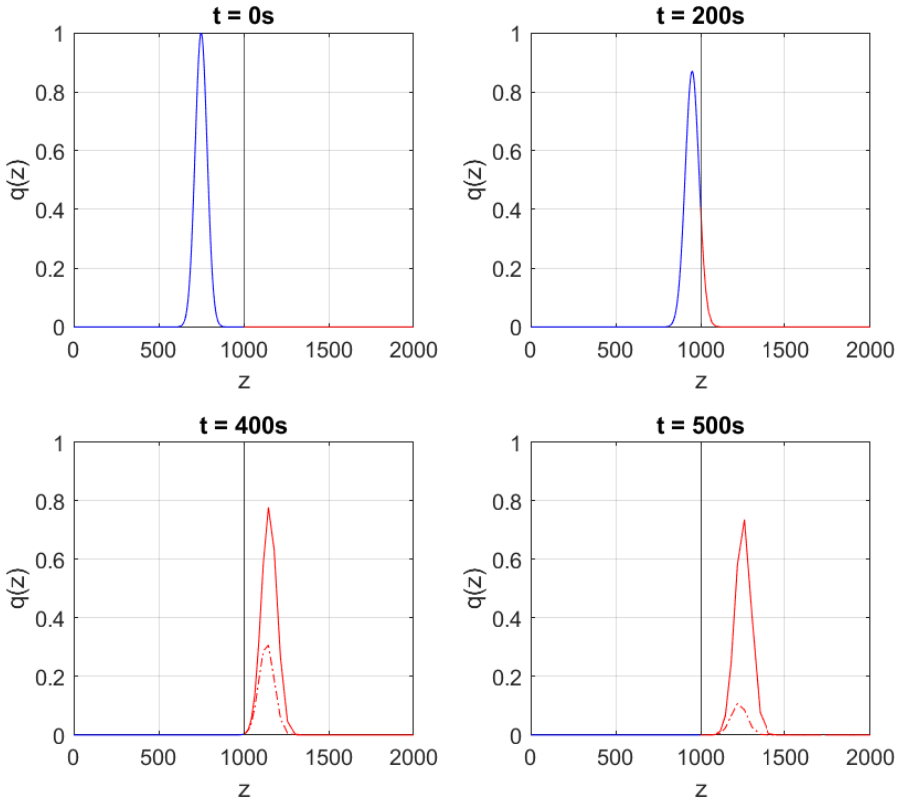

Figure 5.10: Damping of a Gaussian profile. Solid line: $\gamma = 0$. Dash-dot line: $\gamma \neq 0$. Blue: Coupled DG. Red: Coupled Laguerre. $N = 400$, $M = 40$, $\beta = 1/28$, $n = 600$, $\Delta t = 5/6\, s$, $C = 0.33$.

so that the Gaussian profile travels across the finite region with unitary velocity before crossing the interface and being damped. The coefficients of the sigmoid are $\Delta\gamma = 1$, $\alpha = 0.3\ m^{-1}$ and $\sigma_D = L_0/18\ m$ (see also [BB13], [BB19] and [Ben10]). We employ linear or quadratic polynomials in the finite domain and $\theta = 1/2$. The initial data and the numerical solution at $t = 200\, s, 400\, s, 500\, s$ are depicted in Figure 5.10. Further numerical results for several choices of the discretization parameters are reported in Tables 5.26 and 5.27 for the coupled DG-Laguerre scheme; the time step Δt was

chosen so that the Courant number is $C = 0.33$ for all tests. The absolute residual errors are similar to those provided by [BB19]. We also consider the full DG approach, whose results are shown in Tables 5.28 and 5.29. We point out that the spacing Δz is smaller than the one used in [BB19] in order to guarantee the stability of the global matrix $\mathbf{A}$, as seen before.

M	N	n	β	$\mathcal{E}_2$	$\mathcal{E}_1$	$\mathcal{E}_\infty$
40	400	600	1/28	2.4790e-04	3.5651e-04	2.4876e-04
30	400	600	1/21	1.3661e-05	2.7263e-05	1.3369e-05
20	400	600	2/29	6.8709e-05	1.0032e-04	6.8567e-05
10	400	600	2/15	4.2456e-06	9.9023e-06	3.9933e-06
5	400	600	1/4	1.7651e-06	6.6543e-06	1.2501e-06
30	300	450	1/28	1.2229e-03	2.4053e-03	1.0721e-03
20	300	450	1/19	8.7120e-04	1.7148e-03	7.6383e-04
10	300	450	1/10	6.2673e-05	1.2400e-04	5.4987e-05
5	300	450	11/60	6.4668e-06	1.4473e-05	5.6307e-06
20	250	375	1/23	1.0889e-03	2.6896e-03	8.5286e-04
10	250	375	1/12	2.2400e-04	5.4623e-04	1.7621e-04
5	250	375	1/6	1.8454e-05	4.6169e-05	1.4589e-05
10	200	300	1/15	9.8190e-04	3.0288e-03	6.6132e-04
5	200	300	1/7	8.7480e-05	2.7899e-04	5.8367e-05

Table 5.26: Absolute L^2, L^1 and L^∞ residual errors in the finite region for the damping of a Gaussian perturbation, coupled DG-Laguerre scheme for the advection diffusion equation. $C = 0.33$, $p = 1$, $T = 500\,s$.

M	N	n	β	$\mathcal{E}_2$	$\mathcal{E}_1$	$\mathcal{E}_\infty$
40	400	600	1/28	1.1484e-04	1.6170e-04	1.2488e-04
30	400	600	1/21	7.9550e-06	1.3371e-05	9.2091e-06
20	400	600	2/29	3.0774e-05	4.9707e-05	3.2460e-05
10	400	600	2/15	2.0193e-06	7.1450e-06	1.5059e-06
5	400	600	1/4	1.5474e-06	6.2491e-06	8.5797e-06
30	300	450	1/28	4.7009e-04	6.5910e-04	4.6783e-04
20	300	450	1/19	3.4275e-04	4.7678e-04	3.4263e-04
10	300	450	1/10	9.1034e-06	1.7740e-05	8.7312e-06
5	300	450	11/60	1.8633e-06	6.9264-06	1.2725e-06
20	250	375	1/23	3.3049e-04	4.7953e-04	3.0523e-04
10	250	375	1/12	3.2018e-05	4.9755e-05	2.9615e-05
5	250	375	1/6	2.1887e-06	7.5848e-06	1.6091e-06
10	200	300	1/15	1.0661e-04	1.5005e-04	8.9885e-05
5	200	300	1/7	3.5562e-06	9.9407e-06	2.7915e-06

Table 5.27: Absolute L^2, L^1 and L^∞ residual errors in the finite region for the damping of a Gaussian perturbation, coupled DG-Laguerre scheme for the advection diffusion equation. $C = 0.33$, $p = 2$, $T = 500\,s$.

M	N	n	β	$\mathcal{E}_2$	$\mathcal{E}_1$	$\mathcal{E}_\infty$
40	400	600	1/28	1.1346e-04	1.6454e-04	1.1380e-04
30	400	600	1/21	8.6036e-06	1.7966e-05	8.4946e-06
20	400	600	2/29	2.9328e-05	4.4620e-05	2.9157e-05
10	400	600	2/15	1.7895e-06	6.6955e-06	1.2795e-06
5	400	600	1/4	1.4442e-06	6.1064e-06	7.9062e-07
30	300	450	1/28	4.5889e-04	9.0184e-04	4.0236e-04
20	300	450	1/19	3.3819e-04	6.6480e-04	2.9658e-04
10	300	450	1/10	5.5416e-06	1.2653e-05	4.8037e-06
5	300	450	11/60	1.5474e-06	6.5201e-06	9.8777e-07
20	250	375	1/23	3.0948e-04	7.6670e-04	2.4225e-04
10	250	375	1/12	1.6502e-05	4.1436e-05	1.3052e-05
5	250	375	1/6	1.5908e-06	6.8939e-06	1.0477e-06
10	200	300	1/15	6.5441e-05	2.1107e-04	4.3512e-05
5	200	300	1/7	1.8031e-06	8.0631e-06	1.1874e-06

Table 5.28: Absolute L^2, L^1 and L^∞ residual errors in the finite region for the damping of a Gaussian perturbation, fully DG scheme for the advection diffusion equation. $C = 0.33$, $p = 1$, $T = 500\,s$.

M	N	n	β	$\mathcal{E}_2$	$\mathcal{E}_1$	$\mathcal{E}_\infty$
40	400	600	1/28	9.5110e-05	1.3443e-04	1.0307e-04
30	400	600	1/21	5.9751e-06	1.1777e-05	6.7342e-06
20	400	600	2/29	2.5770e-05	4.2453e-05	2.7017e-05
10	400	600	2/15	1.8486e-06	6.8392e-06	1.2798e-06
5	400	600	1/4	1.5203e-06	6.1911e-06	8.1538e-07
30	300	450	1/28	3.5509e-04	4.9929e-04	3.5273e-04
20	300	450	1/19	2.5923e-04	3.6293e-04	2.5861e-04
10	300	450	1/10	4.9958e-06	1.1811e-05	4.5899e-06
5	300	450	11/60	1.6693e-06	6.5652-06	1.0267e-06
20	250	375	1/23	2.3106e-04	3.3549e-04	2.1325e-04
10	250	375	1/12	1.3290e-05	2.3734e-05	1.2130e-05
5	250	375	1/6	1.7434e-06	6.8147e-06	1.1102e-06
10	200	300	1/15	4.5649e-05	6.8301e-05	3.8414e-05
5	200	300	1/7	1.9534e-06	7.4807e-06	1.3075e-06

Table 5.29: Absolute L^2, L^1 and L^∞ residual errors in the finite region for the damping of a Gaussian perturbation, fully DG scheme for the advection diffusion equation. $C = 0.33$, $p = 2$, $T = 500\,s$.

5.3.2 Wave train

In the next experiment we consider a Dirichlet boundary at the left endpoint of the kind $a(t) = A\sin(2\pi k/Tt)$. The initial condition is $q^0 = 0$. In this case, a wave train is generated at $z = 0$, it crosses the interval $[0, L]$ and it is damped by the absorbing layer. We choose again $L = 500\ m$, $\mu = 1\, m^2/s$, $u = 1\, m/s$, $\alpha = 0.3\, m^{-1}$ and $\sigma_D = L_0/18\, m$. The simulation runs until $T = 5000\, s$ in order to make the test more challenging for the absorbing layer, with $n = 16000$ time intervals . The plot of the numerical solution at the final time is shown in Figure 5.11 and Figure 5.12 for $k = 30$ and $k = 60$, respectively, while Tables 5.30 and 5.31 contain the relative errors for $M = 30$ and $M = 15$, respectively. Again, the results are comparable with those obtained by [BB19] in the pure advection case. In particular, a small number of Laguerre modes are enough to damp outgoing perturbations with reflections into the finite domain of negligible amplitude.

On the basis of the tests of this section, we may conclude that the coupled scheme can be employed as an efficient absorbing layer even when a diffusive term is present. This extends the results of [BB13] and [BB19], where the same feature was shown in the case of shallow water equations. We remark that residual errors are smaller in the parabolic case because of the presence of diffusion, which contributes to the damping of signals.

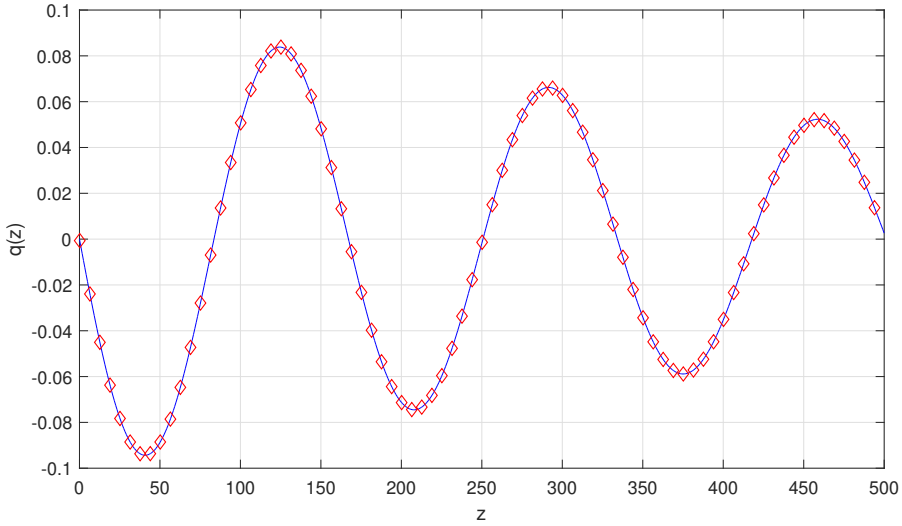

Figure 5.11: Damping of a wave train. Solid line: DG-Laguerre solution. Red diamonds: standalone DG solution. $A = 0.1\,m$, $k = 30$, $M = 30$, $N = 600$, $\beta = 0.143$, $T = 5000\,s$, $n = 16000$.

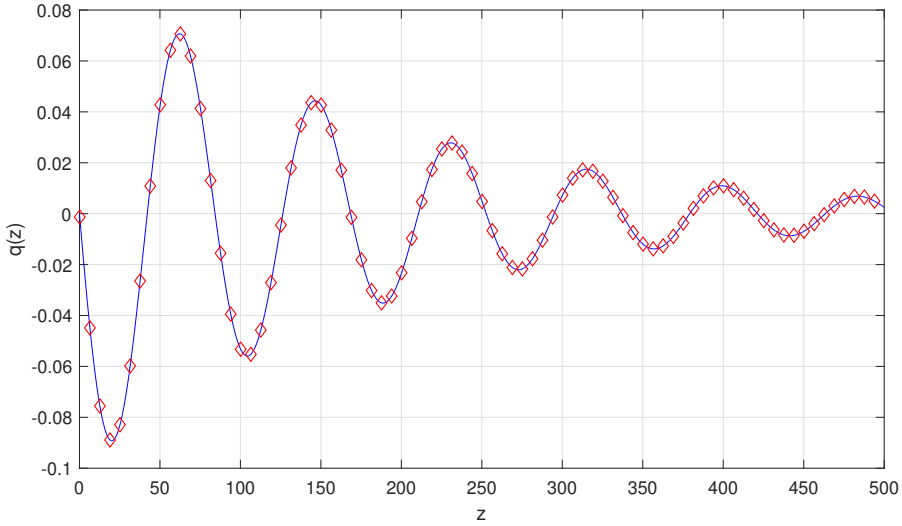

Figure 5.12: Damping of a wave train. Solid line: DG-Laguerre solution. Red diamonds: standalone DG solution. $A = 0.1\,m$, $k = 60$, $M = 30$, $N = 600$, $\beta = 0.286$, $T = 5000\,s$, $n = 16000$.

A	k	N	β	$\mathcal{E}_2^{rel}$	$\mathcal{E}_1^{rel}$	$\mathcal{E}_\infty^{rel}$
0.025	30	600	0.143	3.3609e-06	2.7164e-07	4.3334e-05
0.025	60	1200	0.286	9.7130e-07	6.9462e-08	1.1762e-05
0.05	30	600	0.143	3.8685e-06	3.1312e-07	4.9793e-05
0.05	60	1200	0.286	1.0470e-06	7.4998e-08	1.2697e-05
0.1	30	600	0.143	5.2832e-06	4.2419e-07	6.8717e-05
0.1	60	1200	0.286	1.1982e-06	8.6056e-08	1.4564e-05

Table 5.30: Relative L^2, L^1 and L^∞ errors in the bounded region for the damping of a wave train, coupled DG-Laguerre scheme for the advection diffusion equation. $L = 500\ m$, $p = 1$, $\mu = 1\, m^2/s$, $u = 1\, m/s$, $T = 5000\ s$, $n = 16000$, $M = 30$.

A	k	N	β	$\mathcal{E}_2^{rel}$	$\mathcal{E}_1^{rel}$	$\mathcal{E}_\infty^{rel}$
0.025	30	600	0.286	1.0895e-05	7.9691e-07	1.5531e-04
0.025	60	1200	0.571	9.2336e-07	6.6974e-08	1.1280e-05
0.05	30	600	0.286	4.6748e-06	3.7034e-07	6.1776e-05
0.05	60	1200	0.571	1.0132e-06	7.3535e-08	1.2383e-05
0.1	30	600	0.286	5.6207e-06	4.4860e-07	7.3643e-05
0.1	60	1200	0.571	1.1861e-06	8.5555e-08	1.4460e-05

Table 5.31: Relative L^2, L^1 and L^∞ errors in the bounded region for the damping of a wave train, coupled DG-Laguerre scheme for the advection diffusion equation. $L = 500\ m$, $p = 1$, $\mu = 1\, m^2/s$, $u = 1\, m/s$, $T = 5000\ s$, $n = 16000$, $M = 15$.

5.3.3 Burgers' equation

Finally, we test the efficiency of the damping layer in the non-linear case of the Burgers' equation. We place the interface at $L = 3\,m$, and the initial datum is

$$q_0(z) = A\exp(-(z-3)^2), \tag{5.23}$$

with $A = 1\,m$ or $A = 0.1\,m$. We run the coupled model until the final time $T = 5\,s$ with a time step of $\Delta t = 10^{-5}\,s$. The viscosity is $\mu = 0.05\,m^2/s$ and the penalization parameters for the DG part are $\epsilon = -1$ and $\sigma = 200$. We use linear polynomials, $p = 1$, and we distinguish the cases of $N = 15$ and $N = 30$ sub-intervals in the bounded region. The sigmoid parameters are $\alpha = 0.15\,m^{-1}$ and $\sigma_D = L_0/18\,m$. The plot of the solution at the final time with and without damping is shown in Figure 5.10. The coupled solution is compared to a standalone DG discretization on $[0, 10]$. The relative L^2, L^1 and L^∞ errors for the coupled DG-Laguerre method are shown in Table and 5.32 for $A = 1\,m$, and in Table 5.33 for $A = 0.1\,m$. Tables 5.34 and 5.35 report the results for the fully DG scheme. The errors are at most around a few percent, so that the implemented absorbing layer appears to be efficient in the non-linear case as well.

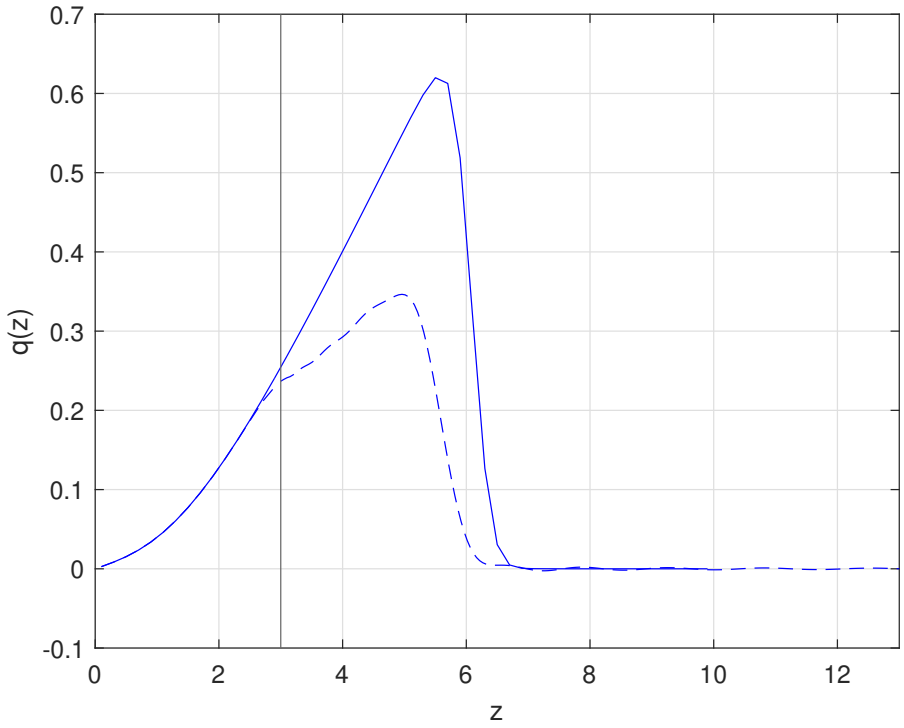

Figure 5.13: Damping for the Burgers' equation. Solution at $T = 5\,s$. Solid line: $\gamma = 0$. Dashed line: $\gamma \neq 0$. $\Delta\gamma = 2$.

M	10	20	40	80
β	1.6	0.85	0.45	0.23
$\mathcal{E}_2^{rel}$	0.0306	0.0182	0.0176	0.0175
$\mathcal{E}_1^{rel}$	0.0133	0.0081	0.0079	0.0079
$\mathcal{E}_\infty^{rel}$	0.0571	0.0338	0.0327	0.0325

M	10	30	60	100
β	3.6	1.2	0.6	0.36
$\mathcal{E}_2^{rel}$	0.0213	0.0151	0.0147	0.0146
$\mathcal{E}_1^{rel}$	0.0092	0.0068	0.0066	0.0066
$\mathcal{E}_\infty^{rel}$	0.0477	0.0333	0.0321	0.0319

Table 5.32: Relative L^2, L^1 and L^∞ errors in the bounded region for the coupled Burgers' equation, $N = 15$ (above) and $N = 30$ (below), $A = 1\,m$.

M	10	20	40	80
β	1.6	0.85	0.45	0.23
$\mathcal{E}_2^{rel}$	0.0292	0.0279	0.0276	0.0275
$\mathcal{E}_1^{rel}$	0.0192	0.0187	0.0185	0.0185
$\mathcal{E}_\infty^{rel}$	0.0459	0.0431	0.0426	0.0425

M	10	30	60	100
β	3.6	1.2	0.6	0.36
$\mathcal{E}_2^{rel}$	0.0214	0.0166	0.0163	0.0163
$\mathcal{E}_1^{rel}$	0.0134	0.0107	0.0105	0.0105
$\mathcal{E}_\infty^{rel}$	0.0381	0.0288	0.0282	0.0281

Table 5.33: Relative L^2, L^1 and L^∞ errors in the bounded region for the coupled Burgers' equation, $N = 15$ (above) and $N = 30$ (below), $A = 0.1\,m$.

M	10	20	40	80
β	1.6	0.85	0.45	0.23
$\mathcal{E}_2^{rel}$	0.0223	0.0257	0.0190	0.0169
$\mathcal{E}_1^{rel}$	0.0099	0.0124	0.0097	0.0088
$\mathcal{E}_\infty^{rel}$	0.0415	0.0459	0.0326	0.0284

M	10	30	60	100
β	3.6	1.2	0.6	0.36
$\mathcal{E}_2^{rel}$	0.0167	0.0120	0.0116	0.0116
$\mathcal{E}_1^{rel}$	0.0072	0.0053	0.0052	0.0052
$\mathcal{E}_\infty^{rel}$	0.0377	0.0264	0.0254	0.0253

Table 5.34: Relative L^2, L^1 and L^∞ errors in the bounded region, Burgers' equation, fully DG scheme, $N = 15$ (above) and $N = 30$ (below), $A = 1\,m$.

M	10	20	40	80
β	1.6	0.85	0.45	0.23
$\mathcal{E}_2^{rel}$	0.0089	0.0076	0.0074	0.0073
$\mathcal{E}_1^{rel}$	0.0055	0.0048	0.0046	0.0046
$\mathcal{E}_\infty^{rel}$	0.0146	0.0125	0.0120	0.0120

M	10	30	60	100
β	3.6	1.2	0.6	0.36
$\mathcal{E}_2^{rel}$	0.0111	0.0067	0.0065	0.0064
$\mathcal{E}_1^{rel}$	0.0065	0.0041	0.0039	0.0039
$\mathcal{E}_\infty^{rel}$	0.0208	0.0123	0.0119	0.0117

Table 5.35: Relative L^2, L^1 and L^∞ errors in the bounded region, Burgers' equation, fully DG scheme, $N = 15$ (above) and $N = 30$ (below), $A = 0.1\,m$.

Chapter 6

Conclusions and perspectives

In this thesis we analyzed a spectral method for the discretization of 1D parabolic problems on unbounded domains. In particular,

1. We performed a stability analysis of the spectrum of the matrix corresponding to the semi-discrete linear advection-diffusion problem for different values of the Péclet number Pe. We compared collocation schemes in strong form, nodal and modal discretizations in weak form, and we considered either Laguerre functions or polynomials. In general, if Pe is fixed, a condition on the scaling parameter β is required to achieve stability, with discretizations based on Laguerre functions providing wider stability ranges of β than those provided by Laguerre polynomials; moreover, our results matched those already available for the advection equation in the limit $Pe \to +\infty$. As in [BB19], the best choice was found to be given by scaled Laguerre basis functions and Gauss-Laguerre-Radau rules for numerical integration.

2. The chosen scheme was tested in several numerical experiments for the advection-diffusion equation. As long as the time error is negligible,

we found spectral convergence in space; the rate of convergence provided by the θ-method also matched the theoretical results. We then performed the coupling with a DG discretization in two different ways, by considering the interface either as the boundary between two different schemes or as the internal node of a global DG discretization. We carried out a stability analysis on the global matrix, and we found out that the grid in the bounded interval must be sufficiently fine to prevent instabilities. The threshold value of the spacing for the fully DG approach is much larger than the one provided by the first method, especially for diffusion-dominated regimes, and it does not depend on the number of spectral modes in the unbounded region. We carried out many validation experiments and we showed that, as in [BB13] and [BB19], reflections at the interface between the two schemes were found to be negligible both in the homogeneous and non-homogeneous case. The fully DG approach achieved better results in terms of absolute and relative errors with respect to a reference solution.

3. We implemented a damping term in the semi-infinite part of the computational domain, and we tested its efficiency in absorbing outgoing perturbations in the form of single Gaussian profiles or wave train initial data for the advection-diffusion equation. A small number of Laguerre modes was found to be sufficient to damp signals without spurious phenomena spoiling the simulation in the finite region. Thanks to the outcomes of points 1, 2 and 3, this work provides an extension to existing results where the same features are proved for hyperbolic problems.

4. As an extension to the results mentioned above, we also tested the coupling on two non-linear problems: the Burgers' equation and a non-

linear reaction-diffusion equation. In this case, an explicit, third-order Runge-Kutta method has been employed for time integration. Also in this case, relative errors with respect to a full DG solution are small enough to make the proposed coupled scheme an interesting technique for the discretization of fluid dynamics problems on unbounded domains.

The work of this thesis may be extended by considering the following future perspectives.

- The coupling strategy can be tested on 2D or 3D domains. For example, one may consider a semi-infinite strip, where the problem is discretized using Laguerre basis functions in the vertical direction and a discontinuous Galerkin approach in the horizontal one. One may also take into account circular domains by switching to polar coordinates and employ Laguerre functions for the radial variable; this may have applications, for example, in the modeling of the solar corona.

- The extension to systems of parabolic equations or to non-linear diffusion may be considered. As an example, we cite the turbulent vertical diffusion, which is described by a system of coupled non-linear diffusion equations, and the gas flow in porous media, where the diffusion coefficient depends on the solution itself (see e.g. [BF14]).

- The numerical tests carried out in the present work rely on the theta-method and a third order Runge-Kutta scheme for time integration, which may neutralize spectral accuracy in space because of their relatively low order. To increase global efficiency, one may employ higher order implicit-explicit (IMEX) methods [BFR16, GKC13, KC03].

Appendix A

Analysis of the outflow case

In this appendix we analyse the advection-diffusion equation in the half-line $[0, +\infty)$ in the outflow case $u < 0$. If this situation happens in the purely hyperbolic case, no boundary conditions should be assigned at the left endpoint in order to have a well posed problem. This is not the case when a diffusion term is introduced, because of the presence of a second order derivative. However, in this section we will also investigate the stability of a discretization of the linear advection-diffusion equation in the outflow case in which the advection term is treated as in the purely hyperbolic regime, without imposing a boundary condition at the outflow boundary. This is of interest to assess robustness of the numerical approach in the inviscid limit and because this approach is often employed in many practical applications in environmental fluid dynamics.

Multiplying (3.1) and (3.2) by a test function and a positive weight and integrating by parts we obtain

$$\frac{d}{dt}\int_0^{+\infty} \varphi(z)q(z,t)\omega(z)\,dz + \mu\varphi(0)\frac{\partial q}{\partial z}(0,t)\omega(0) + \\ + \mu\int_0^{+\infty} \frac{\partial q}{\partial z}(z,t)\frac{d(\omega\varphi)}{dz}\,dz + u\int_0^{+\infty} \varphi(z)\frac{\partial q}{\partial z}(z,t)\omega(z)\,dz = 0 \quad \text{(A.1)}$$

and

$$\begin{aligned}
&\frac{d}{dt}\int_0^{+\infty}\varphi(z)q(z,t)\omega(z)\,dz-\mu\int_0^{+\infty}\varphi(z)\frac{\partial v}{\partial z}(z,t)\omega(z)\,dz+\\
&+u\int_0^{+\infty}\varphi(z)v(z,t)\omega(z)\,dz=0 \qquad\qquad (A.2)\\
&-q(0)\varphi(0)-\int_0^{+\infty}q\frac{d(\omega\varphi)}{dz}\,dz-\int_0^{+\infty}v(z,t)\varphi(z)\omega(z)\,dz=0
\end{aligned}$$

respectively.

A.1 Modal discretization, Laguerre functions

In this case, $\omega = 1$. For the formulation (3.1), by inserting the expansion of the solution on the basis of Laguerre functions we find

$$\begin{aligned}
&\sum_{j=0}^{M}\frac{dq_j}{dt}\left(\hat{\mathscr{L}}_j^{\beta},\hat{\mathscr{L}}_i^{\beta}\right)+\mu\sum_{j=0}^{M}q_j(\hat{\mathscr{L}}_j^{\beta})'(0)\hat{\mathscr{L}}_i^{\beta}(0)+\\
&\qquad+\mu\sum_{j=0}^{M}q_j\left((\hat{\mathscr{L}}_j^{\beta})',(\hat{\mathscr{L}}_i^{\beta})'\right)+u\sum_{j=0}^{M}q_j\left((\hat{\mathscr{L}}_j^{\beta})',\hat{\mathscr{L}}_i^{\beta}\right)=0 \qquad (A.3)
\end{aligned}$$

which gives

$$\frac{d\mathbf{q}}{dt}=\left[\mu\beta^2(\mathbf{L}^T)^2+u\beta\mathbf{L}^T\right]\mathbf{q} \qquad (A.4)$$

where the matrix $\mathbf{L}$ is defined by (3.19).

Starting from formulation (3.2) and acting in the same way we find

$$\frac{1}{\beta}\frac{dq_i}{dt}-\mu\sum_{j=0}^{M}-l_{ji}v_j+\frac{u}{\beta}v_i \qquad (A.5)$$

$$\frac{1}{\beta}v_i=-\sum_{j=0}^{M}q_j+\sum_{j=0}^{M}l_{ij}q_j \qquad (A.6)$$

and then (noting that $l_{ij}-1=-l_{ji}$)

$$\frac{1}{\beta}\frac{d\mathbf{q}}{dt}+\mu\mathbf{L}^T\mathbf{v}+\frac{u}{\beta}\mathbf{v}=0 \qquad (A.7)$$

$$\mathbf{v}=-\beta\mathbf{L}^T\mathbf{q} \qquad (A.8)$$

from which (A.4) follows again.

A.2 Modal discretization, Laguerre polynomials

In this case the weight is $\omega(z) = e^{-\beta z}$. Inserting the representation of the solution in the basis of Laguerre polynomials in the second equation of formulation (3.2) and applying the usual relations concerning the scalar products between basis functions and their derivatives we get

$$\frac{1}{\beta} v_i = -\sum_{j=0}^{M} q_j + \sum_{j=0}^{M} l_{ij} q_j + \sum_{j=0}^{M} \delta_{ij} q_j \tag{A.9}$$

where now the entries of $\mathbf{L}$ are 1 on the lower triangular portion and 0 elsewhere. We notice that $l_{ij} + \delta_{ij} - 1 = -l_{ji}$ so we can write

$$\mathbf{v} = -\beta \mathbf{L}^T \mathbf{q}. \tag{A.10}$$

Acting on the first equation we have instead

$$\frac{1}{\beta} \frac{dq_i}{dt} - \mu \sum_{j=0}^{M} -l_{ji} v_j + \frac{u}{\beta} v_i = 0 \tag{A.11}$$

which, in vector form, reads

$$\frac{d\mathbf{q}}{dt} = -\mu\beta \mathbf{L}^T \mathbf{v} - u\mathbf{v}. \tag{A.12}$$

Inserting the expression for $\mathbf{v}$ we find

$$\frac{d\mathbf{q}}{dt} = \left[\mu\beta^2 (\mathbf{L}^T)^2 + u\beta \mathbf{L}^T\right] \mathbf{q} \tag{A.13}$$

which has the same form as (A.4) with a different definition of the matrix $\mathbf{L}$.

A.3 Nodal discretization, Laguerre functions

We now represent the solution on the basis of Lagrangian functions associated with Laguerre functions and GLR or GL nodes as

$$q(z,t) \approx \sum_{j=0}^{M} q_j(t)\hat{h}_j^{\beta}(z) \tag{A.14}$$

Since Laguerre functions are considered, we choose $\omega = 1$ and substitute the expansion in the second equation of (A.2):

$$\sum_{j=0}^{M} v_j \hat{\omega}_i^{\beta}\delta_{ij} = -\sum_{j=0}^{M} q_j \hat{h}_j^{\beta}(0)\hat{h}_i^{\beta}(0) - \sum_{j=0}^{M} q_j \int_0^{+\infty} \hat{h}_j^{\beta}(z)(\hat{h}_i^{\beta})'(z)dz \tag{A.15}$$

Using the usual notations, we obtain

$$\mathbf{v} = \left(-\hat{\mathbf{\Omega}}_{\beta}^{-1}\hat{\mathbf{H}} - \hat{\mathbf{\Omega}}_{\beta}^{-1}\hat{\mathbf{D}}_{\beta}^{T}\hat{\mathbf{\Omega}}_{\beta}\right)\mathbf{q} \tag{A.16}$$

where $\hat{\mathbf{H}} = \mathbf{h}\mathbf{h}^T$ and $\mathbf{h} = [\hat{h}_0^{\beta}(0), \ldots, \hat{h}_M^{\beta}(0)]$. We notice that, if GLR nodes are used, $\mathbf{h} = \mathbf{e}_1 = [1, 0, \ldots, 0]$. Manipulation of the first equation of (A.2) yields instead

$$\frac{d\mathbf{q}}{dt} = \mu\hat{\mathbf{D}}_{\beta}\mathbf{v} - u\mathbf{v} \tag{A.17}$$

and, substituting the expression of $\mathbf{v}$,

$$\frac{d\mathbf{q}}{dt} = \left[\mu\hat{\mathbf{D}}_{\beta}(-\hat{\mathbf{\Omega}}_{\beta}^{-1}\hat{\mathbf{H}} - \hat{\mathbf{\Omega}}_{\beta}^{-1}\hat{\mathbf{D}}_{\beta}^{T}\hat{\mathbf{\Omega}}_{\beta}) + u(\hat{\mathbf{\Omega}}_{\beta}^{-1}\hat{\mathbf{H}} + \hat{\mathbf{\Omega}}_{\beta}^{-1}\hat{\mathbf{D}}_{\beta}^{T}\hat{\mathbf{\Omega}}_{\beta})\right]\mathbf{q} \tag{A.18}$$

A.4 Nodal discretization, Laguerre polynomials

If polynomials are employed, we choose $\omega(z) = e^{-\beta z}$. Substitutions in the second equation of (A.2) gives:

$$\sum_{j=0}^{M} v_j \omega_i^\beta \delta_{ij} = -\sum_{j=0}^{M} q_j h_j^\beta(0) h_i^\beta(0) + \\ -\sum_{j=0}^{M} q_j \left[\int_0^{+\infty} h_j^\beta(z)(h_i^\beta)'(z)\omega(z)dz - \beta \int_0^{+\infty} h_j^\beta(z) h_i^\beta(z)\omega(z)dz \right] \quad \text{(A.19)}$$

which, in vector notation, is

$$\mathbf{v} = \left(-\mathbf{\Omega}_\beta^{-1}\mathbf{H} - \mathbf{\Omega}_\beta^{-1}\mathbf{D}_\beta^T\mathbf{\Omega}_\beta + \beta\mathbf{I}\right)\mathbf{q} \quad \text{(A.20)}$$

where now $\mathbf{H} = \mathbf{h}\mathbf{h}^T$ and $\mathbf{h} = [h_0^\beta(0), \ldots, h_M^\beta(0)]$. Once again, if GLR nodes are used, $\mathbf{h}$ simplifies to $\mathbf{e}_1 = [1, 0, \ldots, 0]$. From the first equation we obtain

$$\frac{d\mathbf{q}}{dt} = \mu\mathbf{D}_\beta\mathbf{v} - u\mathbf{v} \quad \text{(A.21)}$$

so that

$$\frac{d\mathbf{q}}{dt} = \left[\mu\mathbf{D}_\beta(-\mathbf{\Omega}_\beta^{-1}\mathbf{H} - \mathbf{\Omega}_\beta^{-1}\mathbf{D}_\beta^T\mathbf{\Omega}_\beta + \beta\mathbf{I}) + u(\mathbf{\Omega}_\beta^{-1}\mathbf{H} + \mathbf{\Omega}_\beta^{-1}\mathbf{D}_\beta^T\mathbf{\Omega}_\beta - \beta\mathbf{I})\right]\mathbf{q} \quad \text{(A.22)}$$

A.5 Strong form discretization

In this case we discretize the strong form of the advection-diffusion problem (3.1) substituting the expansion of the solution and evaluating it in the GLR nodes z_i, $i = 0, \ldots, M$. We find

$$\sum_{j=0}^{M} \frac{dq_j}{dt}\hat{h}_j^\beta(z_i) - \mu\sum_{j=0}^{M} q_j(\hat{h}_j^\beta)''(z_i) + u\sum_{j=0}^{M} q_j(\hat{h}_j^\beta)'(z_i) = 0 \quad \text{(A.23)}$$

which, in vector notation, reads

$$\frac{d\mathbf{q}}{dt} = \left(\mu\hat{\mathbf{D}}_\beta^2 - u\hat{\mathbf{D}}_\beta\right)\mathbf{q} \tag{A.24}$$

If Laguerre polynomials are employed, we only need to replace the differentiation matrix $\hat{\mathbf{H}}_\beta$ with $\mathbf{H}_\beta$, so as to obtain

$$\frac{d\mathbf{q}}{dt} = \left(\mu\mathbf{D}_\beta^2 - u\mathbf{D}_\beta\right)\mathbf{q} \tag{A.25}$$

A.6 Analysis of the results

We collect the expressions for matrix $\mathbf{A}$ in the different schemes when an outflow Dirichlet boundary condition is imposed at the left endpoint.

Coll, LF, Out	$\mu\hat{\mathbf{D}}_\beta^2 - u\hat{\mathbf{D}}_\beta$
Coll, LP, Out	$\mu\mathbf{D}_\beta^2 - u\mathbf{D}_\beta$
Nod, LF, Out	$(-\mu\hat{\mathbf{D}}_\beta + u\mathbf{I})(\hat{\mathbf{\Omega}}_\beta^{-1}\hat{\mathbf{H}} + \hat{\mathbf{\Omega}}_\beta^{-1}\hat{\mathbf{D}}_\beta^T\hat{\mathbf{\Omega}}_\beta)$
Nod, LP, Out	$(-\mu\mathbf{D}_\beta + u\mathbf{I})(\mathbf{\Omega}_\beta^{-1}\mathbf{H} + \mathbf{\Omega}_\beta^{-1}\mathbf{D}_\beta^T\mathbf{\Omega}_\beta - \beta\mathbf{I})$
Mod, LF, Out	$\mu\beta^2(\mathbf{L}^T)^2 + u\beta\mathbf{L}^T$
Mod, LP, Out	$\mu\beta^2(\mathbf{L}^T)^2 + u\beta\mathbf{L}^T$

Table A.1: Matrix $\mathbf{A}$. 'Coll': collocation, 'Nod': nodal, 'Mod': modal, 'Out': outflow Dirichlet b.c., 'LF': Laguerre Functions, 'LP': Laguerre Polynomials.

The matrix $\mathbf{L}$ is defined as

- LF

$$l_{ij} = \begin{cases} 1/2 & i = j \\ 1 & i > j \\ 0 & i < j \end{cases}$$

- LP

$$l_{ij} = \begin{cases} 1 & i > j \\ 0 & i \leq j \end{cases}$$

The following table collects the results of the stability analysis of $\mathbf{A}$ in terms of the Péclet number. As in Chapter 3, we employ both definitions $Pe_\beta = |u|/\mu\beta$ and $Pe = |u|L/\mu$. We fix $M = 50$ and $\mu = 1$. In the first case we set $\beta = 1$ and we let Pe_β vary, determining u as $-Pe_\beta\mu\beta$; results are shown in Table A.2. In the second case we set $L = 1$, $Pe = 1$, $Pe = 10$ or $Pe = 100$ and $u = -Pe\mu$; the stability ranges for β are shown in Table A.3.

			Out	
			LF	LP
Strong			$Pe_\beta \geq 1.7$	$\nexists Pe_\beta$
Weak	Nodal	GLR	$Pe_\beta \geq 1.7$	$\nexists Pe_\beta$
		GL	$\nexists Pe_\beta$	$\nexists Pe_\beta$
	Modal		$Pe_\beta \geq 0.5$	$\forall Pe_\beta$

Table A.2: Stability of $\mathbf{A}$ as a function of $Pe_\beta = |u|/\mu\beta$ in the outflow case: condition under which the largest real part of the eigenvalues is non-positive. $M = 50$, $\beta = \mu = 1$. 'Out': Outflow Dirichlet b.c., 'LF': Laguerre Functions, 'LP': Laguerre Polynomials.

			Out	
			LF	LP
Strong			$\beta \leq 0.58Pe$	$\nexists\beta$
Weak	Nodal	GLR	$\beta \leq 0.58Pe$	$\nexists\beta$
		GL	$\nexists\beta$	$\nexists\beta$
	Modal		$\beta \leq 2Pe$	$\forall\beta$

Table A.3: Stability of $\mathbf{A}$ as a function of β in the outflow case: condition under which the largest real part of the eigenvalues is non-positive. $M = 50$, $\mu = 1$. 'Out': Outflow Dirichlet b.c., 'LF': Laguerre Functions, 'LP': Laguerre Polynomials.

The analysis shows that scaled Laguerre functions provide better stability properties than polynomials also in the outflow case. Polynomial-based nodal discretizations are never stable, regardless of the Péclet number, and the same holds true for the discretization in strong form. On the other hand, provided that Pe_β is large enough, or equivalently, β is sufficiently large, Laguerre functions are stable in these cases. Moreover, as in Chapter 3, GLR nodes for numerical integration are a better choice than GL nodes.

Bibliography

[ABCM02] Arnold D.N., Brezzi F., Cockburn B., Marini L.D. *Unified analysis of discontinuous Galerkin methods for elliptic problems*. SIAM Journal on Numerical Analysis, Vol. 39, No. 5, pp. 1749-1779, 2002.

[Akm11] Akmaev R.A. *Whole atmosphere modeling: Connecting terrestrial and space weather*. Reviews of Geophysics, Vol. 49, 2011.

[Arn82] Arnold D.N. *An interior penalty finite element method with discontinuous elements*. SIAM Journal on Numerical Analysis, Vol. 19, No. 4, pp. 742-760, 1982.

[Ben10] Benacchio T. *Spectral collocation methods on semi–infinite domains and application to open boundary conditions*. Master's thesis, Politecnico di Milano, 2010.

[BB13] Benacchio T., Bonaventura L. *Absorbing boundary conditions: a spectral collocation approach*. International Journal for Numerical Methods in Fluids, Vol. 72, No. 9, pp. 913–936, 2013.

[BB19] Benacchio T., Bonaventura L. *An extension of DG methods for hyperbolic problems to one-dimensional semi-infinite domains*. Applied Mathematics and Computation, Vol. 350, pp. 266-282, 2019.

[BF14] Bonaventura L., Ferretti R. *Semi-Lagrangian methods for parabolic problems in divergence form*. SIAM Journal on Scientific Computing, Vol. 36, No. 5, pp. A2458–A2477, 2014.

[BFR16] Boscarino S., Filbet F., Russo G. *High order semi-implicit schemes for time dependent partial differential equations*. Journal of Scientific Computing, Vol. 68, No.3, pp. 975-1001, 2016.

[CHQZ06] Canuto C., Hussaini M.Y., Quarteroni A., Zang T.A. *Spectral Methods. Fundamentals in Single Domains*. Springer–Verlag, Berlin Heidelberg, 2006.

[CL89] Cockburn B., Lin S.Y. *TVB Runge-Kutta local projection discontinuous Galerkin finite element method for conservation laws III: one dimensional systems*. Journal of Computational Physics Vol. 84, pp. 90-113, 1989.

[Dlo82] Dlotko T. *The one-dimensional Burgers' equation; existence, uniqueness and stability*. Zeszyty Naukowe Uniwersytetu Jagiellońskiego. Acta Mathematica, Vol. 623, 1982.

[DSW04] Dawson C., Sun S., Wheeler M.F. *Compatible algorithms for coupled flow and transport*. Computer Methods in Applied Mechanics and Engineering, Vol. 193, pp. 2565-2580, 2004.

[GKC13] Giraldo F. X., Kelly J. F., Constantinescu E. M. *Implicit-explicit formulations of a three-dimensional nonhydrostatic unified model of the atmosphere (NUMA)*. SIAM Journal on Scientific Computing, Vol. 35, No. 5, pp. B1162-B1194, 2013.

[GW07] Guo B.Y., Wang Z.Q. *Numerical integration based on Laguerre-Gauss interpolation*. Computer Methods in Applied Mechanics and Engineering, Vol. 196, pp. 3726-3741, 2007.

[Jac19] Jackson D.R., Fuller Rowell T.J., Griffin D.J., Griffith M.J., Kelly C.W., Marsh D.R., Walach M.T. *Future directions for whole atmosphere modeling: Developments in the context of space weather*. Space Weather, Vol. 17, pp. 1342–1350, 2019.

[KC03] Kennedy C.A., Carpenter M.H. *Additive Runge–Kutta schemes for convection–diffusion–reaction equations*. Applied numerical mathematics, Vol. 44, pp. 139-181, 2003.

[KK17] Karpov I.V., Kshevetskii S.P. *Numerical study of heating the upper atmosphere by acoustic-gravity waves from a local source on the Earth's surface and influence of this heating on the wave propagation conditions*. Journal of Atmospheric and Solar-Terrestrial Physics, Vol. 164, pp. 89-96, 2017.

[LeV92] LeVeque R.J. *Numerical methods for conservation laws*. ETH Zürich. Birkhäuser, 1992.

[LeV16] LeVeque R.J. *Finite volume methods for hyperbolic problems*. Cambridge University Press, Cambridge, 2002.

[Pao98] Pao C.V. *Parabolic Systems in Unbounded Domains. II. Equations with Time Delays*. Journal of Mathematical Analysis and Applications, Vol. 225, pp. 557-586, 1998.

[QSS07] Quarteroni A., Sacco R., Saleri F. *Numerical mathematics*. Springer, Berlin Heidelberg, 2007.

[Qua17] Quarteroni A. *Numerical Models for Differential Problems*. Springer International Publishing, 2017.

[Riv08] Rivière B. *Discontinuous Galerkin Methods for Solving Elliptic and Parabolic Equations: Theory and Implementation*. Frontiers in Applied Mathematics, 2008.

[Rob00] Roble R.G. *On the feasibility of developing a global atmospheric model extending from the ground to the exosphere. Atmospheric Science Across the Stratopause*. Geophysical Monograph Series, Vol. 123, pp. 53–67, 2000.

[RWG99] Rivière B., Wheeler M.F., Girault V. *Improved energy estimates for interior penalty, constrained and discontinuous Galerkin methods for elliptic problems*. Computers and Geosciences, Vol. 3, pp. 337-360, 1999.

[Sal15] Salsa S. *Partial differential equations in action. From modelling to theory*. Springer, 2015.

[ST06] Shen J., Tang T. *Spectral and high order methods with applications*. Science Press, Beijing, 2006.

[WGW09] Wang Z.Q., Guo B.Y., Wu Y.N. *Pseudospectral method using generalized Laguerre functions for singular problems on unbounded domains*. Discrete and Continuous Dynamical Systems Series B, Vol. 11, No.4, pp. 1019-1038, 2009.

[Whe78] Wheeler M.F *An elliptic collocation-finite element method with interior penalties*. SIAM Journal on Numerical Analysis, Vol. 15, No. 1, pp. 152-161, 1978.